

BONE AND SOFT TISSUE REGENERATIVE RESPONSE FOLLOWING
ALVEOLAR RIDGE AUGMENTATION USING MACROPOROUS POLYSULFONE
IMPLANTS WITH AND WITHOUT DEMINERALIZED BONE POWDER
IN MACACA FASCICULARIS

By

Fouad S. Salama, B.D.S.

Submitted to the Faculty of the School of Graduate Studies
of the Medical College of Georgia in Partial Fulfillment
of the Requirements
for the Degree of Master of Science in Oral Biology

June

1987

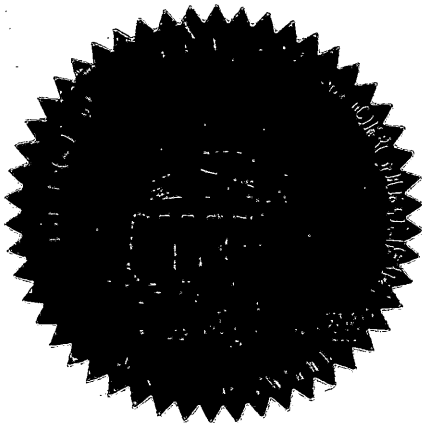
Bone and Soft Tissue Regenerative Response Following
Alveolar Ridge Augmentation Using Macroporous Polysulfone
Implants With and Without Demineralized Bone Powder
In Macaca Fascicularis

This thesis submitted by Fouad S. Salama has been examined and approved by an appointed committee of the faculty of the School of Graduate Studies of the Medical College of Georgia.

The signatures which appear below verify the fact that all required changes have been incorporated and that the thesis has received final approval with reference to content, form and accuracy of presentation.

This thesis is therefore accepted in partial fulfillment of the requirements for the degree of Master of Science in Oral Biology.

8/14/1987
Date



[Redacted Signature]

Advisor

[Redacted Signature]

Department Chairman

[Redacted Signature]

Dean, School of Graduate Studies

ABSTRACT

Successful augmentation of bone surfaces has great clinical application, particularly to the face and oral cavity regions. More than 24 million Americans are edentulous and must depend upon dentures to eat and to restore their normal speech and appearance. Porous polysulfone (PPSF) is frequently used to fill osseous voids. The purpose of this study was to test tooth soft tissue and bone response to porous polysulfone (PPSF), with and without demineralized bone powder (DBP) in *Macaca fascicularis*.

Six adult female monkeys, 12-15 years of age, were used in this study. One animal was sacrificed and used as a bone donor and the other five were recipients. All mandibular molar teeth were extracted and massive alveolectomies were performed. The wounds were left to heal for 5 to 8 1/2 months postoperatively. At the time of implantation, PPSF with DBP was inserted subperiosteally into the left mandibular edentulous areas while PPSF alone was inserted into the right sides. The animals were sacrificed at 42, 60, or 90 days following implantation. Each mandible was cut into 3mm thick coronal sections which were then examined and photographed with a dissecting microscope. Some specimens were then decalcified, embedded in paraffin and sectioned and stained with H & E. Other specimens were processed undecalcified in glycol and methylmethacrylate for histomorphometric measurements and tetracycline labelling. Also, some specimens were processed for scanning electron microscopy. No inflammation or untoward reaction of the implantation sites were noted at the time of sacrifice. Histologically, the 42 day specimens of the DBP-PPSF side (experimental side) revealed penetration of fibrous tissue rich in

fibroblasts and vessels into the pores of PPSF comparing to the PPSF side (control side). The fibrous tissue also surrounded the implant. Some multinucleated giant cells and macrophages were present. At 60 days, the PPSF side showed more organized fibrous tissue and bone grew only for a short distance into the polysulfone. In contrast, the PPSF-DBP side showed large amounts of bone formation within the pores of the polysulfone and almost covered the implant. The newly formed bone contained osteocytes and was surrounded by osteoblasts. At 90 days, the PPSF side showed more bone formation on the lower half of the implant. These results suggested that PPSF is a suitable non-resorbable material that accommodates bone and soft tissue formation. Also, the use of DBP enhanced both rate and amount of the new bone. In conclusion, PPSF with and without DBP is a suitable material that can be used successfully for alveolar ridge augmentation.

ACKNOWLEDGEMENTS

First I would like to express my deep appreciation to my major advisor, Dr. Mohamed Sharawy. He is not only my mentor, but also a friend. I extend my most sincere thanks for his close guidance and support through some difficult times. His inspirational guidance and truly knowledgeable approaches have created an environment conducive to a student's success. His talent and advice have given me an insight and enthusiasm for the future. I would like to thank Dr. Norris O'Dell for his expert advises and Dr. Frank Lake for his help and guidance. I would also like to thank Dr. David Pashley for his cooperation and in making his research facilities available to me.

To the other members of my Committee, Dr. Louis Gangarosa, Dr. Baldev Singh and Dr. Greg Parr, a debt of gratitude is owed for their encouragement, advice, and reading this thesis. I would like to thank Dr. Emad Helmy for his help during the implantation procedures. A special acknowledgment goes to the staff of the Department of Oral Biology/Anatomy. To Mrs. Vera Larke for preparing the photographs, Mrs. Linda Cullum for the long hours spent in typing this thesis, to Mrs. Cathy Pennington and Ms. Linda Shoemake for their skillful assistance.

Acknowledgement is also due to Dr. Lowell Greenbaum and Dr. Thomas Dirksen for their encouragement and support. I would like to thank Dr. Gerald Loft, Dr. George Schuster and Dr. Ken Morris for their help and advice. Also, I would like to thank Dr. Robert Shimp, Mr. Raymond Griffin and Dr. Malcolm Kling for their valuable assistance during the surgical procedures.

Finally, I thank my wife, Faika, and my son, Ahmed, for their patience during difficult times and their understanding has been an important factor for the completion of this work. I dedicate this work with lasting love and thanks to my dear parents, Saad El-Din and Nemat, whose dedication to my childhood instilled in me the desire to achieve high goals and whose tender and loving support has contributed immeasurably to this accomplishment.

Table of Contents

	Page
I. INTRODUCTION	1
A. Statement of the Problem and Aims	1
B. Review of Literature	2
1. Residual Ridge Overview	2
2. History and Background of Atrophic Ridge Management	7
3. Hard Tissue Augmentation	10
a. Background	10
b. Biological Materials	12
1). Bone	12
2). Cartilage	17
3). Demineralized Bone	19
c. Alloplastic Materials	34
1). Metals, Ceramics and Polymers	34
2). Porous Polysulfone	40
C. Rationale	43
D. Specific Aims	46
II. MATERIALS AND METHODS	47
A. Animals	47
B. Food and Care of Animals	47
C. Materials	47
1. Demineralized Bone Powder	47
2. Porous Polysulfone	48
D. Procedures	48
1. Preparation of the Alveolar Ridge	48

	Page
2. Preparation of Porous Polysulfone	50
3. Implantation Procedures	50
4. Animal Sacrifice	51
5. Evaluating Techniques	53
6. Scanning Electron Microscopy	54
III. RESULTS	56
A. Forty-two Days After Implantation (Group I)	56
1. Polysulfone Side	56
a. Gross Appearance	56
b. Stereoscopic Examination	57
c. Histologic Examination	57
2. Polysulfone-Demineralized Bone Powder Side	59
a. Gross Appearance	59
b. Stereoscopic Examination	59
c. Histologic Examination	59
B. Sixty Days Following Ridge Augmentation (Group II)	59
1. Polysulfone Side	59
a. Gross Appearance	59
b. Stereoscopic Examination	60
c. Histologic Examination	60
2. Sixty Days Following Polysulfone-Demineralized Bone Powder	62
a. Gross Appearance	62
b. Stereoscopic Examination	62
c. Histologic Examination	63

	Page
d. Histomorphometric Results	65
e. Tetracycline Labeling	66
C. Ninety Days Following Implantation (Group III)	67
1. Polysulfone Side	67
a. Gross Appearance	67
b. Stereoscopic Examination	67
c. Scanning Electron Microscopy Results	67
d. Histologic Examination	68
e. Histomorphometric Results	69
f. Tetracycline Labelling	69
IV. DISCUSSION	70
V. CONCLUSIONS	90
VI. REFERENCES	149
VII. APPENDIX	175

LIST OF FIGURES

Plate	Figure		Page
1	1	Photomicrograph showing a piece of long bone and DBP	95
	2	Photomicrograph showing a culture of DBP	95
	3	Photomicrograph of PPSF bar	95
	4	Photomicrograph of PPSF block with six holes	95
2	5	Photograph of the mandibular edentulous molar area	97
	6	Photograph of PPSF block on the surface of the edentulous area	97
	7	Photograph of the stone cast of the partially edentulous mandible	97
	8	Photograph of the acrylic splint on the stone cast	97
3	9	Photograph showing the wound closure	99
	10	Photograph of the acrylic splint	99
	11	Photograph of the acrylic splint fixed with circumferential wiring	99
	12	Photograph showing erosion of the mucosa covering the implant	99
4	13	Photograph of the partially edentulous mandible (42 days)	101
	14	Photomicrograph of coronal section of the mandible (PPSF, 42 days)	101

Plate	Figure		Page
	15	Photomicrograph of a histologic section (PPSF, 42 days)	101
	16	Photomicrograph of a histologic section (PPSF, 42 days)	101
5	17	Photomicrograph of a histologic section (PPSF, 42 days)	103
	18	Photomicrograph of a histologic section (PPSF, 42 days)	103
	19	Photomicrograph of a histologic section (PPSF, 42 days)	103
	20	Photomicrograph of a histologic section (PPSF, 42 days)	103
6	21	Photomicrograph of a coronal section of the edentulous mandible (PPSF + DBP, 42 days)	105
	22	Photomicrograph of a histologic section (PPSF + DBP, 42 days)	105
	23	Photomicrograph of a histologic section (PPSF + DBP, 42 days)	105
	24	Photomicrograph of a histologic section (PPSF + DBP, 42 days)	105
7	25	Photomicrograph of a histologic section (PPSF + DBP, 42 days)	107
	26	Photomicrograph of a histologic section (PPSF + DBP, 42 days)	107

Plate	Figure	Page
	27 Photomicrograph of a coronal section of the edentulous mandible (PPSF, 60 days)	107
	28 Photomicrograph of a histologic section (PPSF, 60 days)	107
8	29 Photomicrograph of a histologic section (PPSF, 60 days)	109
	30 Photomicrograph of a histologic section (PPSF, 60 days)	109
	31 Photomicrograph of a histologic section (PPSF, 60 days)	109
	32 Photomicrograph of a histologic section (PPSF, 60 days)	109
9	33 Photomicrograph of a histologic section (PPSF, 60 days)	111
	34 Photomicrograph of a histologic section (PPSF, 60 days)	111
	35 Photomicrograph of a histologic section (PPSF, 60 days)	111
	36 Photomicrograph of a histologic section (PPSF, 60 days)	111
10	37 Photomicrograph of a histologic section (PPSF, 60 days)	113
	38 Photomicrograph of a histologic section (PPSF, 60 days)	113
	39 Photomicrograph of an undecalcified histologic section (PPSF, 60 days)	113

Plate	Figure		Page
	40	Photomicrograph of an undecalcified histologic section (PPSF, 60 days)	113
11	41	Photomicrograph of a coronal section of the edentulous (PPSF + DBP, 60 days)	115
	42	Photomicrograph of a histologic section (PPSF + DBP, 60 days)	115
	43	Photomicrograph of a histologic section (PPSF + DBP, 60 days)	115
	44	Photomicrograph of a histologic section (PPSF + DBP, 60 days)	115
12	45	Photomicrograph of a histologic section (PPSF + DBP, 60 days)	117
	46	Photomicrograph of a histologic section (PPSF + DBP, 60 days)	117
	47	Photomicrograph of a histologic section (PPSF + DBP, 60 days)	117
	48	Photomicrograph of a histologic section (PPSF + DBP, 60 days)	117
13	49	Photomicrograph of a histologic section (PPSF + DBP, 60 days)	119
	50	Photomicrograph of a histologic section (PPSF + DBP, 60 days)	119

Plate	Figure		Page
	51	Photomicrograph of a histologic section (PPSF + DBP, 60 days)	119
	52	Photomicrograph of a histologic section (PPSF + DBP, 60 days)	119
14	53	Photomicrograph of a histologic section (PPSF + DBP, 60 days)	121
	54	Photomicrograph of a histologic section (PPSF + DBP, 60 days)	121
	55	Photomicrograph of a histologic section (PPSF + DBP, 60 days)	121
	56	Photomicrograph of a histologic section (PPSF + DBP, 60 days)	121
15	57	Photomicrograph of a histologic section (PPSF + DBP, 60 days)	123
	58	Photomicrograph of a histologic section (PPSF + DBP, 60 days)	123
	59	Photomicrograph of a histologic undecalcified section (PPSF + DBP, 60 days)	123
	60	Photomicrograph of a histologic undecalcified section (PPSF + DBP, 60 days)	123
16	61	Photomicrograph of a histologic undecalcified section (PPSF + DBP, 60 days)	125
	62	Photomicrograph of a fluorescent histologic unstained section (PPSF + DBP, 60 days)	125

Plate	Figure		Page
	63	Photomicrograph of a fluorescent histologic unstained section (PPSF + DBP, 60 days)	125
	64	Photomicrograph of a fluorescent histologic unstained section (PPSF + DBP, 60 days)	125
17	65	Photograph of the partially edentulous augmented mandible (PPSF, 90 days)	127
	66	Photograph of the partially edentulous augmented mandible (PPSF, 90 days)	127
	67	Photograph of the partially edentulous augmented mandible (PPSF, 90 days)	127
	68	Photomicrograph of a coronal section of the edentulous mandible (PPSF, 90 days)	127
18	69	SEM of polysulfone block	129
	70	SEM of polysulfone block	129
	71	SEM of polysulfone block	129
19	72	SEM of polysulfone block	131
	73	SEM of PPSF 90 days following implantation	131
	74	SEM of PPSF 90 days following implantation	131
20	75	SEM of PPSF 90 days following implantation	133
	76	SEM of PPSF 90 days following implantation	133
	77	SEM of PPSF 90 days following implantation	133
21	78	SEM of PPSF 90 days following implantation	135
	79	SEM of PPSF 90 days following implantation	135
	80	SEM of PPSF 90 days following implantation	135
22	81	SEM of PPSF 90 days following implantation	137

Plate	Figure		Page
	82	SEM of PPSF 90 days following implantation	137
	83	SEM of PPSF 90 days following implantation	137
23	84	SEM of PPSF 90 days following implantation	139
	85	SEM of PPSF 90 days following implantation	139
24	86	Photomicrograph of a histologic section (PPSF, 90 days)	141
	87	Photomicrograph of a histologic section (PPSF, 90 days)	141
	88	Photomicrograph of a histologic section (PPSF, 90 days)	141
	89	Photomicrograph of a histologic section (PPSF, 90 days)	141
25	90	Photomicrograph of a histologic section (PPSF, 90 days)	143
	91	Photomicrograph of a histologic section (PPSF, 90 days)	143
	92	Photomicrograph of a histologic section (PPSF, 90 days)	143
	93	Photomicrograph of a histologic section (PPSF, 90 days)	143
26	94	Photomicrograph of an undecalcified histologic section (PPSF, 90 days)	145
	95	Photomicrograph of an undecalcified histologic section (PPSF, 90 days)	145

Plate	Figure		Page
	96	Photomicrograph of an undecalcified histologic section (PPSF, 90 days)	145
	97	Photomicrograph of an undecalcified histologic section (PPSF, 90 days)	145
27	98	Photomicrograph of a fluorescent undecalcified histologic unstained section (PPSF, 90 days)	147
	99	Photomicrograph of a fluorescent undecalcified histologic unstained section (PPSF, 90 days)	147
	100	Photomicrograph of a fluorescent undecalcified histologic unstained section (PPSF, 90 days)	147
	101	Photomicrograph of a fluorescent undecalcified histologic unstained section (PPSF, 90 days)	147

LIST OF TABLES

	Page
Table I Summary of the Recovery of Implants Following Animal Sacrifice	91
Table II Control Site 60 Days Following Implantation of PPSF	92
Table III Experimental Site 60 Days Following Implantation of DBP + PPSF	93
Table IV Control Site 90 Days Following Implantation of PPSF	94

I. INTRODUCTION

A. Statement of the Problem and Aims

The main objectives in dentistry are the preservation and restoration of dental function, speech and esthetics. Regardless of the cause of loss of teeth, whether it is trauma, disease, or surgical resection, many patients suffer alveolar bone loss which, in some cases, is so severe that conventional prosthetics is nearly impossible (163).

More than 24 million Americans are edentulous and they have to depend on dentures to eat and to restore their normal speech and appearance (36). Also, it is estimated that half of American citizens over age of 50 are without one or more natural teeth (137).

Thoma et al. stated that extreme alveolar ridge atrophy makes the construction of functional dentures difficult and the wearing of dentures almost impossible (213).

Many edentulous patients suffer from marked atrophy of their alveolar ridges and present a problem for construction of an efficient denture. The development of implantable materials that are biocompatible, strong and relatively simple to use would benefit hundreds of thousands of edentulous patients annually.

Demineralized bone powder (DBP) has been shown to be osteoinductive in animals and humans (72, 92). The use of DBP to induce bone formation may be helpful in combination with alloplastic materials as a bone graft substitute.

The aim of this study was to investigate the bone and soft tissue regenerative response following alveolar ridge augmentation using

macroporous polysulfone implants with and without demineralized bone powder (DBP) in *Macaca fascicularis*.

B. Review of Literature

1. Residual Ridge Overview

The residual ridge is that bone of the alveolar process that remains after teeth are lost (29). The subsequent alterations skeletal lead to a considerable change in the configuration of the residual bony ridge. The first to disappear is the alveolar process, but the atrophy eventually may involve parts of the basal bodies of the jaws. In maxilla, there is often a narrowing of the arch relative to its pre-extraction dimensions. This is more pronounced in the premolar, canine or incisor areas. In the mandible, there is often a widening of the arch of the remaining ridge in the molar region while in the anterior region the changes vary individually (191).

If atrophy involves part of the body of the maxilla and mandible, the ridge may approach bony structures which anatomically are located far from the alveolar process. For example, in the maxilla, the ridge may approach the base of the anterior nasal spine, the lower end of the zygomatic alveolar crest, the hamulus of the pterygoid process or even the floor of the maxillary sinus. In the mandible, the atrophy may involve the upper part of the body of the mandible, so the ridge sinks to the level of the mental protuberance anteriorly and to the level of the genial tubercles lingually. In some cases it may even approach the level of the internal oblique line, or the mandibular canal and the mental foramen. In extreme cases, the ridge may drop below the level of the lingual sulcus and the sublingual glands may protrude on the top of the residual ridge (191). After loss of teeth, the residual ridge, under normal conditions, is

covered by a tissue that is identical in its structure with normal gingiva. In other words, it is covered by a keratinized or parakeratinized stratified squamous epithelium with an underlying firm, thick layer of inelastic dense connective tissue, which is also attached to the periosteum of the ridge (191).

The atrophy proceeds toward the line of origin of the muscles which are attached to the bone or near the bone of the alveolar process. In the maxilla, the muscles are the buccinator, upper incisive and nasal muscles. In the mandible, the muscles are the buccinator, lower incisive, mentalis, mylohyoid, geniohyoid and genioglossus muscles. The atrophy may pass below the line of attachment of one or more of these muscles, in which case the muscle fibers lose their direct attachment to the bone and gain an indirect fibrous attachment through the remnants of the periosteum (191).

The mandibular ridge resorbs approximately four times more rapidly than the maxillary ridge (12). The quantity and rate of resorption of alveolar bone not only differ between maxillary and mandibular bone, but also varies with respect to the age, nutritional status and sex of the patient. The original shape, size, and location of the alveolar process are all important factors (49).

In some situations, reduction of residual ridge (RRR) leaves flabby mucoperiosteum, while in others there appears to be well-attached mucoperiosteum with no redundant tissue over the resorbed ridge. Similarly, there may or may not be evidence of inflammation in areas of RRR (9, 10, 99, 100, 101). During the remodeling process, new bone is laid down internally while resorption occurs externally. However, this does not

always work with equal success and in many patients the residual ridge crest has no cortical layer (10, 43).

Atwood (11) termed the atrophy of the residual alveolar ridge as reduction of residual ridge (RRR). He described the morphological changes of RRR in which pre-extraction form is considered (order I), sharp edges remaining after extraction (order II) are rounded off by external resorption leaving a high well-rounded ridge (order III). As resorption continues from the labial and lingual aspects, the ridge becomes increasingly narrow, ultimately becoming knife-edged (order IV). As the process continues further, the ridge becomes shorter and eventually disappears, leaving a low, well-rounded or flat ridge (order V). This, too, resorbs leaving a dwarfed ridge (order VI).

The RRR includes both cortical and cancellous bone, no matter how well bone is calcified (11). Maintenance of alveolar bone is thought to be dependent on stimulation by the periodontal ligament and the presence of teeth. Following loss of teeth, the absence of stimulation to alveolar cancellous bone and overstimulation from denture pressure produce varying degrees of resorption until basilar cortical plates are continuous and less dense alveolar bone is completely resorbed (12). A random arrangement of the trabecular pattern of bone following extractions is thought to be less resistant to prosthetic masticatory forces (144). Forms such as knife edge appearance, undercuts, concave ridge form and complete loss of the ridge which results in a pencil-thin mandible may occur (114). When found in the mandible is usually referred to as atrophied mandible.

The reduction of residual ridges is chronic, progressive, irreversible and cumulative. The reduction usually proceeds slowly over a long period

of time. The annual increments of bone loss have a cumulative effect, leaving less and less residual ridge (11).

The changes in bone morphology following loss of teeth is better termed "bone remodeling" instead of the term bone resorption, which only is a part of the remodeling process that leads to the development of the edentulous ridge. Ridge remodeling is also a better term than ridge atrophy because the latter term implies a passive process (68).

Bone remodeling involves three steps: activation, resorption and formation, all of which are constantly occurring with varying rates, depending upon the specific location, age, metabolic activity and the local stress on the area. The edentulous jaws present challenges due to the characteristic patterns of bone loss without the repetitive stimuli of loading stresses (177).

Alveolar bone loss is considered cumulative and irreversible since it cannot spontaneously regenerate (132). The resorption of the ridge is initially rapid for the first six months (11) or the first two years (177) or within the first few years (42). Thereafter the resorption proceeds at a slower pace. Nevertheless, it continues even after twenty-five years (207). The alveolar bone remodeling differs from one individual to another. It also varies at different sites and at different times (132) and it may or may not be uniform along the entire length of the edentulous ridge (177).

The mechanism of the reduction of the mandible is showed by a modified version of the principle of the "V" seen in long bone. The residual ridge show external resorption accompanied by endosteal deposition - this can be called the principle of the inverted "V" (11).

Moses (138) classified the shape of alveolar ridges and associated a degree of retention with each. Class 1A, inverted U-shaped ridge; Class 1B, flat inverted U-shaped ridge; Class 1C, U-shaped; Class 2, inverted V-shaped ridge; Class 3A, parallel-walled thin ridge; Class 3B parallel-walled ridge, broad crested. He stated that Class 2 ridge is the least retentive while Class 3B is the most retentive.

Patients who lack a convex ridge of adequate height and surface area generally have problems stabilizing and retaining their dentures. The shape of the ridge is often important in developing well-supported and stable dentures (138). The goal of mandibular reconstruction is to recreate, as nearly as possible, normal shape and function. The reconstruction of the mandible is considered unsatisfactory if a good esthetic result is achieved without the restoration of mastication (173).

Factors influencing edentulous bone loss (EBL) are categorized as general and local factors. The general factors include systemic bone diseases, endocrine disorders and nutritional disorders. The local factors include facial morphology, trauma and alveolectomy technique, and prosthetic care (177).

Wical et al. (241), stated that the systemic conditions are important etiologic factors of RRR and that the resistance of bone to mechanical stresses depends on its physiologic state. They found positive correlation among low calcium intake, calcium/phosphorous imbalance, and severe ridge resorption.

Atwood (9, 11, 12) described the RRR as a multifactorial disease and that the rate of RRR depends not on one single factor but on the concurrence of two or more factors which may be called cofactors. He

divided these factors into four categories. The first are anatomic factors, e.g. size, and shape of the ridge, the type of bone and the type of mucoperiosteum. The second are metabolic or biological factors, e.g. age, sex, hormonal balance, osteoporosis. The third are functional factors, the frequency, direction and amount of force applied to the ridge. The fourth are prosthetic factors, e.g. type of denture base, form and type of teeth, and interocclusal distance. Also, since the functional factors must function through prosthetic factors, they may be grouped together as mechanical factors. It may be that when many anatomic, biologic and mechanical factors coexist, the rate of RRR will be high. Whereas, if certain cofactors are absent, even if some cofactors are present to a large degree, the rate of RRR may be little or none.

Mercier et al. (133) have evaluated factors contributing to alveolar ridge atrophy. They stated that the atrophy of the alveolar ridge is a multicausal disease. Systemic factors (e.g. diet) only compound local factors (e.g. early tooth loss, long-term and continuous denture wear). They also found no relationship between bone density and the severity of atrophy. They further stated that ideal bone augmentation material should be able to prevent further atrophy and should be non-resorbable.

2. History and Background of Atrophic Ridge Management

Management of residual alveolar ridges depend on several factors, which include the height and contour of the remaining ridge, adequacy of fixed soft-tissue base, sulcus depth and the potential of the atrophied mandible to fracture (114).

Generally, there are three different approaches for treatment of resorbed alveolar ridges which include soft tissue augmentation,

subperiosteal implant dentures, and hard tissue augmentation. In neither the soft tissue augmentation (in form of vestibuloplasty), nor the implant denture procedure is the ridge restored. These procedures are thought to permit or enhance further ridge resorption (217).

Soft tissue augmentation in form of vestibuloplasty, such as the buccal and labial sulcus extension, as well as lowering of the floor of the mouth, are helpful only if there is adequate alveolar ridge height and convex ridge form. Complete resorption of the alveolar bone to the level of the dense basilar bone would contraindicate soft-tissue vestibuloplasty and necessitate hard tissue augmentation (114).

Kruger (120) stated that even if it was feasible to reposition the structures including muscles to the inferior border of the mandible, there would still be no significant advantage in sulcus depth if the bone is too small. Moreover, such repositioning is limited by natural structures such as the mental foramens and the base of the malar process.

Maggiore (76) in 1809, inserted a lead covered platinum root structure to replace a missing tooth. Greenfield (76) in 1913, used a cylinder of iridioplatinum as an artificial root to which a single tooth crown was attached. Goldberg et al. (74) in 1949, reported the use of a metallic implant for stabilization of a full denture.

Ashman et al. (3), stated that the subperiosteal implant for extremely atrophied mandible has proven to be an excellent modality in the hands of some practitioners and many successes of over twenty years duration have been documented. The main drawbacks of the procedure seem to be: early failures due to placement of the subperiosteal implants directly on the cancellous bone instead of hard cortical bone (setting), the severity of

the surgical two-stage procedure which is sometimes difficult to perform on compromised patients, and the potential of bone infection due to communication between the implant and the oral cavity.

Kent et al. (114), evaluated permucosal implants including transosseous, swiss screw, subperiosteal ramus frame and two phase osteointegrated implants. Many patients are not candidates for permucosal implant devices because of expense, lack of bone height, and concerns about failure of these devices.

The hard tissue augmentation of the residual ridge is considered more physiologic since the ridge is restored to its original height without introducing undercuts and without communications between the oral cavity and the underlying bone. In addition, sometimes the ridge is so small that the remaining ridge is not suitable for the use of vestibuloplasty or subperiosteal implants. Also, in hard tissue augmentation, conventional methods of denture construction are used so there is no need for special training of the prosthodontist, the general dentist and the laboratory technician (217). Hard tissue augmentation is the only available method for the restoration of the alveolar bone that was resorbed to the level of the dense basilar bone (114).

Baker (15) stated the indications of augmentation of alveolar ridge as follows: restoration of bulk and strength to an excessively weakened mandible, inability to provide a stable functioning prosthesis by other means, advanced atrophy. Occasionally, short-span defects will require augmentation to stabilize flexion and torsion of mandible in function. In addition, in cases where buccal vestibular tissues and those of the floor of the mouth are at a significantly higher level than the residual ridge

and when atrophy has exposed the mandibular neurovascular bundle, patients are unable to wear a denture comfortably. The quality and vascularity of overlying soft tissue has an important role on the outcome of augmentation. Although bony augmentation was performed successfully in the presence of extensively scarred oral tissues, the incidence of complications such as wound dehiscence and partial sequestration of the graft has been higher than in patients with uncompromized soft tissues.

Sears (188) stated that augmentation grafting can be used for creating a ridge relationship in which the maxillary and mandibular ridges are in vertical alignment as well as parallel in a horizontal plane. This not only enhances stability of the denture but also minimizes trauma on the grafted ridges. Selection of a corrective procedure should not be determined by any specific ridge height measurement but rather by the degree and type of anatomic deficiency (114). The three requirements for augmentation are re-establishment of ridge height and width, strength of the jaw and morphology.

3. Hard Tissue Augmentation

a. Background

Materials used for hard tissue augmentation are broadly divided into biologic and alloplastic materials. The biologic materials may be an implant of autogenous or allogeneous cortical bone, cartilage, cancellous bone and marrow, or a combination of all these (217, 15). The alloplastic materials are obtained from outside the human body and are broadly classified into three categories which include metals, medical polymers and ceramics (217).

The ideal material for ridge augmentation should be non-antigenic, non-toxic, non-carcinogenic, available in unlimited quantity and easily fabricated and shaped (87). Also, it should be easily handled at insertion, strong, resilient, not cause resorption of underlying bone, allow normal vascularity of overlying mucosa subjected to forces transmitted from dentures, allow attachment of surrounding tissues, be readily sterilized, inexpensive, and replacable with only minor surgical procedures, preferably with use of local anesthetics (217). In addition, it should be porous to incorporate bone ingrowth with subsequent formation of interlocking bonds with surrounding bone that serve to stabilize the implant (194). The ideal material for ridge augmentation has not been found. Advantages can occur from the use of porous materials which are biomechanically compatible with bone (194). A number of studies employing porous ceramics, metals and polymers have demonstrated that bone will form in porous materials that are biocompatible and have a minimum pore size of 100 microns (115).

The modulus of elasticity of the material should be close enough to that of bone, so that stress concentrations in bone can be prevented and stress on the ingrown bone can be minimized, while interface fit of the implant at the time of insertion can be achieved (194). Studies suggest that the shear and tensile strength of the porous materials should be high enough to provide for sufficient strength of the porous material-bone composite interface (195). Also, the modulus and creep resistance should be high enough so that loads applied during placement and function of the prosthesis do not distort the pore structure or cause excessive motion, as might be the case with the lower modulus polymers (193).

b. Biological Materials

1). Bone

The main impetus to the employment of grafting was given by John Hunter (95) (1728-1793). In 1875, Nussbau (147) made one of the early autogenous bone transplants in which he rotated a fragment still attached to the lower end so as to bridge a defect in the ulna. However, the first homogenous bone transplant was reported by Macewen (39) in 1878. In 1889, the first heterogenous bone transplants was reported by Senn (189), in which a decalcified ox bone was transplanted for repairing bony defects in the human calvarium. This was followed by Miller (135) in 1890, who used ox bone chips in a patient with a cystic lesion of the upper tibia.

There have been extensive transplantations of autogenous, homogenous and heterogenous bone in humans in various forms. Clementschitsch, in 1953, (47) was the first to describe augmentation of atrophic mandibular ridge by autogenous bone grafts.

Thoma (213), Gerry (71) and Lane (124) had reported the use of iliac crest bone as a block graft for ridge augmentation. Reitman et al. (174), transplanted iliac crest bone to the inferior border of the mandible for augmentation of atrophic mandible. They found clinical and radiographic evidence of viability and successful attachment of the bone graft, three months postoperatively.

Stoelinga et al. (201) used interpositional bone grafts from iliac crest for augmentation of atrophic mandibles. Vestibuloplasty was needed in more than half of the patients. A 10 to 27% loss of height occurred between 3 and 12 months postoperatively.

Egbert et al. (55) augmented atrophic mandibles by using a three-piece osteotomy procedure and interpositional bone grafts from iliac crest. They showed a reduced rate of bone resorption in the posterior regions and a reduced incidence of sensory nerve disturbances, in comparison with previously used techniques. These results are very similar to those obtained when the posterior portion of alveolar ridge was built up with a composite of hydroxylapatite and autogenous bone.

Terry et al. (211) augmented maxilla by using a contoured rib which was grooved on the medial aspect to allow bending and was supplemented with cortical chips and cancellous bone marrow. The same graft materials were used by Davis et al. (52, 53) for augmentation of atrophic mandibles. When they evaluated the results after 3 to 6 years, they stated that the modality falls short of the ideal aid to the patients. Baker et al. (16) used autogenous onlay rib grafts for augmentation of residual ridge. Farrell et al. (61) augmented atrophic maxillae by a one stage technique of autogenous bone grafting and submucosal vestibuloplasty. Sanders et al. (185) augmented atrophic mandibles by using rib grafting to the inferior border of the mandible so that the graft did not bear the direct pressure of the prosthesis. Boyne et al. (32) restored atrophic residual ridges by transposition of the inferior border of the mandible to the alveolar bone crest and the restoration of the donor site by placement of a metallic mesh implant lined with a cellulose acetate filter and filled with hemopoetic marrow. They found new bone formation at the donor site. Clinically, healing was excellent and only 2 of 12 dogs showed dehiscence. Biopsy specimens 18 weeks after surgery showed evidence of advanced recontouring and internal remodeling of the alveolar ridge grafts. The reactive bone

formation uniting the occlusal graft to alveolar ridge appeared more mature and lamellated.

Anderson (2) and Hey (88) found that ground cortical bone undergoes resorption. Zeiss (247) found that large pieces of cortical bone revascularized poorly. Fonseca et al (67) studied revascularization and healing of two sizes of onlay particulate autogenous bone grafts in primates. They found that the small particle graft was quicker to revascularize, showed more osteoclastic activity and therefore resorbed much more quickly and completely than did the large particle graft. Thus, the resultant net gain in alveolar ridge contour was less with small particle grafts. Jones et al. (102), compared autologous marrow grafts with surface decalcified allogenic grafts, and surface decalcified allogenic grafts with autologous marrow fragments. Findings indicate that mandibular bone grafts composed of a combination of surface decalcified allogenic bone and autologous marrow may have advantages over grafts composed only of autogenous marrow fragments.

Burwell (38) found that cancellous bone revascularized quicker than cortical bone and united with underlying bone in a shorter time. It is not as sensitive to infection as cortical bone and healing occurs over small exposed areas with minimal bone loss. It does tend to resorb quickly with or without the load of a denture.

Connole (48) and Marble (130) successfully used metal crib-supported cancellous grafts in discontinuity defects.

Blackstone et al. (25) reported the use of homogenous freeze-dried bone to restore the contour of the alveolar ridge in dogs. They found that osteogenesis did occur and that the grafts were replaced by living bone.

Boyne et al. (31) used freeze-dried bone with soft tissue ridge extension for augmentation of alveolar ridge.

Maletta et al. (129) compared the healing and revascularization of onlay autologous and lyophilized allogenic rib grafts to the edentulous maxilla in primates. They found that both have minimal osteogenic potential and healing was similar, but resorption of allografts occurred about three months later than that of the autografts.

Kraut (119) augmented atrophic mandibles with a composite graft system consisting of allogenic freeze dried rib, autogenous cancellous bone, marrow, and hydroxylapatite. Patients tolerated the surgery well and showed marked improvement in dental function, with maintenance of 78% of the augmented height one year later and 67% at two years. Two-thirds of the patients underwent split-thickness skin-graft vestibuloplasties.

Kaban et al. (104) found that the visor osteotomy for augmentation of atrophic ridge did not add mass to already weak atrophic mandibles.

Barth (18), in 1893, described the histologic sequence of cranial restoration with autogenous bone grafts. He found no difference in healing between fresh and dead calvarial discs placed into defects in dogs skulls. He therefore concluded that a bone graft acted as a positive scaffolding through which host bone grew. He called this process "Schleichender ersatz". Later, this poetic phrase was literally translated as "creeping substitution". Axhausen (13) extended this idiom to describe the process of resorption of a graft that occurs prior to the laying down of new bone.

Wang et al. (240), in a follow-up of ridge augmentation with iliac crest or rib for periods of 9 months to 3 1/2 years, found almost continual resorption of bone grafts occurred after surgery. Also, some were followed

with vestibuloplasty and some had dentures made. In two cases the bone grafts seemed to stabilize after a period of time with no further evidence of resorption.

Fazili et al. (62), in a follow-up of 39 months after reconstruction of the alveolar process with iliac crest, found that in all cases a second operation of vestibuloplasty and a floor-of-mouth-plasty was done. Almost complete resorption of the bone grafts were observed and only 1/3 of patients were satisfied and 2/3 had problems like mental nerve disturbance or pain at donor and graft sites. Kaban et al. (104) stated that the use of autogenous rib or iliac crest grafts involved a harvesting operation accompanied by increased operating time, blood loss and potential morbidity in an elderly, often compromised patient.

Baker (15) summarized complications of augmentation rib grafting as follows: malposition of the graft, wound dehiscence, infection, sequestration of graft fragments, and donor site complications. Baker et al. (16) evaluated long term results of alveolar ridge augmentation for periods of 4 to 10 years using autogenous onlay rib grafts. All patients required soft tissue surgery. However, despite the degree of bone change and remodeling which occurred early in the clinical course, the patients retained denture function with long-term stability.

Boyne (31) evaluated the use of freeze-dried bone with soft tissue ridge extension for augmentation of alveolar ridges. Clinically and radiographically, the grafts tended to become an integral part of the restored alveolar ridge. Some of the implants were lost early, some showed warpage or curling early and some patients had paresthesia.

Kelly et al. (108) found that the complications involved when using freeze dried allogenic bone included infection, dehiscence and the need for vestibuloplasty. However, it has the advantage of avoiding a harvesting operation.

Koamen et al. (117) reported follow-up for patients who had augmentation of atrophic mandible by interposed bone grafts. They found that the rapid postoperatively reduction in height appeared to cease after 6 months. The results were not satisfactory in all respects. However, this method has more to offer from a prosthetic point of view than the subperiosteal graft techniques.

2). Cartilage

Konig (116), in 1896, was possibly the first to use fresh cartilage transplants in humans. However, Steinhouser et al., European surgeons, were among the first to use autogenous and homogenous cartilage. Kruger (121), in his survey of the literature, credited Verlotsky and Brochman as the first to use cartilage grafts for alveolar ridge augmentation.

Blackstone et al. (25) used freeze dried homogenous cartilage for augmentation of alveolar ridge in dogs. They found homogenous cartilage was a more satisfactory tissue for grafting than bone. Complete osteogenesis of cartilage occurred after a grafting procedure, closely approximating the healing time of an autogenous bone graft.

Lye (128) histologically evaluated homogenous cartilage implants used in preprosthetic surgery and reported that the healthy state of surrounding soft tissues and the absence of inflammatory cell infiltration suggested that cartilage homografts are well tolerated by the host. The grafts remained viable and formed an integral part of the ridge. Resorption was

minimal and attachment to the basal bone seemed to be by fibrous as well as by bony union. The homograft differed little from autograft in that chondroblasts still remained viable. The graft was easy to trim and also stored easily.

In summary, some of the biologic materials that have been used for alveolar ridge augmentation are iliac crest, rib, freeze-dried allogenic bone and cartilage, composite allogenic banked bone, autogenous fresh cancellous marrow grafts, surface decalcified freeze-dried allogenic bone, and autogenous cartilages (122).

Evaluating the biologic materials, it was found they sometimes require special casting or fabrication of trays with additional cost and skilled personnel (217).

Autogenous tissues require a harvesting operation with the associated morbidity and subsequent resorption of at least some of the implanted material (217). Also, Kruger (121) concluded that the use of autogenous tissues in elderly patients with cardiac and other medical problems is impractical due to the hazards of excessive operations.

Non-autogenous materials requires special processing to reduce the antigenicity that affect survival of the graft. Allogenic bone (frozen or freeze-dried) and demineralized bone eliminates the problem of donor-site complications, but sometimes infection from dehiscence may occur. Also, multiple relines for the dentures and varying degree of resorption may occur (108).

Cartilage undergoes little remodeling or resorption. It rarely undergoes true union to underlying bone, and it is mostly held in place by a fibrous membrane. In addition, it has poor resistance to infection due

to lack of vascularity (25, 128). Complications occurs such as infection, dehiscence and paresthesia. Also, vestibuloplasty are often required. The difference in the rate of resorption of cartilage and basal bone may cause the edges of the graft to perforate through the mucosa if they are prominent (128).

3). Demineralized bone

Senn (189), in 1889, reported the efficacy of using antiseptic decalcified ox-tibia for repairing bony defects in the calvarium.

Ray (161) compared the rate of healing of a trephine defect after implantation of allogenic frozen intact bone, deproteinized bone and bone decalcified with EDTA for 12 days. He reported that demineralized bone produced complete bridging in 41.6% of the defects, bridging of two-thirds in 16.6% of the defects, and bridging of only one third of the defect in 33.3% of the cases. He concluded that demineralized allogenic bone was the best substitute for autogenous bone grafting.

Van DE Putte et al. (237) found that cortical bone matrix decalcified in HCl or EDTA or formic-citric acids provided the local conditions for histotypic and organotypic formation of new bone. Undecalcified or recalcified matrix was resorbed more slowly and produced less new bone than decalcified matrix. Also, they found that bone matrix decalcified in nitric acid did not induce bone formation but disintegrated in the extracellular fluid and incited a deleterious inflammatory reaction. Preparations of a complex, prepared from decalcified matrix and chondroitin-sulfates A and C, did not enhance osteogenesis. Differentiation of the osteoprogenitor cells from stem cells occurred in the decalcified matrix. The stem or pluripotent young connective tissue

cells associated with new capillary sprouts and their progeny produced an induction system for osteogenesis. It appears that the process is not metaplasia of previously formed cell types, but is through a sequence of cell divisions and requires new proliferation, modulation and differentiation.

Sharrad (190) used decalcified bone grafts in three scoliotic children to effect spinal fusion. The long term evaluation of the repair process was excellent.

In 1965, Urist (223), reported the bone induction principle. Bone demineralized with 0.6N HCl produced more positive results compared to bone decalcified with EDTA. He also demonstrated the sequence of events leading to bone induction and that the bone induction principle was not freely diffusible and probably moves for short distances through the ground substance along or between cell membranes. In addition, he demonstrated the importance of the bone powder shape and size on bone induction. He reported that the use of cube shaped particles (1mm^3) coincided with increased bone induction and that matrix particles reduced to a size smaller than 0.1 to 0.3 cubic millimeters yielded smaller amounts of new bone with greater amounts of cartilage produced especially within old marrow vascular channels with smooth walls and blind ends. Also, cartilage was dominant in small spaces between opposing surfaces of small particles. He also demonstrated that bone matrix particles measuring 250 to 420 micrometers in diameter inhibit cartilage and bone induction. Reddi et al. (165) also demonstrated the importance of geometry, surface characteristics of demineralized matrix and the site of implantation for induction of new bone. They (164) also demonstrated that coarse particles (420-850

micrometers) were more inductive than fine particles (44-74 micrometers). In another study, Reddi et al. (167) favored the use of particles in the range of 72-450 micrometers. Urist (224) demonstrated that 1mm^3 particles were optimal. The discrepancy between Urist and Reddi may lie in their source of bone and its subsequent treatment. Kaban et al. (103) found that the smaller the particle size, the greater the inductive capacity of demineralized bone powder. Therefore, they favored the use of particles ranging from 72-250 micrometers.

Glowacki et al. (72) found that osteogenesis induced by equal masses of demineralized bone powder (DBP) of various particle sizes (75, 75-250, 25-450, >450 microns) revealed that the smaller particles induced more bone per field than did the large particles.

Urist (224) demonstrated that there was little uptake of calcium or phosphate by demineralized bone particles until the onset of bone induction. He also demonstrated that freezing and thawing destroyed bone induction completely and the highest percentage of positive results was obtained by freezing at -70°C in liquid nitrogen followed by lyophilization. Exposures to temperature up to 50°C and lyophilization promoted bone induction. However, a decline in bone induction resulted after exposure of the matrix to higher temperatures where bone induction was completely abolished.

In addition, he demonstrated that allogenic bone matrix could be stored for up to 3 months in a sterile, non-lyophilized state in sealed containers at room temperature without losing the bone induction property. The possible length of time for storage in a lyophilized state without

deterioration has not been determined. However samples fixed in alcohol and stored for as long as 9 months still produced positive results.

Narang (143) demonstrated that there is an initial decrease in calcium concentration in bone grafts for up to 4 weeks following transplantation. Since decalcification of the bone graft could be accomplished in vitro more rapidly than in vivo, he recommended the use of demineralized bone.

Urist (224) demonstrated that doses greater than 2 million rads of radioactive cobalt inhibit bone induction.

Urist (224) found that the bone induction was inhibited by actinomycin-D, while puromycin, a known protein synthesis inhibitor, did not have the same effect. Parenteral injection of oxytetracyclin in doses of 100 mg/kg and penicillin in doses of 90 mg/kg did not inhibit bone induction. He also found that the time required for transfer of the bone induction principle from the matrix to a competent cell takes less than 3 days. In addition, he found that surface decalcification of bone for 1-2 hours in 0.6 N HCl removes 9-10% of its mineral content and resulted in bone induction which is superior to totally decalcified bone treated with 0.6N HCl for 1 week.

Tuli et al. (220) reported that surface decalcified bone (4-6 hours) produced complete healing of a full osseous ulnar defect in 97.2% of the experimental animals, while completely decalcified (48 hours) allogenic bone produced a 81% success rate. They proposed that the success with the surface decalcified bone was due to its surface osteoinductivity and its superior mechanical stability when compared to completely decalcified bone.

Urist (225) used surface decalcified allogenic bone in humans to repair large bony defects and demonstrate the effectiveness of the bone

induction system. Urist et al. (228) described the sequence of events after implantation of 80 samples of demineralized cortical bone in the anterior abdominal wall of young rats. First, between 0-5 days, ameboid mesenchymal cells migrated from recipient muscle into the old marrow vascular channels of the old matrix or formed an envelope of connective tissue around the implant. These wandering histocytes, become fixed mesenchymal cells and began to proliferate in the interior of the implant. Second, between 5-10 days, some cells may fuse to form multinucleated giant cells and some differentiate into chondroblasts. The multinucleated giant cells were 3 to 10 times larger than the typical osteoclasts and were termed matrixclasts because of their association with nonvital matrix rather than with living bone. Thirdly, in 10 days, the matrixclasts had 50-500 nuclei and were large enough to fill an old vascular channel (35-3500 micrometers). The ratio of multinucleated cells to mononucleated cells then became 10:1. Fourth, in 15 days, woven bone was deposited and large matrixclasts were located mainly in newer, deeper areas of invasion. The other matrix clast that appeared initially became progressively smaller in size (100-500 micrometers). The ratio of multinucleated cells to monocleated cells was 1:10. Finally, from 20-30 days, woven bone started remodeling with the formation of a central pool of bone marrow.

Urist (223) demonstrated that wandering histocytes, foreign body giant cells, and inflammatory connective tissue cells are stimulated by degradation products of dead matrix to grow in and repopulate the area of an implant of decalcified bone. Histocytes are more numerous than any other cell formed and may transfer collagenolytic activity to the substrate to cause dissolution of the matrix. The process is followed immediately by

new bone formation by autoinduction in which both the inductor cells and the induced cells are derived from ingrowing cells of the host bed. The inductor cell is a descendant of a wandering histocyte; the induced cell is a fixed histocyte or perivascular young connective tissue cell. Differentiation of the osteoprogenitor cell is elicited by local alterations in cell metabolic cycles that are as yet uncharacterized.

Reddi et al. (168) found that the sequence of events during matrix - induced chondrogenesis, chondrolysis and osteogenesis are analogous to those occurring during embryonic development. In addition, the early events in biogenesis of bone marrow and the morphology of haematopoietic elements was found to be similar to those of developing medullary bone marrow.

Reddi et al. (166, 168) monitored the process of bone induction in the rat using tritiated thymidine, alkaline phosphatase, ^{59}Fe and ^{45}Ca . They found that by the third day following implantation, thymidine incorporation was increased and that it coincided with the proliferation of invading fibroblasts. There was a second peak of thymidine incorporation before osteogenesis and vascular invasion and a third peak during haematopoiesis occurring around day 18-21. Alkaline phosphatase activity increased prior to mineralization on day nine. Also on day nine, ^{45}Ca incorporation increased along with vascular invasion, and peaked on day 12 during mineralization. On day 12, ^{59}Fe increased when the first haematopoiesis colonies were observed, and peaked between day 23-28 when complete haematopoiesis of newly formed ossicles occurred. In another study, Reddi et al. (169) reported an excellent correlation between increased alkaline phosphatase activity and calcification as indicated by ^{45}Ca incorporation in the mineralization phase. He pointed out that the cascade of events was

similar to those observed during fracture healing in long bones. They suggested that the collagenous matrix may play a role in specifying the morphogenetic information locally at the site of fracture.

Urist et al. (226) found that DBM did not induce bone formation in liver, spleen or kidney parenchyma. However, when they implanted DBM for 5 to 21 days in the abdominal wall and subsequently reimplanted the bone matrix in one of the aforementioned organs, bone was produced. They concluded that differentiation of bone cells postnatally occurred but from a competent mesenchymal cell population and not from blood-born cells or vascular tissues. These cells were probably induced by a substratum of extracellular substances found in bone matrix. They suggested that some mesenchymal cells should be considered differentiated, or at least committed to become osteoblasts since they displayed its strictly prescribed program for further development following transplantation.

Chalmers (44) suggested that for bone induction to occur in extraskeletal sites, three conditions must be met: an osteoprogenitor cell, an inducing material and a suitable environment. While muscle and fascia provided a suitable environment for bone induction, the liver, kidney and spleen were considered inappropriate.

Mulliken et al. (139) implanted demineralized bone prepared according to Reddi's technique and compared it to undemineralized bone implants used for the repair of calvarial defects in rats. They found that the former produced better healing, presumably because it uncovered the bone morphogenetic protein of the calcified matrix. They also concluded that induced osteogenesis is not species-specific since they had similar results when they used human DBP to bridge rat calvarial defects. These results

were confirmed by Kaban et al. (103), who found that demineralized bone produced better healing compared to undemineralized bone in an experimentally created full-thickness mandibular defect. The mineralized bone powder was completely resorbed by 3 weeks, while the demineralized powder induced new bone formation by endochondral ossifications without being appreciably resorbed prior to bone induction.

Lindholm (127) demonstrated that allogenic, demineralized bone produced more new bone when combined with bone marrow diluted in culture media than when used by itself. However, the addition of bone marrow to allogenic demineralized bone is advantageous only in the first phase of bone formation, while later stages of implant formation seemed to be unaffected (245).

Osbon et al. (151) successfully reconstructed maxillary and mandibular defects in humans using composite grafts consisting of allogenic cancellous surface decalcified bone and autogenous particulate cancellous bone and marrow. They reported the following advantages of demineralized bone; the reduced amount of autologous bone required, ease of adaptability of the material at the time of surgery, and the high biocompatibility and biodegradability.

Urist et al. (227) referred to the substance responsible for the bone induction as bone morphogenetic protein (BMP). They demonstrated the importance of temperature, time and concentration of exposure to decalcifying solution, in order to prevent denaturation of the cross-linked structure of the bone matrix. They also demonstrated the importance of devoting sufficient time for bone demineralization in order to acid gelatinize the bone matrix. Also, Urist et al. (228) suggested that the

BMP is protected from thermal denaturation by the mineral. Bone minerals in vivo insulate the BMP and prevent the transmission of the morphogenetic property from bone matrix to mesenchymal cells. Urist et al. (230) stated that the bone induction capacity of BMP changed according to the species of the experimental animals in the following order: rabbit, guinea pigs, mouse, with rabbit being the most favorable. Also BMP induced bone formation in the rat.

Urist et al. (233) noted that BMP is transferred from bone matrix to a responsive mesenchymal-like population of cells within 24 hours after implantation. The BMP activity was estimated by the increase of the following: hyaluronate within 24 hours, hyaluronidase within 48 hours, ^{35}S uptake within 7 days, increase in alkaline phosphatase activity within 10 days and ^{45}Ca uptake by mineralization tissue within 10-14 days.

Urist, et al. (234) demonstrated that BMP is a glycoprotein and that mesenchymal response to it is growth hormone-dependent. Bone formation was partially restored when growth hormone was given to the hypophysectomized rat. This is in agreement with the work of Reddi and his group (166, 168, 169), who found that hypophysectomy delayed the formation of the ossicle and it also profoundly inhibits haematopoiesis.

Urist (235), in a review article, suggested that bone-derived growth factors and BMP are coeffective. Also, he indicated that bone induction starts with a morphogenetic phase followed by a cyto-differentiation phase. The former consists of mesenchymal cells disaggregation, migration and reaggregation and proliferation. He suggested that with the onset of the morphogenetic phase, a chondroosteogenetic activation starts and is controlled by BMP activity. He postulated that the binding of BMP to

membrane receptors on mesenchymal cell surfaces alter cell surface electric charges which in turn, may induce a cascade of cell-to-cell interactions, transmitting the genetic program of the induced cells to their progeny. At this point, the human skeletal growth factor (BDGF) comes into play.

Urist (235) reported that BMP-induced bone development is irreversible, while BDGF bone growth stimulation is reversible. In addition, he reported that the BMP has a molecular weight of 17.5K and is associated with variable quantities of 14K, 24K and 34K proteins. He also found that BMP yields less bone when isolated in the pure state, than when it is associated with other proteins. He suggested that presence of collagen is not required for BMP activity, which could be transferred across a distance of 450 micrometers through pores as small as 25 nanometers. In doses of up to 5 milligrams, the yield of new bone was directly proportional to the quantity of implanted BMP. This was in contrast to what he (234) previously reported, that BMP implanted alone diffuses away before inducing the competent mesenchymal cells (Urist 1982). In addition, he indicated that cortical bone contains more BMP than cancellous bone. This agrees with the work of Nade and Glowacki (1981), who demonstrated superior osteoinductive ability of cortical over cancellous bone.

Huggins (94) suggested that a solid state physicochemical alteration of cell surface is responsible for the phenotype transformation caused by DBP.

Urist et al. (232) showed that the demineralization time of 3 hours in Reddi's system produced less bone formation and more fibrous tissues. He suggested that this was due to defective demineralization. In addition, he

pointed out that the demineralization procedure and the subsequent washing with different chemicals used by Reddi, denaturated the bone matrix. He stressed again that, unlike demineralized dentin, bone matrix ground to a particle size which is less than 400 microns results in the loss of bone morphogenetic activity. He suggested that the mineral content of bone insulates BMP and prevents the transmission of the inductor from the bone matrix to the proliferating mesenchymal cells.

Reddi et al. (165) noted that cartilage persisted in the deeper regions of the transplant where oxygen tension was presumably low. According to Bassett (20), oxygen tension as low as 5% favors chondrogenesis while levels of 35% favor osteogenesis.

Reddi et al. (167) found that DBP prepared from the diaphysis of long bones was more inductive than that from flat bone. This was attributed to the marked difference in collagen fibers orientation between weight-bearing bone and flat bones.

Reddi et al. (167) noted that the transformation of fibroblasts to chondroblasts and osteoblasts was always restricted to the center of the implant and not the periphery, which indicates a difference between these two locations.

Reddi et al. (170) found Type III collagen on day 3 around invading fibroblasts, Type I collagen on day 5, Type II collagen associated with chondrogenesis, Type I collagen associated with osteoblastic activity on day 10, and Type III collagen reappearing during haemopoiesis on day 12.

Rath et al. (160) found that glucoronidase, acid phosphatase, and especially aryl sulfatase, were increased during bone remodelling. These enzymes peaked between day 12 and 16 following implantation of DBP.

Urist (235) found that the collagen of bone matrix was not essential for osteoinduction.

Sampath et al. (181) investigated the osteoinductive molecule to determine its mitogenic activity on human and rat fibroblasts as well as bovine endothelial cells. He reported that while human and rat fibroblasts responded by with a increase in proliferation of 250 and 300% respectively, the endothelial cells did not respond.

The bulk of the basic information gained from the research reviewed above was applied to solve clinical problems.

Narang et al. (142) used decalcified allogenic bone matrix for alveolar ridge augmentation in dogs. After 16 weeks, no infection was found around the wound sites. The grafts were not rejected and new bone was formed at the implantation sites and did not evoke any significant immunologic response.

Kaban et al. (104) augmented the rat mandibular ridge with demineralized bone implants in submucosal pockets on the edentulous segment of the rat mandible. These implants induced osteogenesis and the mass of induced bone and implant was united to the ridge by 2 weeks and there was little or no resorption over a 6 months follow-up period.

Mulliken et al. (140) used demineralized allogenic bone to augment, contour, fill defects or construct bone within soft tissues in humans. The implants were clinically solid after 3 months and radiographically healed by 3 to 6 months. Infection occurred in 4 of 44 patients and 4 patients showed resorption of the implant. The advantages of allogenic demineralized implants over conventional bone grafting are: avoidance of harvesting operation, ease of manipulation and potentially unlimited

material in banked form. Healing by induced osteogenesis may bypass the resorption seen with healing of mineral-containing grafts. Available autogenous bone is limited, especially in infants and young children. In some instances, the harvesting operation may be of greater magnitude than the surgical procedure for example, the closure of a bony oronasal fistula.

Induced osteogenesis with demineralized implants is different from osseous healing that occurs with conventional bone grafts. Fresh cancellous grafts are rapidly revascularized and survive to produce new bone from the transplanted living osteoblasts (20, 81, 162). The predominant mechanism of healing with fresh, preserved, cortical grafts is "creeping substitution", i.e. concomitant resorption of the bone graft and its replacement via ingrowth of vascular and osteoblastic tissue from adjacent bone (13, 155). Induced osteogenesis, in contrast, is a phenotypic change of host pluripotential cells into osteoblasts. The process is one of local cellular transformation, in contrast to osseous transplantation with living cortical or cancellous grafts (140).

Glowacki et al. (72) evaluated the fate of mineralized and demineralized osseous implants placed into cranial defects in rats. By 2 weeks, 100% of the defects that had been filled with demineralized bone powder (DBP, 75-250 microns) showed bony repair as judged by histomorphometric analysis and incorporation of ^{45}Ca . The DBP was not resorbed but rather was amalgamated within the new bone. In contrast, mineralized bone powder was completely resorbed by 3 weeks without bony repair of the cranial defect. These specimens contained large multinucleated cells and connective tissue. Implants of bone minerals were also evaluated. Bone

ash and disorganized bone powder were surrounded by multinucleated cells within 7 days and completely resorbed by 3 weeks.

Inoue et al. (97) showed that outgrowth of cells from rat muscle, dermis and subcutaneous tissue, bone marrow cells and periodontal ligament cultured in vitro with demineralized bone matrix for up to 35 days, induced chondrogenesis.

Glowacki et al. (73), used demineralized bone implants for cranio-maxillofacial reconstruction and construction in patients with congenital deformities and acquired defects. Early healing was assessed by clinical and radiographic examinations and sometimes by biopsy. They concluded that the clinical advantages of DBP are rapid union, healing of large defects, avoidance of harvesting procedures and the potentially unlimited supply of banked material.

Sampath et al., (184) implanted DB matrix subcutaneously into rats. This induced cartilage and bone formation in vivo. When mice skeletal muscle was cultured on hemicylinders of demineralized bone in vitro, mesenchymal cells are transformed into chondrocytes.

Blumenthal et al., (26) tested a combined collagen gel-autolysed antigen-extracted allogenic bone implant for its effect on growing new attachment in surgically-created defects in dogs. As controls, bone implants alone, nonimplanted, and untreated defects were evaluated. The collagen gel encouraged ingrowth of regenerative tissue fibroblasts in the early stages of wound healing, while the allogeneic bone induced new bone formation. The graft materials were bicompatible, technically manageable and clinically effective.

Mulliken (141) defined osteoinduction or bone induction as a process involving cellular change or cellular interaction. In other words, the cells are made to differentiate and do something they normally would not do. The classic material for this is either autogenous marrow, because of the capacity of marrow cells to differentiate into bone forming osteoblasts, or extracts of bone marrow or treated bone.

Syftestad et al. (203), assayed urea and guanidine extracts of demineralized beef and rabbit bone matrix both in vivo and in vitro. One month following intramuscular implantation into mouse thighs, these extracts induced ectopic cartilage and bone. Seven days following continuous in vitro exposure to the same extracts, mesenchymal cells in cultures had differentiated into greater numbers of chondrocytes than controls.

Hosny and Sharawy (92) tested the osteoinductivity of demineralized bone powder in Rhesus monkeys in subcutaneous tissues. Decalcified and undecalcified sections of the implants were studied. Large numbers of undifferentiated mesenchymal and fibroblast-like cells were observed around and within the DBP matrix particles on day 20. Cartilage formation was also evident at that time and had increased by day 40, when chondroid bone also appeared. By day 72, the implants showed mature and immature bone and bone marrow formation. Areas of DBP that were incorporated within the induced bone contained empty lacunae and stained similarly to mineralized bone.

From the above reviewed research work, the evidence for bone induction using DBP in rodents, non-human primates and humans are strong and

convincing. This encourages us to use DBP in combination with alloplastic material as a bone graft substitute.

c. Alloplastic Materials

1). Metals, Ceramics and Polymers

Although metals have been used widely as internal prostheses, their physical characteristics discouraged their use for replacement of residual ridges. Holland (89) and Thoma (214) used subperiosteal gauze made of tantalum to block undercuts of lower residual ridges. The rolled-up gauze was fixed in place subperiosteally with fine wires passing through the bone. The gauze was well tolerated and a denture was constructed 3 months postoperatively. However, in some cases dehiscence occurred.

Ceramics are generally brittle, have no ductility, low flexure strength, low impact resistance, freedom from notch sensitivity, and mechanical reliability. However, many ceramics are inert and possess interconnecting pores (217).

Bahn (14) implanted porous plaster-of-paris for augmenting edentulous ridges. Resorption was rapid with little permanent augmentation of the ridge. Although its tissue acceptance is good, its high solubility appears to limit its value as a scaffold for new bone formation.

Calcium aluminate with interconnecting pores was used for augmentation of dog alveolar ridges (218). Tissue acceptance was good. Fibrous tissue and bone grew into the implant (83).

The principle limitation of calcium phosphates are their mechanical properties. Like most ceramics calcium phosphates are brittle, have low impact resistance and a relatively low tensile strength. However, there is a lack of local or systemic toxicity, little or no inflammatory or foreign

body response, an absence of intervening fibrous tissue between implant and bone and its ability to become directly bonded to bone by what may be natural bone cementing mechanisms. The solid materials are stronger than bone, while porous ones have similar properties to cancellous bone (114).

Tricalcium phosphate (TCP) was used either for replacement or to supplement bone grafting (63) where bony regeneration was expected and when a temporary substitute of bone was necessary (34). The process of bone replacement of the implant begins with an ingrowth of cellular loose connective tissue which is replaced later by dense bone. Around the periphery of this dense fibrous connective tissue, osteoid tissue becomes evident and later this mixture converts to bone which, at first, is in the form of spicules but later takes on the characteristics of lamellar bone with TCP particles seen within its lacunae. However, this replacement of TCP is slow and takes up to 18 months. When porous TCP was used in cancellous and cortical bone it was rapidly infiltrated with bone and slowly resorbed. There were no untoward tissue or systemic reactions.

Following TCP implantation in animal experiments, DeGroot (34) found that tricalcium phosphate was detected in regional lymph nodes. Krempien (1985) reported an unexplained osteoporosis in animals that received TCP implants. Fischer (34) suggested that clinical utilization of the material be discontinued until the unfavorable results of these observations are clarified. Replamineform hydroxylapatite was used subperiosteally for augmentation of alveolar ridges in dogs (156). Finn et al. (64) used interpositional grafting with autogenous bone and coralline hydroxylapatite for augmentation of alveolar ridge on dogs. They found early consolidation and remodeling of the grafted bone and implant with minimal alterations of

the morphologic form and architecture of the repositioned bone. Piecuch et al. (157), indicated the use of block porous HA in cases of severe resorption of the mandible to the level of basal bone, especially when broad flat ridge contour areas are found. Grossly irregular ridge contours and knife-edge ridges are better treated with porous non-resorbable hydroxyapatite granules. Hydroxyapatite, with or without autogenous cancellous bone (112), was used for augmentation of alveolar bone where a permanent augmentation was required and where bone regeneration would not occur on its own.

Beirne et al. (23) evaluated tissue response to dense HA. They found minimal inflammation but the implant had not induced new bone formation and was instead surrounded by a fibrous connective tissue scar and occasionally epithelial macrophages and multinucleated giant cells immediately adjacent to the implant.

Gumaer et al. (78) studied tissue response to dense HA after 6 to 8 years in dogs femurs. They found that the implants were totally encased in dense mature bone and in some cases at the periosteal surface showed interdigitation of connective tissue stalks with large multinucleated cells at the interface with the implant.

Hydroxylapatite (HA) used for reconstruction of residual alveolar ridges, with or without autogenous cancellous bone, has been evaluated over a six year period. It was found that the complications that arise involve incision dehiscence or erosion of the mucosa from the use of splints, parasthesia and hyperesthesia of mental nerve, migration and displacement of particles, nonattachment of HA to bone, overfill, and hematoma formation (113). In another study, they found that problems facing dentists wishing

to construct complete dentures following use of HA, regardless of the technique used and in the presence or absence of a stent, included diffusion of HA into adjacent area, irregular distribution and extrusion of the material, incorrect position, excessive increase in alveolar ridge height, paresthesia, and settling, migration and resorption (54).

Kent et al. (112) evaluated dense HA used with or without autogenous cancellous bone for 4 years. They found improved ridge height and width. Dentures were constructed 3 to 6 months postoperatively and vestibuloplasty was done in some patients. Complications included anesthesia of the lower lip, pain, inflammation, particle migration, ulceration and dehiscence. Some patients underwent fewer subsequent denture relines.

Beirne et al. (23) concluded from their studies on augmentation of alveolar ridge of mandible with hydroxyapatite that HA was biocompatible, caused minimal inflammatory response and could increase denture retention. However, a large number of patients developed lip paresthesia and showed migration and displacement of HA.

Lew et al. (126) used autogenous rib graft with particulate HA for augmentation of atrophic mandible. They found that mandibular morphology was restored with good prosthetic function and insignificant resorption. Problems encountered were migration of HA particles and dehiscence of overlying mucosa.

Kent, et al. (114) described the important advantages of using HA which included excellent compatibility, absence of antigenic reactions, availability of the material, allow surgery under local anesthesia, low risk of infection, low risk of permanent hyperesthesia, no resorption of the material granting long-lasting results, high rate of good results and no

need of a perfect oral hygiene. He described the complications as hyperesthesia of the mental nerve, dehiscence which sometimes leads to loss of some materials and pressure necrosis.

Guerra (77) stated difficulties encountered with HA were overbulking, malplacement, paresthesia or hypersthesia, required secondary vestibuloplasty and sometimes skin grafting. Also, sometimes the mandible became wider than the maxilla. Sometimes patients need a long time for HA to stabilize and during this period they would be without their dentures.

There are many polymers used for ridge augmentation. Epstein (59) placed subperiosteal polyvinyl alcohol sponges (Ivalon) into the labial and lingual undercuts. Histologically, there was fibrosis and giant cell response but no evidence of inflammation. The material was elastic, tough and of great tensile strength.

Cranin (50) implanted polyvinyl sponge subperiosteally in the anterior maxilla to reconstruct the resorbed ridge in humans.

Gatewood (70) used silastic covered with a dacron mesh subperiosteally to augment alveolar ridge. The surrounding tissue showed normal response. Boucher (27) augmented the upper anterior region of maxilla with medical grade, liquid silicone rubber. He (28) also used a modified form of silastic for ridge extension procedures both in animals and humans.

Small et al. (192) evaluated Teflon and silastic for replacing portions of the mandible. Teflon seemed more adaptable to restoration of large mandibular resections, whereas silastic seemed better for small mandibular resections. Bone will not proliferate in either substance and when combined with bone grafts, bone was not be retained if there was

contamination or inadequate fixation. Silicone rubber is more bio-inert but did not directly attach to bone leading to slippage and extrusion.

Moore et al. (136) blocked the undercut regions by using gelatin sponge (Gelfoam) subperiosteally which created better alveolar ridges and produced more stable and comfortable denture-bearing areas.

Henefer et al. (87) inserted acrylate-amide sponge in undercuts in primates and humans. New bone which formed in the spaces of the sponge extended beyond the original contours of the labial cortical plate. No evidence of rejection or carcinogenesis of the material was noted.

Laskin (125) injected a sclerosing solution of 5% sodium morrhuate subperiosteally for augmentation of residual ridges. This treatment produced fibrosis in hypermobile edentulous ridge without a need for surgery. It also maintained alveolar height and avoided the necessity for a second vestibuloplasty.

Kent et al. (109, 110) used porous proplast, which is made of polytetrafluoroethylene and carbon fiber, in dogs and humans for ridge augmentation. It increased denture stability, reduced pressure and eliminated pain. However, large implants did not improve denture function and were more likely to develop sepsis.

Proplast showed early stability by connective tissue ingrowth, but if the tissue did not completely infiltrate the material, lead to infection of the voids (110).

Flohr (66) used acrylic resin in subperiosteal tunnels for augmentation of mandibular residual ridges. Methylmethacrylate is not completely inert and promotes excessive encapsulation with fibrous connective tissue which leads to displacement, extrusion and infection.

Ashman et al. (3) used an alloplastic material called hard tissue replacement (HTR) for augmentation of alveolar ridge. Problems encountered include postoperative swelling and ecchymosis, plaque accumulation within the pores if not primary closed, paresthesia, vestibuloplasty sometimes needed and the requirement of a special dielectric oven for fabrication.

Generally, alloplastic materials offer an advantage over the biologic materials for replacement of tissues because they are readily available in large quantity, are easily fabricated and adjusted at the time of surgery and do not require operation on the donor site (217).

2). Porous Polysulfone

The aliphatic polysulfones were originally synthesized in 1898 by Russian workers and subsequently investigated by German, Dutch and English researchers (145). In 1958, the aromatic polysulfones were synthesized. The materials were produced from the reaction of P, P' - dihalodiphenyl sulfone with sodium salt of an aromatic dithiol. Subsequently, in 1964, aromatic polysulfones containing ether links were introduced commercially by Union Carbide Plastic Company (145).

The commercial aromatic polysulfones are produced by reacting the disodium salt of bisphenol A with P,P' - dichlorodiphenylsulfone in dimethyl sulfoxide and chlorobenzene. The molecular weights range from 30,000 to 60,000 (145).

The aromatic polysulfones were introduced as molding powders and as an adhesive system (145). Blocks of polysulfone were produced by sintering particles of medical grade polysulfone (850-1180 microns in diameter) in aluminum molds at 222-246°C for 15 minutes. Molds were quenched and chips were removed, rinsed and stored in 70% ethanol at 4°C. It has a molecular

weight of 25,000 and glass transition temperature of 190°C . Its chemical composition satisfies the American Society of Testing and Materials (ASTM) (145, 194).

Polysulfone is biocompatible (195, 197) highly resistant to aqueous mineral acids, and alkalis and salt solutions (145). It has modulus of elasticity in the range of 2000 to 7000 MN/m^2 which fill the gap between the high modulus of ceramics and metals and the low modulus of polymers. This modulus can be increased to over $14,000 \text{ MN/m}^2$ by the addition of 30% by weight of carbon fiber reinforcement (194).

The modulus of elasticity of the polysulfone was low enough to allow the near normal remodeling of bone in the pores of the implant, behavior not provided by imporous ceramics and porous metals. This behavior should provide for the long-term viability of the bone-polysulfone composite interface (194). Also, this low modulus is desirable so that stress concentration produced in the surrounding bone are avoided (194). However, the modulus of elasticity and creep resistance of polysulfone is high enough to prevent distortion of the pore structure under initial placement and functional loading and also does not cause excessive motion, as might be the case of lower modulus polymers (196, 198).

It has a high enough shear strength to allow the highest interfacial shear strength possible to be developed. Polysulfone has no adverse tissue reactions. The size of the pores can be predetermined. It can be shaped as needed and the material is non-radiopaque (145, 194).

The ingrowth of bone within polysulfone proceeded at what might be considered normal rate of osseous repair, thereby suggesting that the material has sufficient interconnecting porosity (194).

In addition to its favorable mechanical properties, polysulfone has been found to have good thermal and hydrolytic stability and has satisfied the biotoxicity tests for U.S. Pharmacopeia class VI plastics (212, 194, 199).

Ballintyne et al. (17) tested the mechanical properties of polysulfone and its performance as a surface coating on orthopedic implants in the form of coated femoral prosthesis in dogs. Also, as a coated tooth roots in healed extraction sockets in Rhesus monkeys. They found that the shear strength of the polysulfone was comparable to that of trabecular bone. Bone and fibrous tissue were identified in the pores of the coated specimens. The clinical evaluation of the functioning dental implants revealed no instability and radiography and pocket depth measurements revealed no loss of bone from around the implants.

Spector et al. (194) implanted pellets of sintered polysulfone into canine femurs. Bone ingrowth into polysulfone proceeded in such a fashion as to mimic the normal repair at the site. Mechanical testing of cortical and cancellous implants revealed that the interfacial shear strength of the polysulfone bone composite was similar to that achieved using porous metals.

Spector et al. (199) investigated polysulfone-coated cobalt-chromium femoral prosthesis implanted in dogs for up to three years. Radiographic and scintigraphic features were demonstrated, bone ingrowth to some degree in 12 of 14 dogs. One of two failed implants was recovered 4 days after implantation and the second was loose due to overreaming.

Spector et al. (194) inserted 16 porous polysulfone (PPSF) coated canine femoral stems into 14 dogs. Coating was approximately 40% porous.

Bone was formed within at least 30% of the surface pores of the implants. The tissue ingrowth filling the pores included marrow and fibrous tissue. Correlated roentgenographic and histologic observations revealed a trabecular "lamina dura-like" at the coating bone interface and relatively dense trabeculae distal to the stem tip.

Behling et al. (22) studied the quantitative and qualitative tissue and cellular response to PPSF particles implanted subcutaneously in rats for 100-118 weeks. The PSF particles were sequestered within a subcutaneous fibrous capsule. The long term response was a characteristic foreign-body granuloma and consisted of a monolayer of macrophage at the surface of the implant surrounded by a zone of fibrous tissue. Also, fibroblasts and giant cells were found.

Vandersteenhaven et al. (238) investigated the subcutaneous implantation composite of demineralized allogenic bone matrix (DABM) and PPSF, and PPSF only, whole demineralized allogenic bone matrix, and particulate demineralized allogenic bone matrix in rats. Microradiographically and histologically the DABM and PPSF composite revealed chondrogenesis within the pores of the specimens at 10 days followed by the ossification and fatty marrow production at 21 and 43 days. This histologic sequence was similar to that seen with DABM controls. The PPSF did not prevent the osteoinductive process.

C. Rationale

We selected Rhesus monkeys as our animal model because they have jaw bones similar to the human from the functional and anatomical point of view. They were from 12 to 15 years of age which is comparable to humans of 45-53 years of age (149). This age group and older demonstrates an

increased incidence of edentulous jaws. We selected female monkeys because ridge resorption affects females more than male in a proportion of 4 to 1 (133). We also selected the lower jaw because resorption is four times greater in the mandible than the maxilla (133).

We selected porous material because a thoroughly porous material that would allow soft tissue and bone infiltration would be desirable (217). One of the main reasons of failure of alloplastic material is the extrusion of the implant (192) due to its failure to become structurally united with the surrounding living tissues. In addition, previous studies have demonstrated that bone ingrowth into porous materials produces an interlocking composite interface which is capable of stabilizing orthopedic and dental prosthesis (17-194).

We selected porous polysulfone (PPSF) for our experiment because of its favorable mechanical properties which includes a modulus of elasticity that fills the gap between the high-modulus of ceramics and metals and lower-modulus polymers (194). This is desirable because it is low enough so that stress concentrations produced in the surrounding bone are avoided. The material also undergoes sufficient elastic deformation to uniformly transmit some portion of the loads applied to the implant to bone spicules within the pores. The transmitted stress would effect remodeling of bone in the cortical region of the implant, as might normally occur (194). The normal remodeling of bone in the pores of the implant is not seen in porous ceramic or porous metals (194). This behavior should provide for the long-term stability of the bone-PPSF composite interface. Also, PPSF has a high enough modulus of elasticity and creep resistance to prevent distortion of the pore structure under initial placement and functional

loading. Such property help in preventing excessive motion, as might be the case with lower modulus polymers (17,149). PPSF also has a high enough shear strength to allow the highest interfacial shear strength possible to be developed without breaking or tearing. It also has no adverse tissue reactions, the size of the pores can be predetermined, the modulus of elasticity can be increased if needed, it is biomechanically compatible with bone, it can be shaped as needed and it is radiolucent thus allowing roentnographic identification of bone ingrowth. In addition to its favorable mechanical properties, PPSF has been found to have good hydrolytic stability and has satisfied the biotoxicity tests for U.S. Pharmacopoeia Class VI plastics (194).

We selected the demineralized bone powder (DBP) in our experiment because it had several advantages over conventional bone grafting, such as avoidance of a harvesting operation, ease of manipulation and potentially unlimited supply in banked form. Healing by induced osteogenesis may bypass the resorption seen with healing of mineral-containing bone (140). It was shown that DBP has osteoinductive abilities in both young and old rats (93), in dogs (142), and in Rhesus monkeys in subcutaneous tissues (92). We followed Reddi's technique (164) for obtaining DBP except for increasing the decalcification time from 3 to 18 hours. We did not use higher concentrations of acid to demineralize bone and we did not use long periods of time which might have a detrimental effect on the bone induction capacity of the bone matrix, since it might denature the protein content and therefore delay or prevent bone induction. We did not pulverize bone with a liquid nitrogen micromill which might also denature the protein.

The sacrifice time selected to be on days 42, 60 and 90 was based on the work done by Hosny and Sharawy (92) who observed undifferentiated mesenchymal cells and fibroblast-like cells and evidence of cartilage on day 20, more cartilage formation and chondroid tissue on day 40, and mature and immature bone and bone marrow formation on day 72.

D. Specific Aims

1. To extract mandibular molar teeth bilaterally in five monkeys and to wait for healing of the wound and resorption of the alveolar bone.
2. To obtain long bones from one monkey and prepare demineralized bone powder.
3. To prepare porous polysulfone implant to conform the shape of residual alveolar ridges.
4. To insert the porous polysulfone implants on one side and the porous polysulfone with DBP on the other side.
5. To sacrifice two monkeys after 42 days, two monkeys after 60 days and one monkey after 90 days by perfusion fixation.
6. To process the blocks for light microscopy using paraffin, glycol methacrylate and methyl methacrylate embedding technique.
7. To quantify bone formation using histomorphometric techniques and tetracycline label measurements.
8. To process specimens for scanning electron microscopy.

II. MATERIALS AND METHODS

A. Animals

Six adult (12-15 years of age) female Macaca fascicularis were used in this experiment. The animals were previously ovariectomized by the vendors and therefore had no ovarian cycles. One animal was sacrificed and used as a bone donor and the other five were recipients.

B. Food and Care of Animals

The monkeys were caged individually in an air-conditioned room at the MCG animal resources facility. They were fed Purina monkey chow, supplemented with fresh fruits and water was available ad libitum.

C. Materials

1. Demineralized Bone Powder

One monkey was sacrificed using pentobarbital sodium (100 mg/kg) intravenously. The diaphysis of long bones of the donor animal were dissected out and were freed of muscles and bone marrow. These bones were cut into small pieces (Fig. 1) using autopsy saw and bone cutting rangeur, washed and stirred in distilled water using a magnetic stirrer for two hours. They were then dehydrated in absolute ethanol for 90 minutes followed by 30 minutes in ethyl ether.

The bones were dried overnight under a vacuum at 37°C. The following day, the bones were ground at 20 second intervals at room temperature with a water cooled micromill (Bel Art Supplies, N.J., USA). The resultant powder was sieved to a particle size of approximately 420 micrometers. The bone powder was demineralized in 0.5 N HCl (25 meq/g) or 50 ml of acid/gm of bone powder) for 18 hours with continuous stirring. The acid was changed seven times during the process of demineralization.

At the end of demineralization, the solution was centrifuged at 3,000 rpm for ten minutes and acid was separated from the precipitate. Distilled water was added to the precipitate and stirred for two hours and the distilled water was changed three times. The solution was then centrifuged at 3,000 rpm for ten minutes and water separated from the precipitate. This was followed by dehydration in absolute ethanol for 30 minutes.

The dry, demineralized bone powder (Fig. 1) was divided into twelve portions of 100 mgs each and placed into 1cc plastic syringes. Random samples (100 mgs) of DBP was mixed with sterile water and left to settle. The resultant solution was cultured in agar plate for 48 hrs at 37°C to check for any microbial growth (Fig. 2). The other eleven samples were kept at room temperature until their use.

2. Porous Polysulfone

Blocks of PPSF implants (Fig. 3) were kindly supplied by Dr. Myron Spector, Department of Orthopedics, Emory University School of Medicine. The porosity of the polysulfone ranged from 25-45% with the darker specimens having the higher strengths and lower porosities. All specimens were fabricated from medical grade polysulfone (P-1700).

D. Procedures

1. Preparation of the Alveolar Ridge

(a) The animals were initially anesthetized by experienced animal resources personnel using a combination of Ketamine (20-25mg/kg) and acepromazine (.5-1 mg/kg) IM. These were supplemented with surital (sodium thiamylal) IV as needed. Atropine 400 mg subcutaneously, was given on the day of surgery.

(b) The animals were draped with sterile towels to expose only the field of surgery. The operator and his assistant scrubbed and dressed in standard aseptic techniques for operating rooms.

(c) The mandibular molars of the right side were infiltrated using 1.8ml of Xylocaine-epinephrine (1:100, 000).

(d) The mucoperiosteum was reflected with a periosteal elevator on both buccal and lingual surface and held back. The molar teeth of the lower jaw on the right side were extracted. The ridge was kept free of blood by use of a suction apparatus throughout the operation. By using a side-edge, bone-cutting rongeur, bone was removed from buccal and lingual cortical plates. The interseptal osseous projections were removed with an end-cutting rongeur. The buccal and lingual surfaces of the ridge were smoothed with a bone file. Any spicules of bone or tooth structure that may have dropped into the socket were removed and the wounds were then irrigated with normal saline. The flap was returned to its original position and the edges of the soft tissue was approximated. The overlapping soft tissue was trimmed with scissors and then the cut edges were approximated again. The mucoperiosteum was sutured with 3-0 vicryle (made of polyglactin and calcium stearate) resorbable sutures. Both continuous and interrupted suturing techniques were used.

(e) The same protocol was repeated for the left lower molar teeth.

(f) Pressure was applied to the wound area with ice bags for approximately one-half hour following the surgery. The animal was returned to its cage and observed until fully recovered from the anesthesia.

(g) The animals were left for healing and remodeling of the alveolar bone for periods of 5 to 8 1/2 months after extractions.

2. Preparation of Porous Polysulfone

- (a) One week before the final surgical procedure, the animal was anesthetized using the same protocol mentioned above.
- (b) An alginate impression was taken of the partially edentulous lower ridge using a preformed special tray. The impression was poured using mount stone and a cast made and trimmed.
- (c) The PPSF was shaped to fit the edentulous area of the cast. It was prepared in a rectangular form $1 \times 0.5 \times 0.2$ cm. Six holes, approximately 0.5 mm in diameter, at equal distances, were made on each rectangular form implant (Fig. 4). Polysulfone can be sterilized by autocaving. However, a hot air oven was used for sterilization. Each implant was wrapped and sterilized in a hot air oven for two hours at 165°C and stored at room temperature until its use.

3. Implantation Procedures

- (a) The animal was anesthetized using the same protocol as mentioned before and all procedures were done under aseptic techniques.
- (b) On the left side of the partially edentulous ridge (Fig. 5), a longitudinal incision of 2-5 cm was made over the crest of the edentulous ridge from the retromolar pads to the second premolar. Another oblique incision was made at 45° from the second premolar to the mucobuccal fold.
- (c) A mucoperiosteal flap was reflected using a periosteal elevator and retracted. The ridge was kept free from blood by suction throughout the operation.
- (d) A very shallow box was made on the crest of alveolar ridge and buccally with a #169 fissure bur to help the retention of PPSF blocks (Fig. 6). Only in the first monkey was the PPSF prevented from dislodgement by

using a preformed acrylic splint (Fig. 7 & 8) fixed in place by circumferential wiring (Fig. 11). The splint was in a supraocclusion position. Since the splint caused ulceration of the underlying mucosa, no more splints were used in this study.

(e) The wound was irrigated with normal saline. The PPSF and DBP (200mg) were inserted on the left side, 100mg below the implant and 100mg above the implant. The flap was approximated and sutured with 3-0 vicryl resorbable sutures (Fig. 9).

(f) The same procedures were performed on the right side except that PPSF was inserted without DBP.

(g) The animals were returned to their cages and observed until fully recovered from the anesthesia.

4. Animal Sacrifice

Fifteen days before sacrificing of the animal, the first dose of tetracycline hydrochloride (25mg/kg) was given intramuscularly. The second identical dose was given 10 days following the first dose. The animal was sacrificed 5 days after the second dose.

The animals were sacrificed at 42, 60 and 90 days after implantation. The animals were anesthetized with ketamine. A central incision in the midline of the neck was made and with blunt dissection, the carotid sheaths on each side of the neck were exposed. The common carotid artery, the internal jugular vein and the external jugular vein was cleaned of connective tissue and 00 black silk ligatures were placed around each vessel.

The common carotid artery was occluded with a bulldog clamp distally and then ligated proximally. A small incision was made in the isolated

segment and a plastic cannula was introduced into the artery (bilaterally) as the clamp was released. The canulae were secured in the artery by tying the ligatures around the cannulated artery. Both right and left cannulae were connected to a perfusion pump. In the meantime, the internal jugular veins were ligated and the external jugular veins incised to allow drainage of the blood and perfusate. Heparinized saline (10,000 μ /L) was pumped into the arteries at a rate of 50-75 ml/min until clear saline drained from the external jugular veins. The monkey was then perfused with Millong's phosphate buffered formalin (pH 7.2). Submucosal injections at the partially edentulous areas were used to supplement the perfusion procedure. In one monkey, we perfused through the heart and in another one we perfused through femoral vessels.

Each perfused monkey was decapitated. The head was placed in Millong's phosphate buffer for about three weeks. Then a band saw was used to make a coronal cut through the rami of the mandible. Then another cut was made sagittally at the symphysis menti area of the mandible. Photographs were taken. Both the right and left side of the alveolar ridges were then cut into 3mm thick sections using a diamond saw. Each section was photographed using a Zeiss dissecting microscope equipped with fibro-optic light cables and an automatic camera (Carl Zeiss, West Germany). All gross topography was recorded. The tissue sections of each side were divided into two groups. The first group was decalcified in a solution containing 12.7 M formic acid and 0.0035 M sodium citrate. The formic acid was prepared by diluting concentrated formic acid 1 to 1 with distilled water. The sodium citrate solution contained 0.007 M sodium citrate. This mixture of formic acid and sodium citrate is considered

to be a mild decalcifying solution that requires 6-7 weeks for decalcification. The second group was left undecalcified.

5. Evaluating Techniques

After decalcification, each jaw section containing the implant was dehydrated in ascending grades of ethanol, then cleared in xylene and infiltrated overnight in paraffin under a vacuum and then embedded in the same substance. The samples were cut into 5 micron thick sections using a steel blade mounted on a 820 Spencer microtome (American Optical Corporation, Buffalo, N.Y.) The sections were stained with the Harris Hematoxylin and Eosin Stain (H & E).

This technique was used to demonstrate the general histology of the alveolar ridge containing the implant. In the H & E sections, the nuclei appeared blue and cytoplasm and intercellular fibers stained pink which allowed different tissue components to be identified. The stained sections were studied and photographed with a Zeiss photomicroscope (Carl Zeiss, Inc., Thornwood, N.Y.) The undecalcified specimen was processed for plastic embedment in methyl methacrylate. The samples were dehydrated in ascending grades of ethanol, infiltrated in methyl methacrylate monomer for 3 months (3 infiltrations) and then embedded in methylmethacrylate under vacuum for polymerization. The specimens were cut into 3 and 10 micron-thick sections using a Polycut S microtome (Reichert Scientific Instruments, Buffalo, N.Y.) The 3 micron sections were deplactisized using xylene and then stained by the modified Masson stain which colors mineralized tissue blue and osteoid tissue red. These sections were used to calculate the number of points that fall over bone

and soft tissue. The images of the sections were transferred via a camera mounted on a microscope to a television screen interfaced to an Apple Microcomputer (Apple Computer, Inc., N.Y., N.Y.) equipped with a Houston Hipad digitizing table (Houston Instruments, Austin, Texas).

Three microscopic fields were selected from each slide from the upper, middle, and lower parts of the specimens. A grid composed of 651 points was superimposed on the microscopic field projected through the camera to the TV screen. The number of points that fall over the soft tissue, bone and osteoid were counted. All counts were made using the same magnification (60X). The total number of points overlying each structure, which is equivalent to the relative surface area, was expressed as a percentage of the total points. The mean values of the control and experimental sides were compared using the Student's t-test. The micron thick sections were mounted unstained for tetracycline identification. The fluorescent specimens were photographed with a Zeiss photomicroscope under ultraviolet light.

The tetracycline labelling was diffuse and not in lamellar form. This did not allow the measurement of the appositional rate as we expected.

6. Scanning Electron Microscopy

Scanning electron microscopy, thick sections approximately 500 microns were prepared from both PPSF blocks before implantation and 90 days following implantation. The specimens were washed in water to remove any surface contaminants and then dehydrated in ascending grades of alcohol. For final dehydration, we used the critical point drying technique. The specimens were placed in a pressure vessel containing 100% ethanol. Once loaded, the pressure vessel is sealed and cooled to a few degrees below

room temperature by cool water. The carbon dioxide is allowed to enter the vessel under pressure. This covered the specimen and almost filled the vessel. While continuing to supply the carbon dioxide under pressure, the chamber exhaust valve was opened slightly to allow the fluid to flush through the vessel and sample, carrying out the ethanol and most or all air. Once ethanol was no longer detectable in the exhaust, the chamber was resealed at both the exhaust and inlet valves isolating it in a moderately high pressure, cool state. This procedure was repeated three times. Then, the temperature of the vessel is gradually increased during which time the pressure of the carbon dioxide also increased. The carbon dioxide thus passed through or around its critical point, resulting in a gaseous phase within the vessel under high pressure. Then, it is bled off gradually through the exhaust vent. During the gas exhaust, the pressure vessel must remain at a temperature above the critical temperature and the pressure release must be very gradual to avoid any condensation of the carbon dioxide. The dried specimens were then mounted on aluminum stub using double-stick Scotch tape. The specimens were coated with gold for 2 minutes (Ernest F. Fullam Inc., N.Y.). The specimens were studied and photographed using an AMR (Model 100A) scanning electron microscope.

III. RESULTS

Table I summarizes the records of recovery of implants following animal sacrifice.

A. Forty-two days after implantation (Group I)

In one of the two monkeys used in this group (monkey #11446), an acrylic splint was fabricated and inserted post-operatively (Fig. 10). The mucosa under the splint was ulcerated and eroded (Fig. 12) causing bilateral exposure of the implants two weeks after implantation.

The animal was rescheduled for surgery and the mucosa was trimmed and resutured on one side, while on the other side, the implant was not found. At the time of sacrifice, there were no signs of infection or tissue necrosis at the implant site or adjacent areas but examination of the coronal sections of the augmented area of the jaw indicated the loss of the implants on both sides. We decided not to use acrylic splint to cover the areas of the implants in subsequent animals.

From the second monkey in this group we could recover the implants on both sides (Table I).

1. Polysulfone side

a. Gross Appearance

Forty-two days after implantation of porous polysulfone on the lower edentulous area, the animal was sacrificed. The animal was in good health throughout the course of the experiment. In general, the animal did not exhibit any evidence of pain, lameness, or other indications of intolerance. No changes in appearance or behavior of the animal attributable to the implant was noticed.

The mucosa covering the implant was intact and smooth (Fig. 13). On palpation the implantation site felt firm. There were no signs of infection, at the implantation site or the adjacent areas.

b. Stereoscopic Examination

Thick coronal sections of the edentulous lower augmented area 42 days following implantation with polysulfone were examined under a dissecting stereomicroscope. The implant could easily be seen to occupy the outer, superior surface of the alveolar ridge. The implant was covered with normal mucosa and was surrounded with normal looking tissues. The micropores of the implant appeared filled with connective tissues (Fig. 14). The cortical bone of the alveolar ridge, the cancellous bone and bone marrow spaces appeared normal with no sign of untoward reaction.

c. Histologic Examination

The examination of histological sections of the augmented edentulous lower ridge, at low magnification, complemented the results of the stereoscopic examinations of thick sections which were described in the previous section of this thesis.

The decalcified coronal sections at the implant site were stained with H & E. It was clearly evident that fibrous connective tissue invaded the pores of the polysulfone (Fig. 15 & 16). Both loose and dense connective tissues were found. At high magnification, the tissue contained primarily fibroblasts and collagen fibers (Fig. 17).

The loose connective tissue consisted of loosely arranged collagen fibers while the dense connective tissue was formed of closely packed collagen fibers. The loose connective tissue also contains more cells than the dense ones (Fig. 17).

The collagen bundles were either regularly arranged in an orderly parallel orientation or irregularly arranged in an interwoven or whorled arrangement.

The cellular components consisted mainly of fibroblasts. Occasionally, a few multinucleated giant cells, mononuclear inflammatory cells and macrophages were seen within the fibrous tissue (Fig. 18). This finding is consistent with a foreign body reaction seen with other synthetic materials. Fibroblasts were recognized by their fusiform spindle-shaped appearance and their long cell processes, well-defined basophilic cytoplasm, and oval or elongated nuclei.

The fibrous layer which surrounded the implant was continuous with the connective tissues that penetrated the pores of the implants and surrounding the particles of polysulfone (Fig. 19). The fibrous tissue within the pores of the implant was also richly vascularized. A few large vessels (Fig. 18) penetrated into the larger opening between polysulfone particles whereas many smaller vessels were observed in greater numbers surrounding the implant (Fig. 20).

Adjacent to the fibrous tissue which surrounded the implant, cancellous bone and marrow were found (Fig. 19). Cortical alveolar bone with typical haversian system surrounded the cancellous bone and marrow. The gingiva overlying the implant area showed normal cellular components with no evidence of inflammatory reaction in the underlying connective tissue (Fig. 20). The collagen fibers of the lamina propria blended with the fibrous tissues surrounding the implant.

2. Polysulfone-Demineralized Bone Powder Side

a. Gross Appearance

Examination of the polysulfone-demineralized bone powder implantation site on the lower augmented edentulous ridge 42 days following implantation revealed the same appearance described on the polysulfone side in the same monkey (Fig. 13).

b. Stereoscopic Examination

Stereoscopic examination of the polysulfone-demineralized bone powder-polysulfone (DBP-PPSF) implantation site on the lower augmented edentulous ridge revealed the same appearance described on the polysulfone side of the same animal (Fig. 21).

c. Histologic Examination

The examination of histological sections of the augmented edentulous lower ridge on the DBP-PPSF side, 42 days following implantation revealed the same appearance as the control side except that the fibrous tissue was more cellular (Figs. 22, 23 & 24) and showed more blood vessels. Also, DBP particles were fused, interconnected and contained remnants of osteocytes (Figs. 24 & 25).

B. Sixty Days Following Ridge Augmentation (Group II):

Three out of four implants were recovered from two monkeys. One implant was recovered from the polysulfone side and two implants from the demineralized bone powder-polysulfone side (Table I).

1. Polysulfone side

a. Gross Appearance

Sixty days after implantation, the animals appeared in good health and

did not exhibit any evidence of pain, lameness, or other indications of intolerance. No changes in appearance or behavior attributable to the implant was noticed.

The mucosa of the implant site was firm on palpation. There were no signs of infection or tissue necrosis at the implantation site and the adjacent areas. The wound healed by with primary intention and the implant was covered with a normal mucosa, both in appearance and texture.

b. Stereoscopic Examination

Similar to the previous group, coronal sections of the edentulous lower augmented alveolar ridge area were examined and photographed under a dissecting stereomicroscope. The implant was found at the same site where it has been originally placed 60 days ago. The implant was surrounded with normal-looking tissues and the overlying mucosa was intact and appeared normal (Fig. 27). The polysulfone implant was incorporated into the edentulous ridge. Tissue clearly grew through the micropores of the implant and into one of the macropores (Fig. 27). The cortical bone of the alveolar ridge and the cancellous bone and marrow all appeared normal with no sign of untoward reaction.

c. Histologic Examination

The examination of histological sections of the augmented lower edentulous alveolar ridge 60 days following implantation of PPSF, at lower magnification complemented the results of the stereoscopic examination of thick sections which were described previously in this thesis.

The coronal decalcified sections of the implant site stained with H & E produced blue nuclei, while collagen, bone and cytoplasm were pink.

Newly formed bone grew at the periphery surrounding the inner half of the implant and for a short distance within the pores of PSF (Fig. 28). This new bone contained osteocytes and was covered with osteoblasts (Figs. 29 & 30). It also contained bone marrow (Fig. 29). Along the advancing edge of the newly formed bone (Figs. 31 & 32), osteoblasts were present. The new bone also contained osteocytes and marrow (Fig. 32). The implant-bone interface revealed normal bone with active osteoblasts and vascular spaces (Fig. 33). There was a fibrous tissue layer between the bone and the implant.

Fibrous tissue was seen within the micropores of the polysulfone interconnecting and surrounding polysulfone particles (Fig. 34). The fibrous tissue around the polysulfone was continuous with the fibrous tissue within the micropores and that along the contours of the polysulfone particles (Figs. 35 & 36).

The fibrous tissue was well vascularized and more organized than that found in the earlier time periods. The fibrous tissue consisted of both dense and loose connective tissue. This tissue contained fibroblasts and collagen fibers (Fig. 37 & 38). The loose connective tissue was formed of loosely arranged fibers while the dense connective tissue was formed of closely packed fibers (Fig. 37). The loose connective tissue contained more cells than dense connective tissue. The cells were mainly fibroblasts which were identified by their typical fusiform spindle shape, their long cell processes, a well defined basophilic cytoplasm, and oval or elongated nuclei. In addition to fibroblasts, some mononuclear inflammatory cells, multinucleated giant cells and macrophages were found (Fig. 38).

The fibrous tissue surrounded the implant and within the pores showed remodelling changes which were evident by the parallel orientation of the fibroblasts and collagen fibers to the implant surface and to the polysulfone particles (Figs. 37 & 38).

A few large vessels penetrated into the large pores between polysulfone particles whereas many smaller vessels were observed in greater numbers within the connective tissue which surrounded the implant. The gingiva overlying the implant area showed a normal cellular architecture with no evidence of inflammatory reaction in the underlying tissue.

The coronal undecalcified sections of the lower edentulous region 60 days following implantation with polysulfone were stained with modified Masson. This staining method stain osteoid (undemineralized bone matrix) red and mineralized matrix blue. The osteoid and mineralized matrix could be easily recognized in these tissues after using this stain. Histologic examination revealed mostly fibrous connective tissue with little osteoid (red) and very little bone (blue) (Figs. 39 & 40). The surrounding bone acquired a deep blue stain (Fig. 40).

2. Sixty Days Following Polysulfone-Demineralized Bone Powder

a. Gross Appearance

The mucosa covering the augmented ridge looked normal and similar in appearance to the control side.

b. Stereoscopic Examination

Stereoscopic examination of the coronal sections of the augmented ridge 60 days following implantation revealed incorporation of polysulfone into the edentulous ridge. The implant was at its original insertion site i.e. the outer top surface of the ridge.

Tissues invaded the micropores of the implant and crossed the whole length of the polysulfone block. In some areas this tissue had a marble like appearance of bone (Fig. 41). The soft tissues surrounded the whole implant. The overlying mucosa was intact and appeared normal. The polysulfone-tissue interface was intact, smooth and showed no areas of separation. The cortical bone of the alveolar ridge, and the cancellous bone and marrow appeared normal with no sign of untoward reaction.

c. Histologic Examination

The examination of histological sections of the augmented edentulous alveolar ridge 60 days following implantation at low magnification complimented the results of the stereoscopic examinations of thick sections which were described in the previous section of this thesis.

Newly formed bone grew at the periphery and around the implant and almost covered the implant (Figs. 42, 43 & 44). The advancing edges of bone surrounding the implant were covered with osteoblasts and contain osteocytes (Figs. 45 & 46). A layer of what appeared as undifferentiated mesenchymal cells (preosteoblasts) was adjacent to active osteoblasts. The implant-bone interface revealed normal bone with active osteoblasts and vascular spaces (Figs. 47, 48, 49 & 50). In some areas a direct contact between the bone and polysulfone with no intervening connective tissue was present (Fig. 51). However, in other areas a thin fibrous layer intervened between the bone and polysulfone (Fig. 52). Bone and fibrous tissue were seen within the micropores of the polysulfone (Fig. 44). Some pores contained only bone (Fig. 53), some pores contain only fibrous tissue (Fig. 48), and some contained both bone and fibrous tissue (Fig. 43). The fibrous tissue and bone within the micropores and surrounding polysulfone

particles were continuous with each other and followed the contours of the polysulfone particles. The bone within the micropores were covered with osteoblasts. A layer of preosteoblasts were also seen adjacent to active osteoblasts. The bone contained lacunae which, in turn, contained osteocytes. The osteoblasts were found in juxtaposition to the bone surface where osteoid matrix was being deposited (Fig. 54). The cells varied in shape some being cuboidal and others pyramidal, and were frequently organized in a continuous layer. The cells usually contained large nuclei and basophilic cytoplasm. The osteocytes contained darkly stained nuclei and a faintly basophil cytoplasm (Fig. 53).

The fibrous tissue within the micropores of the polysulfone were continuous from one pore to another. It sometimes blended into the osteoblastic layer of cells actively forming bone (Figs. 44 & 48).

The fibrous tissue was well vascularized and more organized than that found in the earlier time periods. The fibrous tissue consisted of thick collagenous bundles and fibroblasts. Loose connective tissue, which was also found in the pores of polysulfone at earlier time periods, was not totally replaced by a dense connective tissue. This connective tissue was not as organized as the fibrous tissue found around the entire implant or around the individual particles of polysulfone. The streaming of fibroblast-like cells into polysulfone micropores was noticed. Some of these cells, particularly near the implant appeared as if they were more differentiated. A few large vessels penetrated into the large openings between polysulfone particles (Fig. 55) whereas many small vessels were observed in greater numbers just outside the fibrous layer (Fig. 56). Vascular penetration was also common adjacent to the dense fibrous layer

which surrounded the polysulfone particles (Fig. 57). The gingiva overlying the implant area showed a normal cellular pattern of stratified squamous epithelium and no evidence of inflammatory reaction within the submucosal connective tissue (Fig. 58). The organization of the gingival epithelial and connective tissues suggested its adaptation to external forces. The collagen fibers of the lamina propria ran parallel to the surface and blended with the fibrous tissues which surrounded the implant.

Examination of the coronal sections of undecalcified sections stained with modified Masson complemented the results of the H & E stained decalcified histologic sections described above.

Modified Masson stained osteoid (unmineralized bone matrix) red and mineralized matrix (bone) blue. In contrast to the control side, the osteoid and mineralized matrix was easily recognized in these tissues after using this stain. Some areas acquired a blue stain suggesting that they were mineralized. At the interface between osteoblasts and the blue stained bone surface, a layer of red stained osteoid was found suggesting active bone deposition by the osteoblasts (Figs. 59, 60 & 61).

The amount of bone and osteoid appeared to be more than that found in the control side (polysulfone side).

d. Histomorphometric Results

The results of the histomorphometric measurements 60 days following implantation of polysulfone with and without demineralized bone powder are presented in Tables II and III.

The quantitative data tend to support our qualitative histological findings. Sixty-days following implantation, the DBP-PPSF side had significantly more bone and osteoid than the PSF side.

The percentage of points overlying bone and osteoid which was proportional to the relative surface area of bone on the DBP-PPSF side (44.57%) was significantly higher than the PSF side (6.90%). In contrast, the percentage of points overlying fibrous tissue of the DBP-PPSF side (35.56%) was less than the PSF side (59.4%). Although the number of the specimens recovered from our study was not as large as we would have liked, the specimens used for the histomorphometric analysis may be enough to give us at least an idea about the amount and difference in bone formation between the control and experimental sides. The histomorphometric results supported the histological, tetracycline labelling and scanning electron microscopic results.

e. Tetracycline Labeling

Examination of undecalcified unstained histologic sections of the edentulous lower ridge 60 days following implantation of polysulfone and demineralized bone powder under ultraviolet light complemented the histologic and histomorphometric results of the previous sections.

Tetracycline double-labelling fluorescence with reflected ultraviolet light was used. Tetracycline fluorescence gives an indication of recently formed bone. The observed fluorescence of tetracycline showed a distinct yellow color on recently formed bone. The fluorescence was noticed within the pores of the polysulfone (Figs. 62, 63 & 64) and at the bone-polysulfone interface (Fig. 63). This fluorescence almost surrounded the implant.

The fluorescent yellow color of the double labelling tetracycline occasionally showed two-distinct layers. However, in many areas these two layers were indistinguishable and appeared diffuse (Fig. 64).

C. Ninety Days Following Implantation (Group III)

This group contained only one monkey. Only one implant was recovered from this monkey (Table I).

1. Polysulfone Side

a. Gross Appearance

The animal was in good health throughout the course of the experiment. In general, the animal did not exhibit any evidence of pain, lameness or other indications of intolerance. No changes in appearance or behavior attributable to the implant was noticed.

Examination of the lower augmented edentulous ridge 90 days following implantation of polysulfone showed normal mucosa, both in appearance and texture, covering the implant (Figs. 65, 66 & 67). The mucosa was smooth and slightly elevated. On palpation, the augmented area felt firm and elevated. There was no sign of infection, or tissue necrosis at the implantation site and the adjacent areas. The wound closed with a well-healed soft tissue covering. There was no sign of dehiscence.

b. Stereoscopic Examination

The implant was found on the outer superior surface of the alveolar ridge and was surrounded with tissues of normal appearance and the overlying mucosa was intact and appeared normal. Tissue grew through the micropores of the implant (Fig. 68). The cortical bone of the alveolar ridge and the cancellous bone and marrow appeared normal with no sign of untoward reaction.

c. Scanning Electron Microscopy Results

Scanning electron microscopy examination of the porous polysulfone

block showed the polysulfone particles and the micropores (Fig. 69). Also, it showed the size, arrangement, and the contour of the polysulfone particles (Figs. 70 & 72). In addition, it showed the interconnecting macropores and tunnels between the polysulfone particles (Figs. 71 & 72).

Ninety days following implantation, examination of the PPSF block showed incorporation of the polysulfone into the mandibular augmented ridge. The polysulfone was completely surrounded and invaded with connective tissue and bone (Fig. 73). Fibrous tissue was seen within the pores and around the polysulfone particle (Figs. 74 & 75). Fibrous tissue within the macropores showed parallel-arranged collagen fibers (Fig. 76). Bundles of collagen fibers were seen within the micropores (Fig. 77). In addition, SEM showed the arrangement and networks of collagen fibers (Fig. 78). The fibrous tissue consisted of collagen fibers and fibroblasts (Fig. 79). There was close adaptation of the connective tissue to the polysulfone surface (Fig. 80). Bone invaded the micropores of the polysulfone (Figs. 81 & 82) and surrounded part of the implant (Fig. 83). Numerous Howship's lacunae were observed on the surfaces of the thick, bony trabeculae. Lacunae, representing the spaces in which osteocytes reside in the living tissue, appeared as oval depressions (Fig. 82). The mucosal tissue covering the implant showed an epithelial layer and submucosal layer (Fig. 84). This mucosal covering was in close adaptation and continuous with the fibrous tissue within the polysulfone (Fig. 85).

d. Histologic Examination

The coronal decalcified sections of the implant site stained with H & E show the same features (Figs. 86, 87, 88, 89 & 90) described after 60

days except that more bone was formed within the pores of the polysulfone (Figs. 91, 92 & 93) and the bone showed evidence of remodelling (Fig. 93).

Examination of the coronal sections of undecalcified sections stained with modified Masson complemented the results of the decalcified histologic sections stained with H & E. In contrast to the polysulfone side after 60 days, the osteoid and mineralized matrix was easily recognized (Figs. 94, 95, 96 & 97).

e. Histomorphometric Results

The quantitative data tended to support our qualitative histologic findings. Ninety days following implantation, the PSF side showed significantly more formed amount of bone and osteoid (Table IV) than the same side (PSF side) after 60 days (Table II). In contrast, the amount of fibrous tissue 90 days following implantation was less than that formed after 60 days.

f. Tetracycline Labelling

Examination of undecalcified histologic unstained sections of the edentulous lower ridge 90 days following implantation of polysulfone under ultraviolet light complemented the histologic and histomorphometric results of the previous sections.

Tetracycline uptake by bone gives an indication of recently formed bone. The observed fluorescence of tetracycline showed a distinct yellow color which was an indication of recently formed bone within the pores of polysulfone (Figs. 98 & 99) and around it (Figs. 100 & 101). The fluorescence of the double labelling tetracycline within the micropores showed indistinguished layers and appeared diffuse (Fig. 99).

IV. DISCUSSION

The purpose of this study was to determine the soft tissue and bone response following edentulous ridge augmentation using porous polysulfone (PPSF) with and without demineralized bone powder (DBP) in non-human primates. We used DBP to induce bone formation and bone ingrowth into the polysulfone micropores. The soft tissue and bone ingrowth into the micropores produce an interlocking that serves to stabilize the polysulfone. Although many experimental and clinical studies using autogenous, allogeneous and alloplastic grafting materials with varying success had been done, the ideal method and material of augmentation of an edentulous ridge has not yet been discovered. We selected PPSF as our experimental material because it accommodates bone and soft tissue ingrowth (194, 197). In addition its favorable mechanical properties encourage its use as a bone substitute material. Animal research is an important part of implant development and is prerequisite before human clinical trials. We used the monkey as an animal model in this study because their dental arches and teeth morphology closely resemble human. Also, monkeys are similar to humans in bone metabolism and the function of the orofacial complex (58), which should make our results applicable to future clinical trials using the same materials. We used animals from 12 to 15 years of age which is comparable to humans of 42-53 years of age (149). This age group and older have increased incidence of edentulous jaws. We selected female monkeys in our study because ridge resorption affects females more than male in a proportion of 4 to 1 (177). The rate and amount of residual bone resorption varies between maxillary and mandibular arches and within a single arch. However, the amount of resorption in the mandible of complete

denture patients were at least 4 times greater in the mandible than the maxilla (204, 205). This variability between maxillary and mandibular arches was also found in other studies (98) in which the mandible exhibited between 4% to 45% greater bone loss than the maxilla. Mindful of these facts, we selected the lower jaw as the site of implantation. We also selected the lower molar region as the site of implantation and augmentation because previous studies of ridge resorption in Rhesus monkeys (158) and humans (244, 98) indicated that the largest amount of bone loss of the alveolar ridge occurred in the posterior ridge area. This is also evidenced by the results of other studies (98) in which the area mesial to the canine showed 4% bone loss and the posterior area, 45%. However, the posterior area was not uniform in losing bone in that the area distal to the second molar exhibited less bone loss than the area just distal to the first molar.

We extracted the lower molar teeth and made a massive alveolectomy to create the human condition of atrophied residual alveolar ridge. The time of augmentation was selected at 5 to 8 1/2 months following extraction, to allow time for healing and remodeling of the residual ridge. After tooth extraction, resorption of alveolar crest occurred shortly (158). However, it has been shown in humans and pigs (4, 5) that the remodelling process occurs in bone structure throughout life and even aging human edentulous mandibles were still being remodelled (6). This was supported by a 4 1/2 year study that reported that 50% of the total amount of alveolar bone loss occurred during the first year (98). In another study (6) over a 2 year period, monkeys showed 70% to 80% loss of alveolar bone in the first year. These two studies indicated there is an initial rapid rate of alveolar bone

loss followed by a slower, more gradual rate of loss. In the monkey (6), the plexiform bone forms first showing the tendency towards haversian remodelling.

The polysulfone blocks were implanted on the buccal superior aspect of the residual ridge as it is known that (6) remodelling influences bone texture and that the buccal alveolar cortex is more affected than the lingual alveolar cortex.

The implants could not be found on one side in two animals. Since the implants were retained in one side, the loss of the implants could not be due to immunologic rejection. It may be the animal gained access to the implant site and removed the polysulfone block. However, this occurred only on one side in which the number of sutures may have not been adequate. A prefabricated splint was used to cover the implant site of the first monkey. The splint was in supraocclusion and caused ulceration of the underlying mucosa. It was noticed that the monkey was continuously opening, closing and biting on the splint and one could easily hear the sound of biting the splint. The excess biting force on the splint may have been due to the presence of opposing natural teeth. It was estimated that the biting force using natural teeth is about 5 to 6 times greater than in denture wearers (86). Also, the presence of the splint must have abnormally influenced the oral masticatory system. This view is supported by a study that showed that wearing removable prostheses evoked initial discomfort that led to unusual patterns of behavior in the surrounding musculature. The presence of the prostheses in an edentulous mouth also produced different stimuli of the sensory-motor system, which in turn

affected oral motor behavior (246). Regardless of the cause of the implant loss it seems that future researchers in this field should refrain from covering their implants with a splint particularly if it would be opposed by natural teeth. The excessive occlusal forces probably produced local mucosal ischemia leading to pressure necrosis.

The importance of the shape of the implant on the reaction of tissue had been reported in rat gluteal muscle (131) in which they reported that rods with triangular cross sections showed the highest tissue reactions while those circular cross sections showed the lowest reaction. In our study, we used rectangular-shaped blocks of PPSF for ridge augmentation. In our study, the rectangular cross section did not hinder a favorable bone and soft tissue response. However, it may be of interest in the future to compare the response of different shapes of the implant in order to standardize and evaluate the effect of the shape of the implant on tissue reaction.

We used blocks of PSF with 30% to 40% porosity and with pore sizes 150 to 250 microns. This amount and size of pores accommodated soft tissue and bone ingrowth. Our results support the idea that the ideal pore sizes range that encourage bony ingrowth should be 150 to 200 microns (243). Also this agrees with other studies showing that PPSF with 33% porosity and 150 to 250 microns pore sizes accommodates bone and soft tissue growth (17, 197). It is known that variations in pore sizes could produce differences in the total pore opening area available to ingrowing bone and could produce structural differences in the invading bone (146).

In this study, the fibrous connective tissue and bone penetrated the pores of PPSF and also surrounded the implant. However, the thickness of the fibrous capsule and the number of certain types of cells were not homogenous throughout the implant. This may be due to the difference in particle morphology and surface texture of the polysulfone. It was shown that the surface texture of the implant material affects the foreign body response, the interfacial cell response and the kinetics of the fibrous capsule formation (209). It was found that a textured implant surface promotes an increased adhesion of cells. The cells were macrophages and foreign body giant cells. In the same study using thick specimens, the fibrous capsule was thinner around a textured specimen than around a smooth one. However, at a later time period the thickness of the fibrous capsule are similar. These results demonstrate that surface texture of the implant is a critical variable in determining the soft tissue response to alloplastic material. In our study, the variation we noted in the quantity and quality of cells at different sites of the implant may be due to the difference in surface texture of the polysulfone probably created during preparation of the specimens prior to surgery and may also be due to differences in polysulfone particle morphology. The difference in surface texture may also account for the areas in which bone was in direct contact with the implant (osseous integration) and the areas where fibrous tissue intervened between the implant and surrounding bone. It has been shown that roughened surface implants exhibit direct bone apposition while smooth surface implants exhibit various degrees of fibrous tissue encasement. This may account for the observation that roughened surface implants demonstrated greater strength than smooth ones.

In our study, multinucleated giant cells and a moderate number of macrophages were observed close to the polysulfone which is consistent with a foreign body reaction seen with other synthetic materials. However, the number of these cells vary with different materials (17, 23, 196, 210, 238). All implants produce a giant cell response in the surrounding tissues. Such a response is considered to be an acceptable part of tissue repair in the presence of any foreign body. The foreign body response may be present for years after implantation with no detrimental effect on the implant and surrounding tissue (46).

In previous studies using PSF particles, it was found that the rough surface of the polysulfone was covered mostly with foreign body giant cells while its smooth particles had more macrophages and fibrous tissue (17).

Taylor (209) suggested that the presence of macrophages and multinucleated giant cells may be due to the direct action of absorbed exudate proteins, the physical nature of the texture spikes of the implant or humoral components of unknown nature released by the interfacial cells themselves. In another study (180) they showed that, with a rough implant surface, macrophages and giant cells persisted for many months with the formation of chronic granulomatous reaction. Superior tissue compatibility was found to be associated with smooth, well-contoured implants that had no acute angles. In the present study the foreign body reaction did not appear to be detrimental to the retention of the implant or to tissue growth within its pores. This reaction also did not affect the osteoinduction in the experimental side which is consistent with other studies (238). The absence of lymphocytes and plasma cells at the

interface of PPSF and the surrounding perivascular area indicate that the PSF did not elicit an immune response.

Our histologic results provide strong evidence that polysulfone is a biocompatible implant material in non-human primates. The fibrous tissue contained abundant collagen fibres and fibroblasts. Such a reparative response may be caused, in part, by secretion of macrophages or growth agents secreted by other cells which stimulated the production of collagen by fibroblasts. It has been shown that (180) the presence of macrophages was essential for the activation of collagen synthesis by fibroblasts. The fibroblasts and collagen fibers were arranged parallel to the implant surface suggesting their adaptation to the applied stress. Usually fibroblasts and fibers lie parallel with the forces of mechanical stress (134). This was considered one of the most important factors in successful retention of an implant (7). The fibrous tissue around the implant was continuous with the surrounding bone and the micropores of the implant. This may transmit some of the applied forces during mastication of food to the underlying bone. Also, the pores may increase the surface area of regenerated alveolar bone which, in turn will transmit forces to the underlying basal bone. It was found that the loss of teeth cause a 3.5-fold decrease in mandibular basal seat as compared to naturally present teeth (246). The orientation of the fibrous tissue within the pores of PPSF varied suggesting remodelling changes. The fibrous connective tissue, bone and blood vessels penetrated the pores of PSF in both the experimental and control sides which agrees with other studies (199, 238). However, the experimental side was more cellular and vascular than the control side.

Both biocompatibility and strength are important properties of any biomaterial-bone interface and the zone a few hundred microns deep into the pores of the implant. The type and maturity of tissue which penetrates an implant determine the mechanical properties of the interfacial complex (146). Observations of microstructural and biomechanical behavior suggested that the bone-porous implant region act as a dynamic composite material which, if closer-matching of the implant and parent bone moduli reduce stress concentration at the implant surfaces (146).

In our study, osseous integration was found in some areas of the implant-tissue interface while fibrous tissue of variable thickness was interposed between the implant and bone at other areas. Because of the high shear strength of PSF, osseous integration will help in the transmission of forces to bone, therefore enhance the viability of the surrounding tissue. This is consistent with results of another study (194) that showed the interfacial shear strength of PPSF-bone interface was similar to that of some metals.

The bone observed within the pores of the PSF showed remodelling changes indicating that some of applied forces may be transmitted to the bone within the pores. It has been reported (194, 199) that the modulus of elasticity of PSF was low enough to transmit part of the applied forces to the bone within the pores which, in turn, affect its remodeling in the cortical region of the implant. This important property was not found in high modulus metals and ceramics. In porous metals, the remodelling of bone within the pores does not affect the interfacial shear strength. However, the remodelling and viability of bone within the pores of an

implant may be an important factor particularly when a load is applied for a long time.

In our study with one exception (using splint in one animal), no external fixation of the implant was done. We depended on a shallow depression that was created as the only method of fixation. We predicted that the ingrowth of tissue around and into the pores of the implant would serve to stabilize it.

Since the majority of the implants were recovered, we think that the surgical technique employed is sufficient and that there is no need for external fixation using a splint. It is safe to assume that the polysulfone blocks were loose at the initial period of the experiment. Whether or not the vibratory motion has contributed to the bone growth at the base of the implants or at the control side it is hard to determine. The initial fit of the prosthesis through the period of bone healing was found to be required for bone to adapt to and form within the pores of an implant (40, 159, 199). Mobile implants with small pore sizes were found to be more likely to develop fibrous tissue instead of bone (40, 199). In other studies, however, many implant failures resulted from loosening of the implant caused by inadequate postoperative fixation and infection (7).

The polysulfone side (control) showed penetration of the pores with fibrous tissue and little bone at 60 days following implantation. However, at 90 days the amount of bone increased. This proliferative bone growth suggest that the implant material was accepted by the body and that PPSF, with its favorable mechanical and physical properties and sufficient porosity accommodated soft tissue ingrowth and bone formation around and within the pores of the implant did not prevent or hinder these responses.

In addition, the polysulfone does not distort under mechanical compression which is a disadvantage of some porous alloplastic materials (153). The bone formed within the pores of polysulfone on the control side had probably originated from the underlying bone. This is supported by other studies where bone migrated from the basal bone to the superior aspect of the implant rather than from the periosteum (43). In our study, it may be that if we allowed more time for bone regeneration (beyond the 90 days observation period), bone may have filled all of the pores and reached the superior border of the implant.

The addition of DBP to polysulfone induced bone formation within and around the polysulfone in larger amounts when compared with the polysulfone alone. This is consistent with another study on rats in which bone was induced within the polysulfone using DBP at subcutaneous sites (238). Although the end results were the same in both studies, the sequence of events leading to bone induction was different. In our study, the undifferentiated mesenchymal cells (UMC) which infiltrated the pores of the implant were apparently induced to differentiate into osteoblast that formed bone matrix. In another study by Vandersteenhaven et al. (238), the undifferentiated mesenchymal cells were induced to differentiate into chondroblasts that formed cartilage which was subsequently resorbed and replaced by bone. In both studies, DBP served as a stimulus for osteoinduction. However, under our experimental conditions, the induction was through intramembranous ossification while in the other study was through endochondral ossification. It has been shown that osteoinduction can occur by both mechanisms, namely intramembranous and endochondral ossification (35, 93, 79, 164, 165, 220, 222, 227). The source of

responding UMC at the experimental sides may be the fibrous tissue within and around the PSF which may have provided a pool of osteoprogenitor cells, or it could have been derived from periosteal progenitor cells from adjacent bone. These cells were attracted to DBP probably through the action of a bone-derived chemotactic factor known to be found within bone matrix (235). The difference between the results of Vandersteenhaven et al. (238) and our study may be due to the fact that we used PPSF-DBP at osseous sites while they placed their implants subcutaneously. We also used 200mg of DBP while they added only a few particles of DBP. Also, we did our experiment in monkeys and they did it in rats. These differences may also account for the large amount of induced bone and its extension into the pores of the PSF in our study while it remained localized around the DBP particles and did not extend into the pores of PSF in the other study (238).

The newly formed bone at the experimental sites contained osteocytes and were covered with a layer of osteoblasts. In addition, marrow cavities were seen. The DBP particle size used in this study ranged from 75 to 425 microns which is supposed to be the optimum range that produce large masses of new bone and marrow (170). This is consistent with other studies that used the same range of particle size and induced large amounts of new bone (72). However, this is in disagreement with Urist, et al. (224) who stated that small particles, 0.1 to 0.3 cu. mm induce small amounts of new bone in contrast to larger particles. It has been shown that the extent of bone induction is a function of the surface area of the implanted powders (72). It was also shown that osteogenesis proceed more slowly in response to demineralized bone blocks than to powders (73).

The new bone at the augmented ridge was apparently induced by intramembranous ossification which may be due to the abundant vascularity of the connective tissue in the vicinity of polysulfone. Urist et al. (224) stated that, in areas of sprouting capillaries, the responding undifferentiated mesenchymal cells differentiate directly into osteoblasts whereas in nonvascularized areas the cells differentiate into chondroblasts. It is generally accepted that the cells in the presence of capillaries would differentiate into osteoblasts, while they would differentiate into chondroblasts in the absence of capillaries. This is supported by the work of Bassett (20) who concluded that an O_2 concentration of 35% favors osteogenesis while concentrations as low as 5% would favor chondrogenesis. This is further supported by another study using tissue culture (19), in which they concluded that O_2 concentration was the determining factor with regard to whether certain cells form bone or cartilage.

The rich capillary blood supply noted around the polysulfone in our study would imply that there was an adequate supply of O_2 and which would therefore favor bone formation. The new bone within the polysulfone is an indication that capillary growth kept up with the invading osteogenic cells.

We believe that the new bone formed in the experimental site was due to osteoinduction by DBP for more than one reason. First, it has been shown that DBP induces bone formation in soft tissue and osseous sites (92, 164, 167, 238). Second, more bone was formed in DBP-PPSF side and in considerably less time in comparison to the PPSF side. Third, the bone was formed uniformly within the pores and around the implant, which suggest

that its formation was not limited to creep substitution from the edges of bone underneath the PPSF. This is in contrast to the PPSF side, in which bone grew only from the basilar bone side in areas of contact with the PPSF and failed to reach the surface of the PPSF. Fourth, the histologic evidence that, in some areas, one could identify the old DBM being incorporated into the newly induced bone.

This observation is in disagreement with the work of Narang, et al., (142) who used demineralized allogenic bone matrix (DABM) for ridge augmentation in dogs. They found that DABM was removed by osteoclastic resorption and that it had been replaced by new bone and marrow. This is also consistent with the work of Kaban and Glowacki (104) who used DBP for ridge augmentation in rats. They found that DBP was not resorbed during induction of new bone and that it remained amalgamated in the mass of the induced new bone. However, later in the course of their investigation, DBP showed evidence of remodelling into dense bone with cement lines and marrow spaces and it was difficult at this stage to distinguish the DBP in random sections made through the bone defect.

It has been shown that mineral-containing powder (104) used for augmentation of alveolar ridge in rats was resorbed and did not induce new bone formation. We increased the demineralization time from 3 hours in Reddi's method (164), to 18 hours which may have enhanced the inductive process and delayed the DBP resorption.

It has been shown in in vitro studies that DBM has the property of attracting calcium to its surface which may also play a role in its mineralization in vivo (221). This is also supported by the observation of

mineral deposits within the DBP two weeks after implantation (238). This notion is also supported by the work of Hosny and Sharawy (93) on old rats in which they attributed the mineralization of DBP to osteonectin. It has also been reported that there is a non-cell-mediated mineralization of human and rabbit bone matrix (221). In our study we observed both woven and lamellar bone. This is in contrast to the work of Hosny and Sharawy (92), who observed woven, lamellar and chondroid bone. This difference may be attributed to the absence of chondroblasts in the alveolar ridge response which would have been responsible for forming chondroid-type bone. Woven bone is believed to undergo remodeling changes to mature, lamellar bone (150). This is supported by the presence of remodelling and cement lines in the newly formed bone in our study. However, we do not know if this woven bone will change to lamellar bone or not. In our study we used the diaphysis of long bones to prepare the DBP. This bone is known to develop in the embryo by enchondral ossification. However, using this DBP in the alveolar ridge which is intramembranous in origin, yielded typical membranous ossification without an intervening stage of cartilage. This is in contrast to the study of Mulliken et al (115) who used DBP from long bones for the repair of calverial defects and showed that bone was induced by endochondral ossification.

In our study, the new bone was observed 60 days following implantation in monkeys. This is in contrast to the work of Hosny and Sharawy (92) in which bone was shown at 72 days following implantation of DBP in subcutaneous sites in male monkeys. This difference may be due to the fact that our implantation site was on bone which may have enhanced the recruitment of osteoprogenitor cells. It has also been shown that the

physical and chemical microenvironment in different locations may differ in its influence on the genetic machinery of the undifferentiated mesenchymal cells (171). The time for bone induction in rodents is faster than in monkeys. This has been attributed by Hosny and Sharawy (92) to the species differences or the presence of inhibitory protein in monkey bone or the possible remineralization of some of the DBP in monkeys. Sampath and Reddi (182) found that guanidine-HCl bone matrix extract of monkey bone produced little or no bone induction when implanted in rats. However, partial purification of this matrix protein and its reconstitution with the inactive rat residue restored the bone induction property of DBP, suggesting that the purification may have removed the inhibitory components.

The monkeys used in this study were comparable in age to middle aged human adults. Urist (224) reported that the age of the recipient influences the time of appearance of the bone induced by DBM. In another study (167), a two year old rabbit produced less new bone 6-8 weeks following implantation than that found in young animals. Young rabbits and rats produced new bone about 25 days after implantation. It is also known that old animals show a decrease in their regenerative ability in healing fractures. This agrees with the work of Hosny and Sharawy (93), who reported that the rate and amount of induced bone and marrow were reduced in old age. In our study, we increased the demineralization time to 18 hours instead of the 16 hours used in the work of Hosny and Sharawy (92). This may have enhanced the process of bone induction and agrees with the results of Urist (228) who stressed the importance of devoting more time for demineralization. The presence of minerals inhibits the

osteoinductivity of bone matrix. Sampath and Reddi (183) reported that the mineral phase was associated with 15% of the total biological activity of bone induction, while 85% of the activity was associated with the bone matrix. It was also shown (224) that adequate removal of the mineral was important to unmask the osteoinductive proteins and to reduce or remove the antigen expression of the bone matrix.

It has been suggested by Hosny and Sharawy (92) using histomorphometric analysis, that the process of osteogenesis continues for a long period following the initial induction. It has also been shown that the quantity of new bone is proportional to the mass of the matrix implanted or the dose of the BMP (229, 235). The histological study of the undecalcified sections using the modified Masson stain which stains unmineralized bone (osteoid) red and the mineralized bone blue, complemented the histologic examination using H & E stain. The quantitative and qualitative impression of the soft tissue and bone ingrowth around and within the PPSF, in both the control and experimental sides, was confirmed by the histomorphometric analysis and tetracycline labelling findings. The relative surface area of bone/unit area was statistically significantly higher in the experimental side than in the control side after the same period of implantation. The increase in the amount of bone formation in the experimental side should be due to the presence of DBP, since the control and experimental implant occurred in the same animal. The presence of the osteoid provides unequivocal evidence of the continuing process of bone deposition. The histomorphometric results correlated well with the tetracycline labelling study in which the

experimental side exhibited more fluorescent bone than the control side at comparable times of implantation.

It is known that tetracycline molecule has the capacity to chelate with several biologically active ions including calcium (67). This antibiotic (41) tends to deposit in areas where new bone is mineralized following the same pattern of calcium. According to Frost et al (69), tetracycline incorporated into bone matrix during bone formation becomes fluorescent under ultraviolet light.

We used tetracycline double labelling for measuring the appositional rate of bone. We depended on the density of the tetracycline labelling rather than the percentage, since both bone and matrix take up tetracycline. We used 25mg/kg of tetracycline hydrochloride, intramuscularly. This dose has been used in monkey (187) and has no effect on bone formation. The use of low doses is important since it has been shown that large doses of tetracycline may inhibit mineralization (148).

We wanted to measure the appositional rate of bone over a 10 day period which may include active and inactive appositional time. It has been shown in rats (208) that the measured bone apposition rate depends on the dose interval. At intervals of 24, 48 and 72 hours, the rates are the same. At larger intervals (96 and 192 hours) the rates fall significantly due to periods of cellular inactivity. We used double labelling as an indication of bone formation and to measure the rate of bone formation. The use of the technique was recommended by another study (219) that emphasized using a double labelling particularly in determining the rate of bone formation. Single doses of tetracycline may not confirm the results

and may only be an indication of accessibility of the tetracycline to bone by the blood supply.

Although we used small numbers of the experimental animals, the data provided valuable information on the histologic sequences of healing following implantation of a new implant material. At the same time, we used DBP to enhance the healing pattern of the reconstructed residual ridge through the biological principle of bone induction. The mandible is a unique bone in the craniofacial complex and is subject to continuous motion and significant compression and shear forces. In our study, it was not possible to determine how much forces was applied on the implant during function. Furthermore, the animals were partially edentulous and the masticatory forces may be different in totally edentulous animals. However, there was no doubt that there were some forces on the implant during mastication. It is also encouraging, that in another study (199) using PPSF as a coated tooth root for dental implants in monkeys, the clinical examination revealed zero mobility after 2 months and radiographic examination and pocket depth measurements revealed no loss of bone from around the implants.

In our study, the porous polysulfone with its excellent mechanical and physical properties and sufficient porosity with and without demineralized bone powder, accommodated soft tissue and bone formation around and within the pores. The implantation of PPSF with and without DBP caused no adverse tissue reaction. The complications encountered with other allogeneous autogenous and alloplastic materials (15, 24, 34, 54, 62, 77, 111, 112, 240) were not encountered in this study with the exception of loss of few implants due to the reasons that were discussed above. The published

complications include migration of the implant, inflammation, dehiscence, diffusion to surrounding areas, irregular distribution, extrusion, incorrect position, settling, resorption, pain, and excessive increase alveolar ridge height. The results of our study agrees with most clinical criteria for a successful augmentation of the alveolar ridge (34). However, other criteria still to be investigated include normal sensibility of the mental nerve, and a well fitting denture with good function. The ultimate goal of the implant is to withstand daily oral masticatory function and the unique environment of the oral cavity. In addition, the implant should be physiologically acceptable and should not be altered by bone resorption and the variables of prosthetic function.

The augmentation of residual alveolar ridge with PPSF with and without DBP has advantages that include excellent biocompatibility, absence of antigenic reactions, availability of the material, lack of inflammation, non-degradability, surgery under local anesthesia and good mechanical and physical properties.

With the use of DBP, more rapid bone induction will occur. In addition, the DBP will permit the operator to avoid using autogenous and allogeneous bone as is commonly the practice with alloplastic materials. DBP has many advantages that include (73, 142) avoidance of harvesting operations, potentially readily available, can be stored, little or no immune response, easily shaped and excellent inductive properties.

More investigations need to be performed on PPSF for evaluation of its ability to withstand stress in the oral cavity, the effect of particles morphology and the shape of the implant on the tissue response, and its use for longer time periods for ridge augmentation. The reduction of residual

ridges is a problem of multifactorial origin which cause psychological, economic and physical problems for millions of people all over the world (11). We hope that prevention or at least control of this problem will prevent their need for treatment. However, until this happens, an ideal method of treatment should be provided for them. Our results, and the tolerance of the PPSF with and without DBP by the soft tissue and bone are strongly encouraging and allow us to recommend the use of DBP and PPSF for clinical trials for ridge augmentation in humans.

CONCLUSIONS

1. Porous polysulfone is a biocompatible alloplastic material that accommodates bone and soft tissue ingrowth.
2. Healthy fibroblasts, osteoblasts, collagen and blood vessels were found within and around the pores of the polysulfone at the light and electron microscopic level.
3. Implantation of the demineralized bone powder with the polysulfone induced new bone formation within the micropores and around polysulfone.
4. The histologic, histomorphometric measurements, and tetracycline labelling supported the conclusion that more bone formed more quickly when using the demineralized bone powder.
5. The demineralized bone powder may serve to create an osteoinductive environment that may enhance bone coverage of polysulfone augmented ridges in humans.
6. Porous polysulfone with and without demineralized bone powder successfully augmented the mandibular edentulous molar areas with no evidence of resorption of the implant or untoward reactions of the surrounding tissues.
7. Porous polysulfone is a suitable material that can be used successfully for bone augmentation for future study in humans.

Table I

The Following Table Shows the Summary of the
Records of Recovery of Implants Following Animal Sacrifice

Group Number	Monkey Number	Edentulous Period-Mos.	Implantation Period-Days	PPSF Side	PPSF and DBP Side
I	11446	5	42	Missing	Missing
	11438	8 1/2	42	Intact	Intact
II	11443	5	60	Missing	Intact
	11436	5	60	Intact	Intact
III	11434	8 1/2	90	Intact	Missing

Table II

Control Site 60 Days Following Implantation of PPSF*

<u>Structure</u>	<u>Total Number of Points</u>	<u>Mean of Number of Points</u>	<u>Standard Deviation</u>	<u>Standard Error</u>	<u>Percentage of Points</u>
Bone and Osteoid	674	44.9	69.4	17.9	6.9
Fibrous Tissue	5802	38.7	109.6	28.3	59.4

* Calculated from one animal

Table III

Experimental Site 60 Days Following Implantation of DBP + PPSF

<u>Structure</u>	<u>Total Number¹ of Points</u>	<u>Mean of Number² of Points</u>	<u>Standard Deviation</u>	<u>Standard Error</u>	<u>Percentage of Points</u>
Bone and osteoid	4352	290.1	138.4	44.6	44.6
Fibrous tissue	3473	231.1	104.6	35.6	35.6

¹ 15 readings were made/5 slides/animal

² Means were calculated by dividing total number of points by 15 (readings)

* Statistical comparison of bone and osteoid (Student's t-test)
Control (Table II) vs experimental (Table III) - t value = 6.140 n=2 P<0.05

Table IV

Control Site 90 Days Following Implantation of PPSF*

Structure	<u>Total Number of Points</u>	<u>Mean of Number of Points</u>	<u>Standard Deviation</u>	<u>Standard Error</u>	<u>Percentage of Points</u>
Bone and osteoid	3117	207.8	157.7	40.7	31.9
Fibrous Tissue	4032	268.8	128.1	33.1	41.3

* Calculated from one animal

PLATE 1

FIGURE 1: Photomicrograph showing a piece of long bone (arrow) and the demineralized bone powder (arrowhead) ready for implantation.

FIGURE 2: Photomicrograph showing a negative culture of the demineralized bone powder on agar plate, incubated for 48 hours at 37°C.

FIGURE 3: Photomicrograph showing a porous polysulfone bar before preparation of a block similar to the one seen in Fig. 4.

FIGURE 4: Photomicrograph of the porous polysulfone block with six holes prior to implantation.

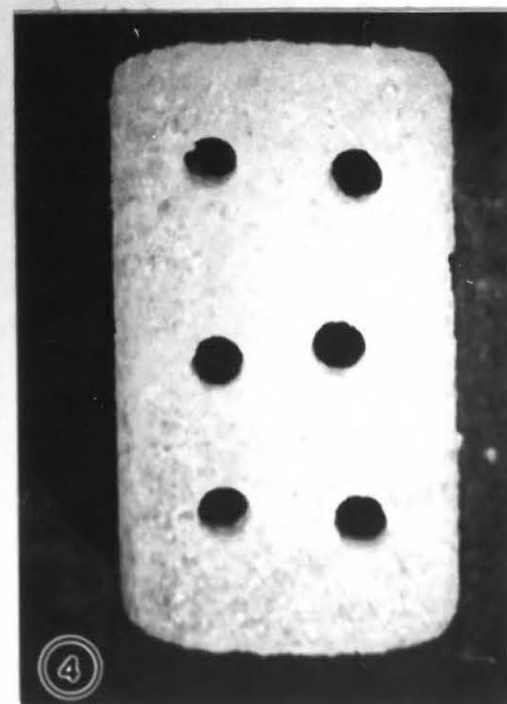
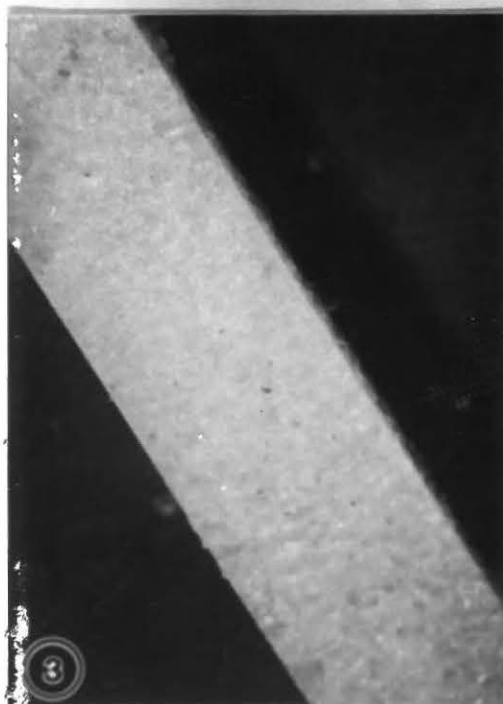
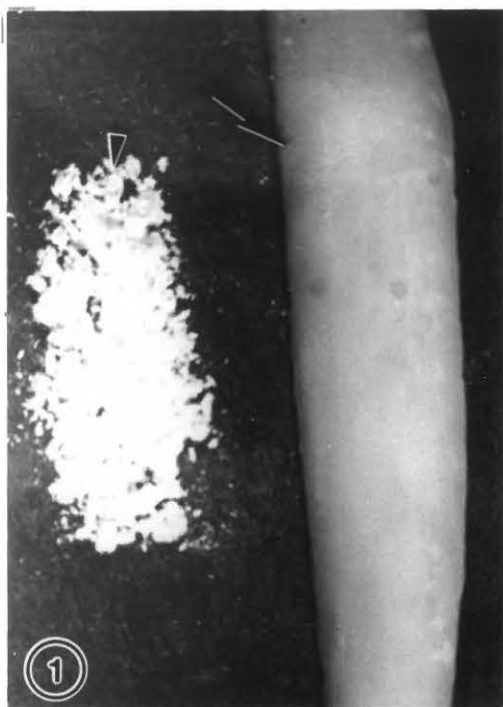


PLATE 2

FIGURE 5: Photograph showing the mandibular edentulous molar area (arrow) five months following extraction of lower molar teeth.

FIGURE 6: Photograph showing the position of polysulfone block (arrow) immediately after insertion on the outer top surface of the edentulous area.

FIGURE 7: Photograph of the stone cast of the monkey partially edentulous mandible (arrows).

FIGURE 8: Photograph of the acrylic splint placed on its stone cast.

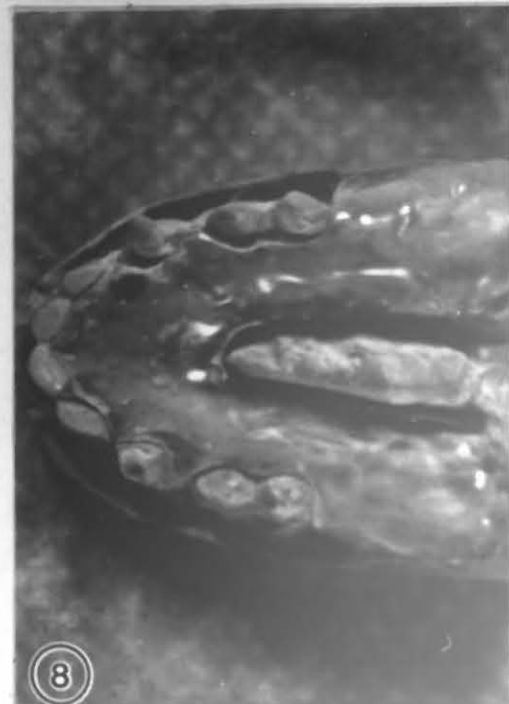
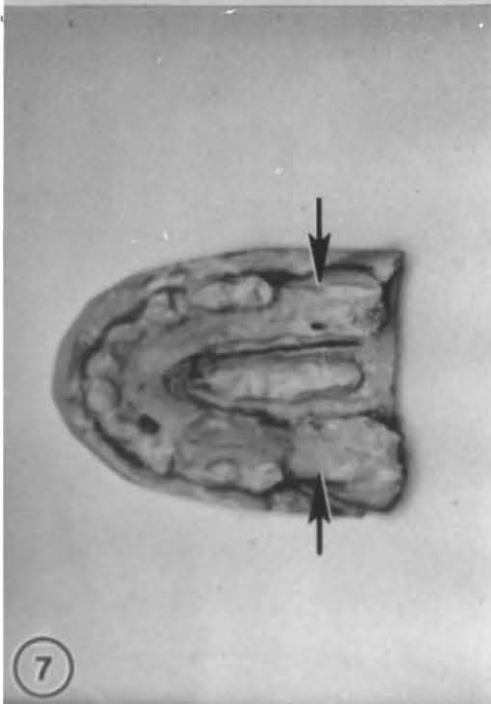


PLATE 3

FIGURE 9: Photograph showing the wound following closure with sutures.

FIGURE 10: Photograph of the acrylic splint used for fixation of the polysulfone implants.

FIGURE 11: Photograph showing the acrylic splint (asterisk) fixed with circumferential wiring postoperatively.

FIGURE 12: Photograph showing erosion and ulceration (arrow) of the mucosa covering the implant (arrowhead) 15 days following the placement of supraocclusion acrylic splint.

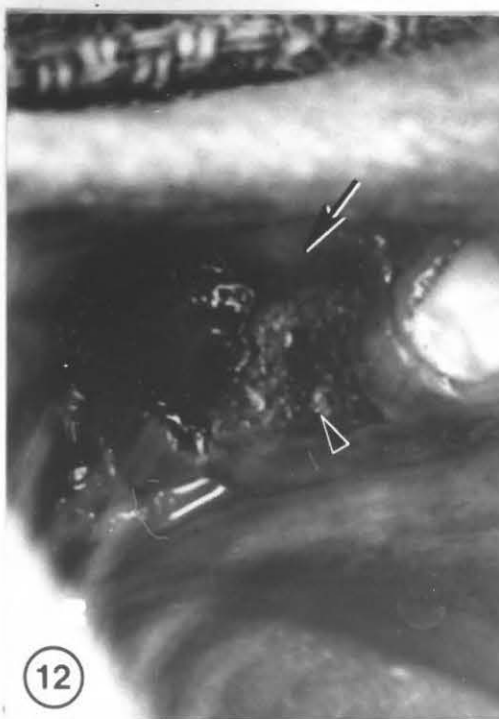
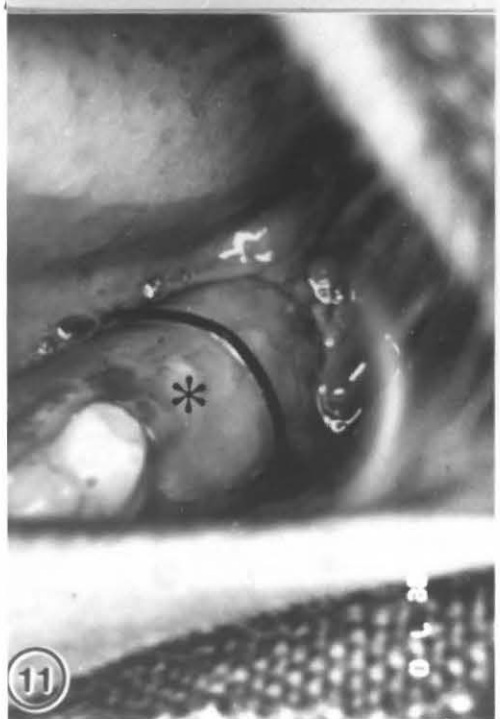


PLATE 4

FIGURE 13: Photograph of the partially edentulous mandible 42 days following implantation. Note that the ridges were obviously augmented (arrows).

FIGURE 14: Photomicrograph of a coronal section of the edentulous mandible 42 days following implantation of polysulfone. Note the connective tissue within the pores (arrows) and also surrounding the implant (arrowhead).

FIGURE 15: Photomicrograph of a histologic section 42 days following implantation of PPSF showing fibrous tissue (arrows) within the micropores of the polysulfone (PS) (H & E). (34 X)

FIGURE 16: Photomicrograph of a histologic section 42 days following implantation of PPSF showing the continuation of the fibrous tissue from one pore to the other (arrows) and around the PPSF particles (PS) (H & E). (34 X)

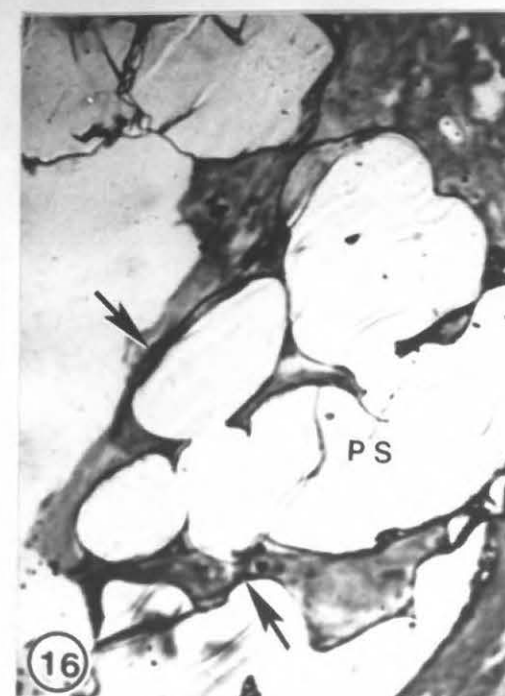
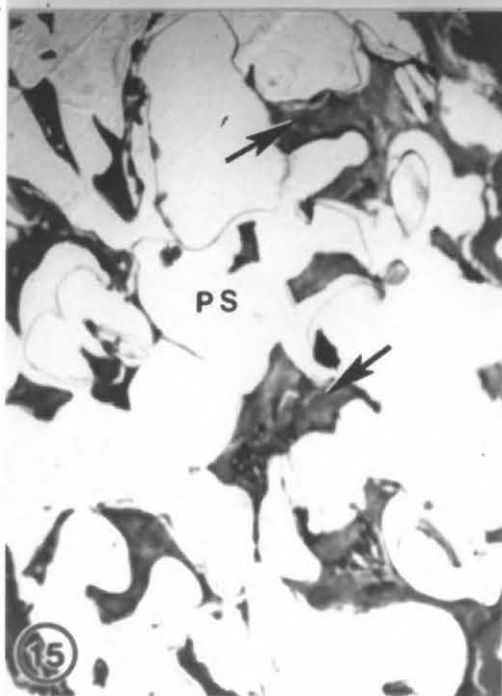
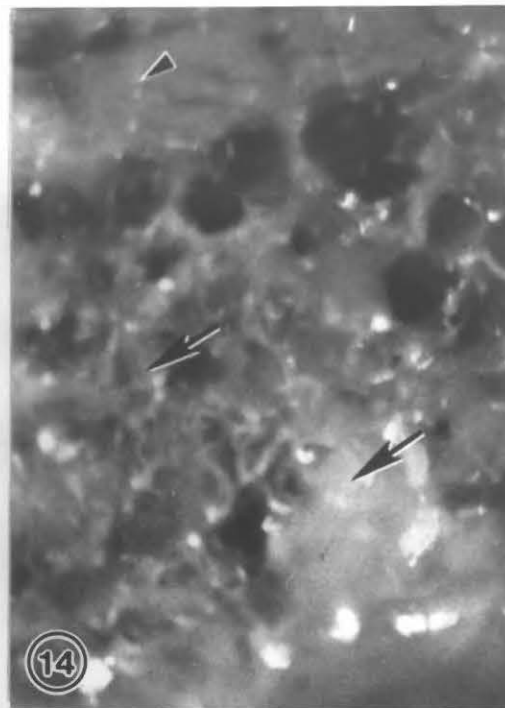
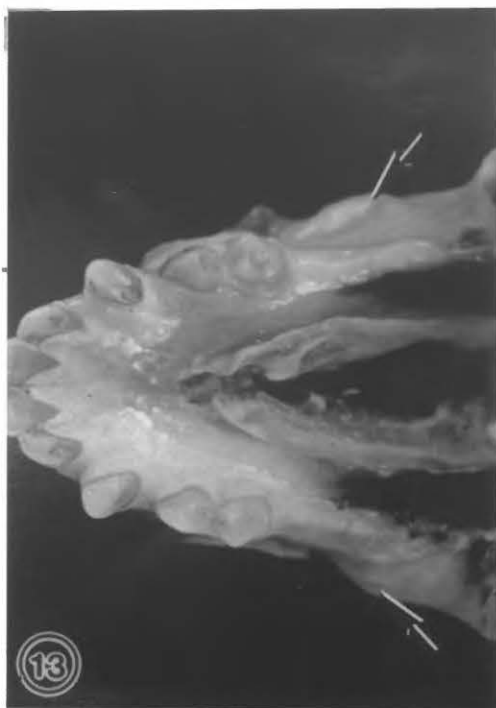


PLATE 5

FIGURE 17: Photomicrograph of a histologic section 42 days following implantation of PPSF showing the collagen fibers (arrows) and fibroblasts (arrowhead) within the pores of polysulfone (H & E). (481 X)

FIGURE 18: Photomicrograph of a histologic section 42 days following implantation of PPSF showing fibrous tissue containing fibroblasts (FB-arrow), collagen fibers (CC), multinucleated giant cells (arrowhead) and blood vessels (asterisk) (H & E). (481 X)

FIGURE 19: Photomicrograph of a histologic section 42 days following implantation of PPSF showing bone-PPSF interface (asterisk). Note osteocytes (arrowhead), bone marrow (arrow) and the fibrous capsule (C). Note that fibrous tissue around the implant continued within the pores of polysulfone (PS) (H & E). (138 X)

FIGURE 20: Photomicrograph of a histologic section 42 days following implantation of PPSF. Note the gingiva (arrow) and submucosal tissues (asterisk) covering PPSF (PS). Also note the absence of inflammatory reaction and the presence of blood vessels (arrowhead) close to the implant surface (H & E). (34 X)

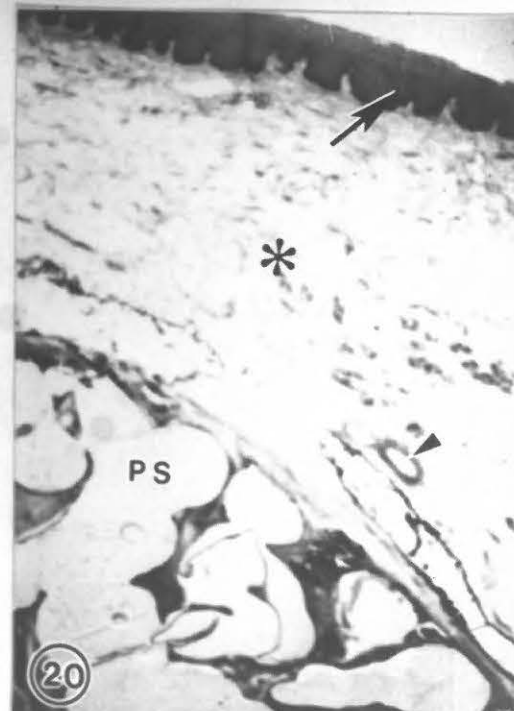
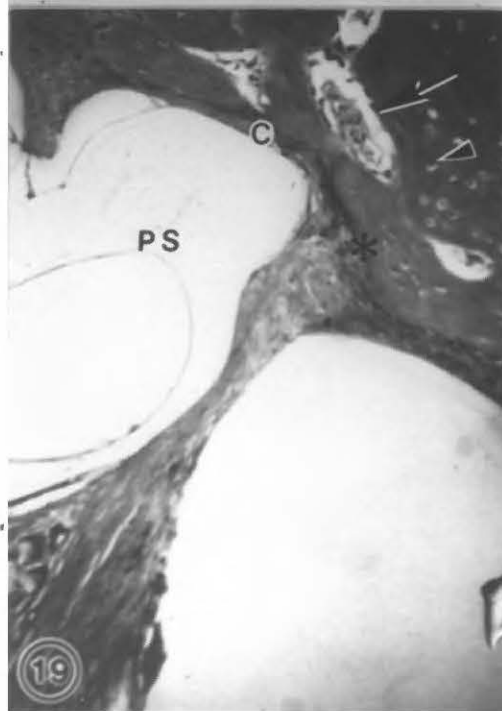
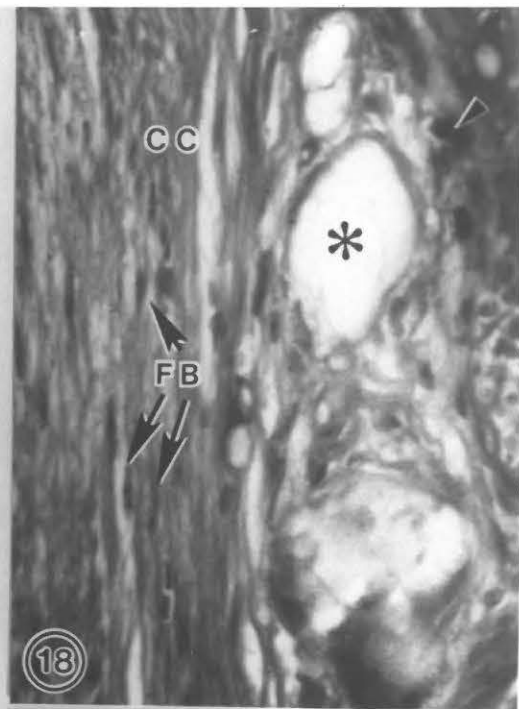
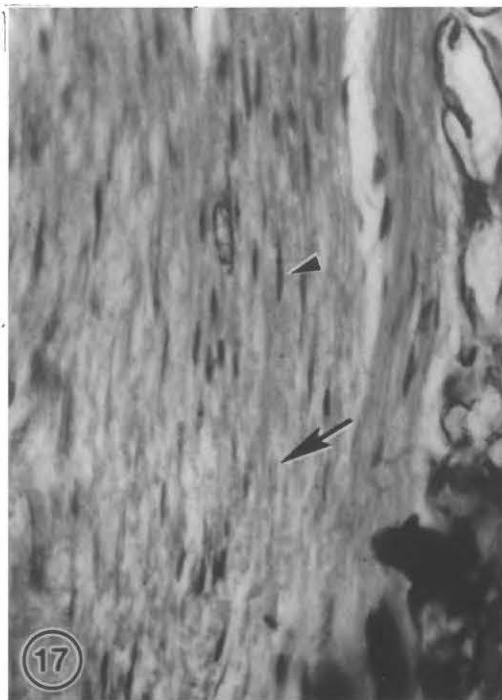


PLATE 6

FIGURE 21: Photomicrograph of a coronal section of the edentulous mandible 42 days following implantation of PPSF+DBP. Note the connective tissue within the micropores (arrow) and surrounding the implant (arrowhead).

FIGURE 22: Photomicrograph of a histologic section 42 days following implantation of PPSF+DBP showing the interconnecting fibrous connective tissue (arrow) within the pores of the polysulfone (PS) (H & E). (34 X)

FIGURE 23: Photomicrograph of a histologic section 42 days following implantation of PPSF+DBP showing the fibrous tissue (asterisk) at higher magnification surrounded by polysulfone particles (PS) (H & E). (138 X)

FIGURE 24: Photomicrograph of a histologic section 42 days following implantation of PPSF+DBP showing the collagen fibers (arrow) and fibroblasts (arrowhead) within the pores of the polysulfone. There was no bone formation at this stage (H & E). (481 X)

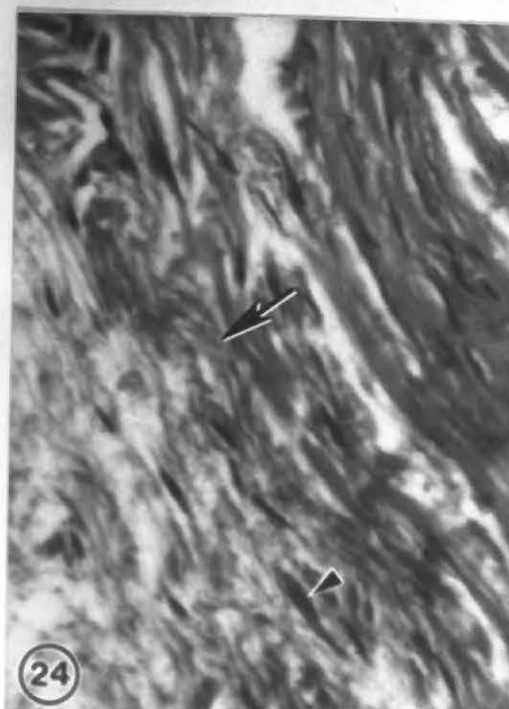
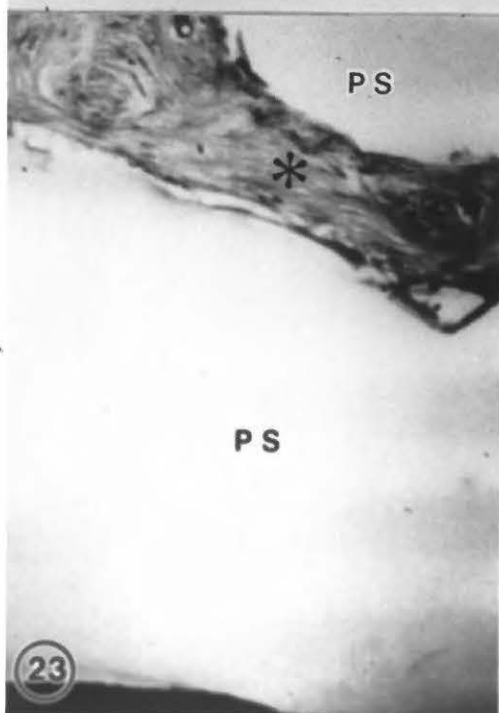
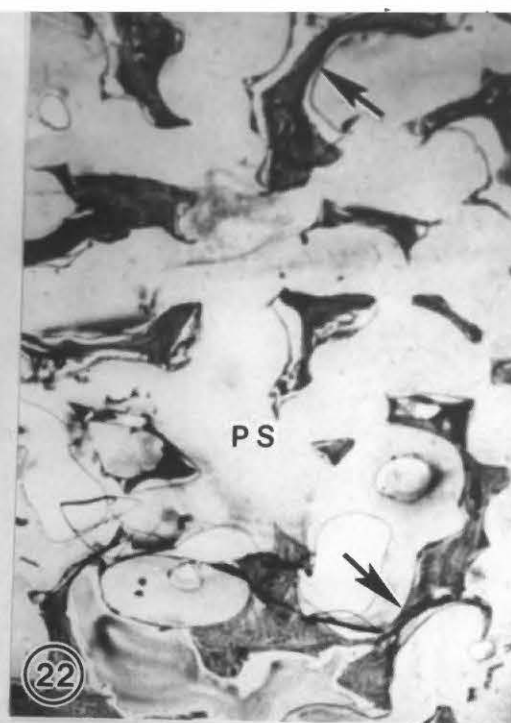


PLATE 7

FIGURE 25: Photomicrograph of a histologic section 42 days following implantation of PPSF-DBP showing interconnection and fusion of the DBP particles (arrows) (H & E). (138 X)

FIGURE 26: Photomicrograph of a histologic section 42 days following implantation of PPSF+DBP showing the DBP particles (arrow) with remnants of osteocytes (arrowhead) in their lacunae (H & E). (138 X)

FIGURE 27: Photomicrograph of a coronal section of the edentulous mandible 60 days following PPSF implantation. Note the connective tissue within the micropores (arrow), one of the drilled holes (asterisk) and surrounding the implant (arrowhead).

FIGURE 28: Photomicrograph of a histologic section 60 days following implantation of PPSF showing the fibrous tissue within the pores (arrowhead). Note that the newly formed bone (arrow) grew for a short distance within the pores of PPSF (H & E). (55 X)

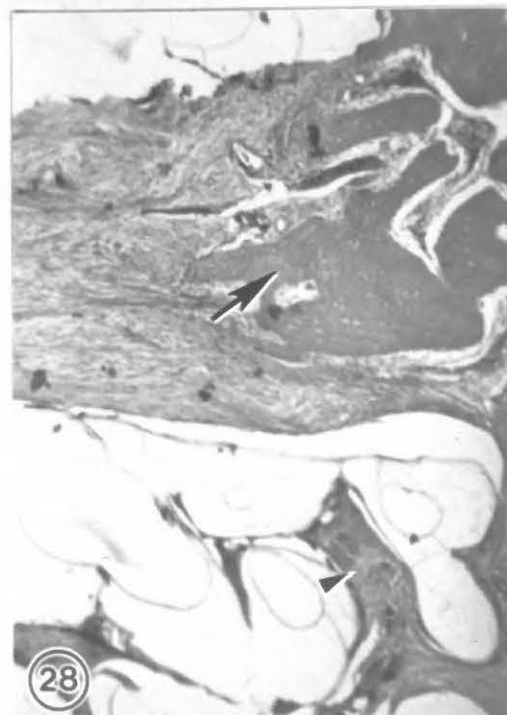
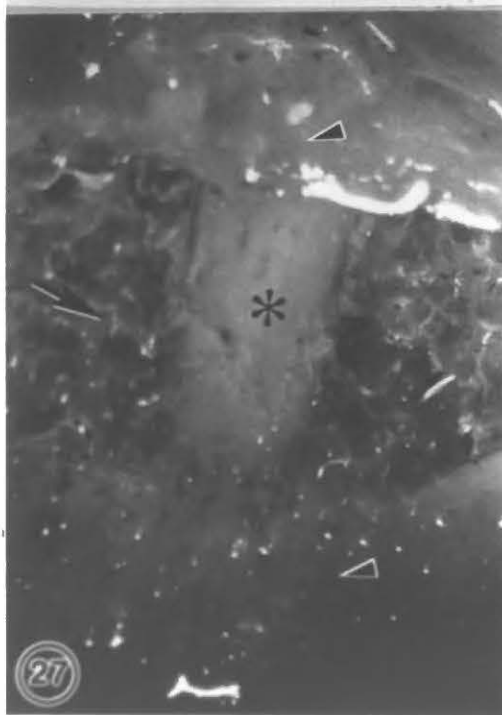
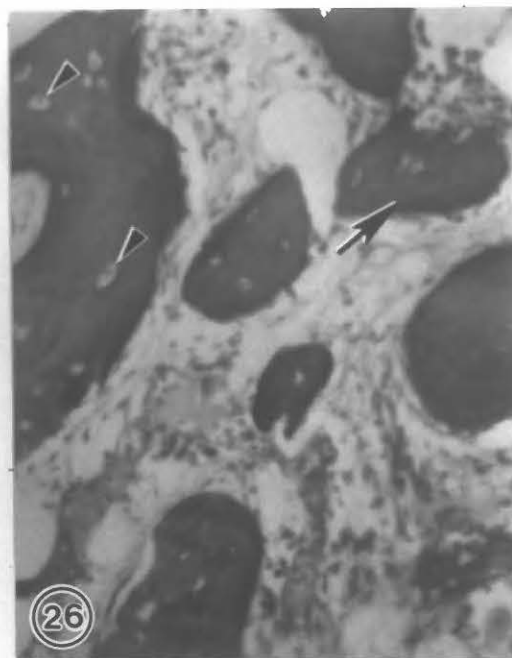
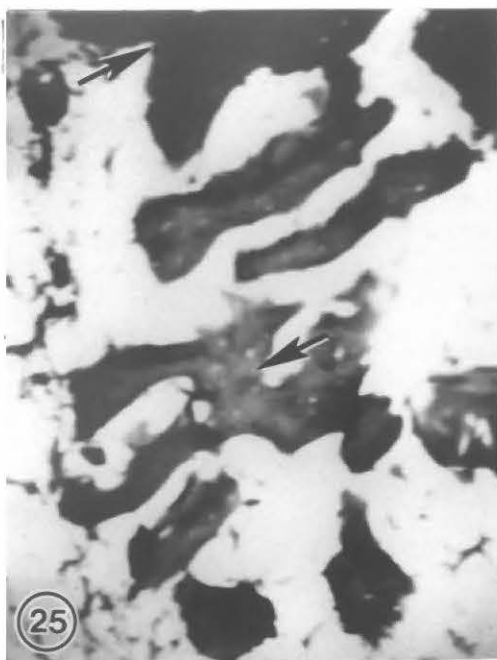


PLATE 8

FIGURE 29: Photomicrograph of a histologic section 60 days following implantation of PPSF showing the newly formed bone (arrow) surrounded with fibrous tissue (asterisk). Also note the presence of bone marrow (arrowhead) (H & E). (70 X)

FIGURE 30: Photomicrograph of a histologic section 60 days following implantation of PPSF showing the newly formed bone containing osteocytes (arrowhead) and covered with osteoblasts (arrow) (H & E). (86 X)

FIGURE 31: Photomicrograph of a histologic section 60 days following implantation of PPSF showing the advancing edge of bone (arrow) adjacent to polysulfone (PS) (H & E). (34 X)

FIGURE 32: Photomicrograph of a histologic section 60 days following implantation of PPSF showing the advancing edge of bone contained osteocytes (arrowhead), marrow (asterisk) and covered with osteoblasts (arrow) (H & E). (220 X)

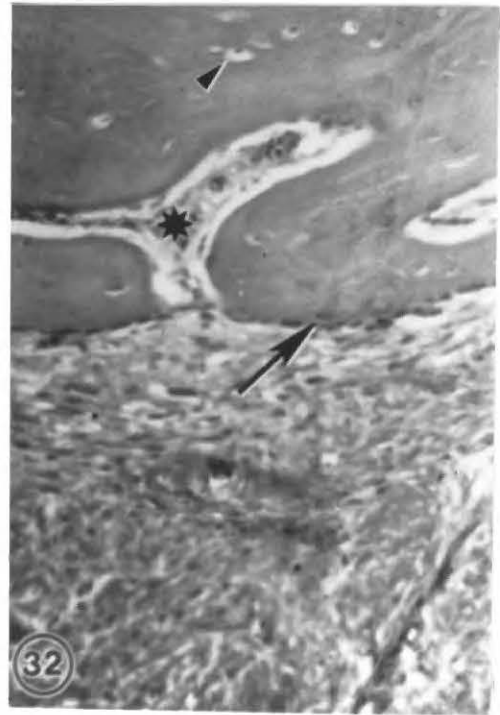
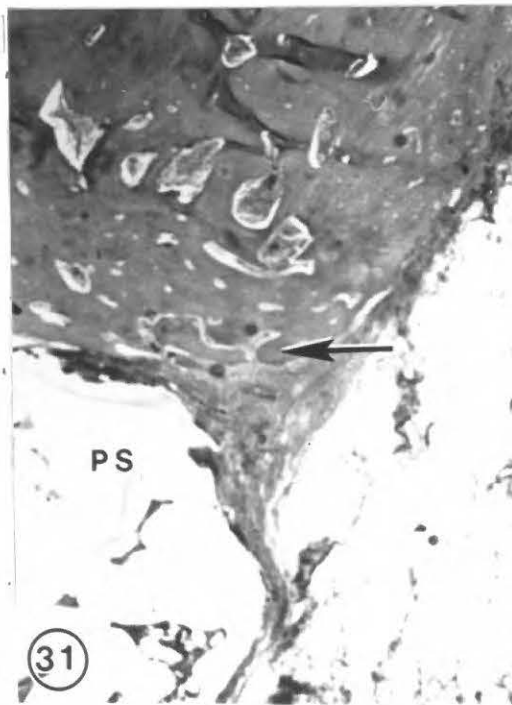
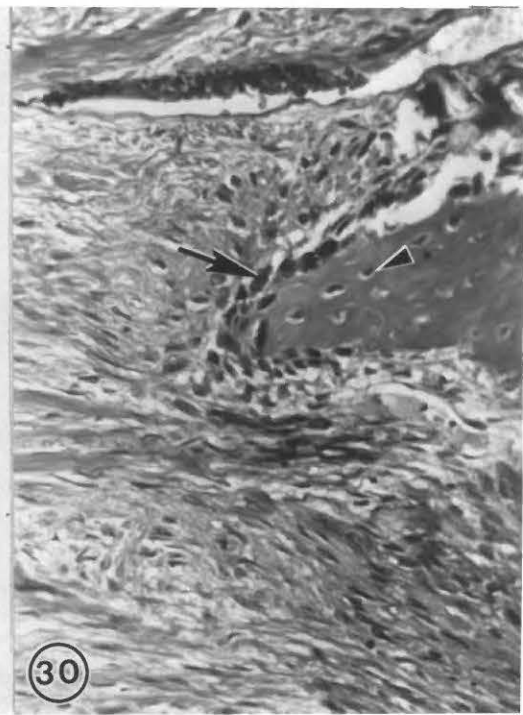
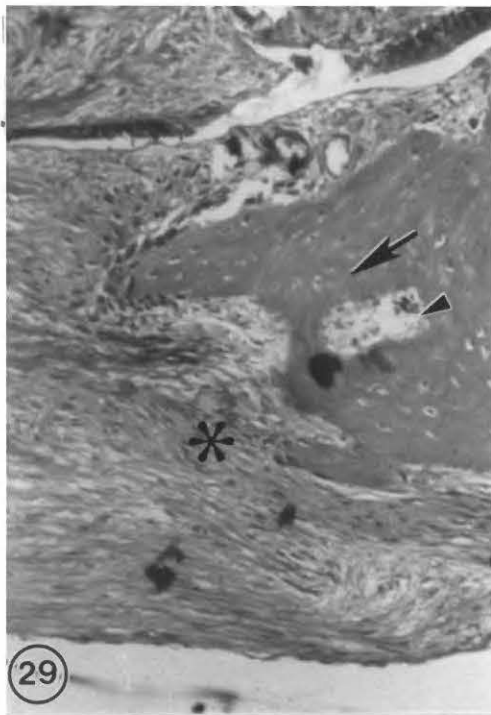


PLATE 9

FIGURE 33: Photomicrograph of a histologic section 60 days following implantation of PPSF showing bone-PPSF interface (arrow) (H & E). (34 X)

FIGURE 34: Photomicrograph of a histologic section 60 days following implantation of PPSF showing the fibrous tissue (arrows) within the micropores of the implant interconnecting and surrounding the polysulfone particles (PS) (H & E). (34 X)

FIGURE 35: Photomicrograph of a histologic section 60 days following implantation of PPSF showing the fibrous tissue around (arrow) the polysulfone was continuous with the fibrous tissue (arrowhead) within the micropores of polysulfone (PS) (H & E). (55 X)

FIGURE 36: Photomicrograph of a histologic section 60 days following implantation of PPSF showing the organization of the fibrous tissue (arrow) along the contours of the polysulfone (PS) particles (H & E). (138 X)

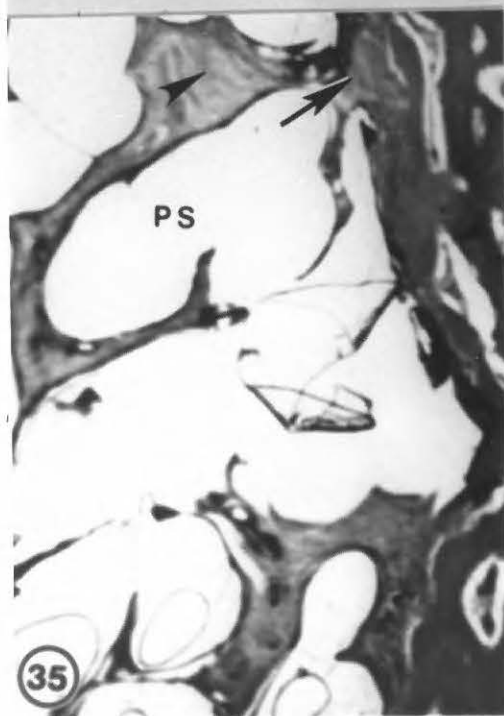
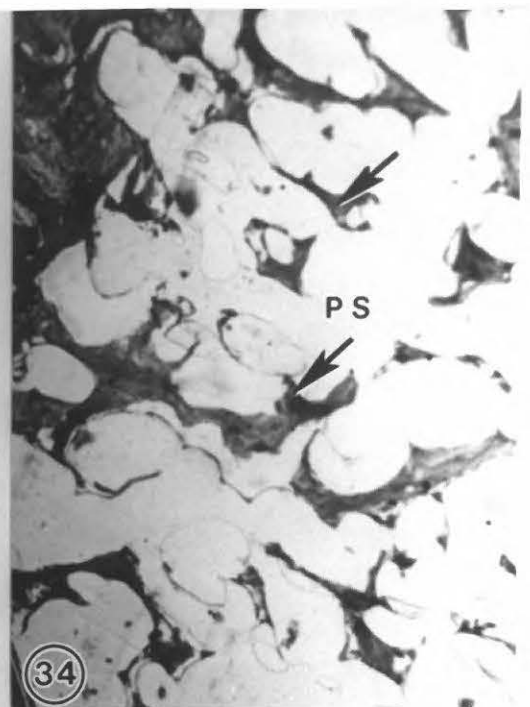


PLATE 10

- FIGURE 37: Photomicrograph of a histologic section 60 days following implantation of PPSF showing the loose (arrow) and dense (asterisk) connective tissue within the pores of the polysulfone (H & E). (55 X)
- FIGURE 38: Photomicrograph of a histologic section 60 days following implantation of PPSF showing the collagen fibers, (asterisk) fibroblasts (arrow) and multinucleated giant cells (arrowhead) within the pores of the polysulfone. (H & E). (55 X)
- FIGURE 39: Photomicrograph of a undecalcified histologic section 60 days following implantation of PPSF showing bone (blue) and osteoid (red) within the pores of the polysulfone (PS) (M. Masson). (344 X)
- FIGURE 40: Photomicrograph of an undecalcified histologic section 60 days following implantation of PPSF showing bone (blue) and osteoid (red) adjacent to the polysulfone (PS) (M. Masson). (344 X)

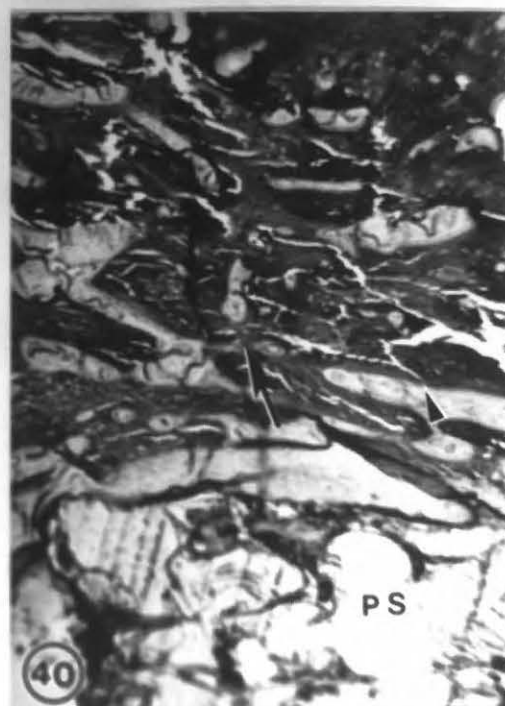
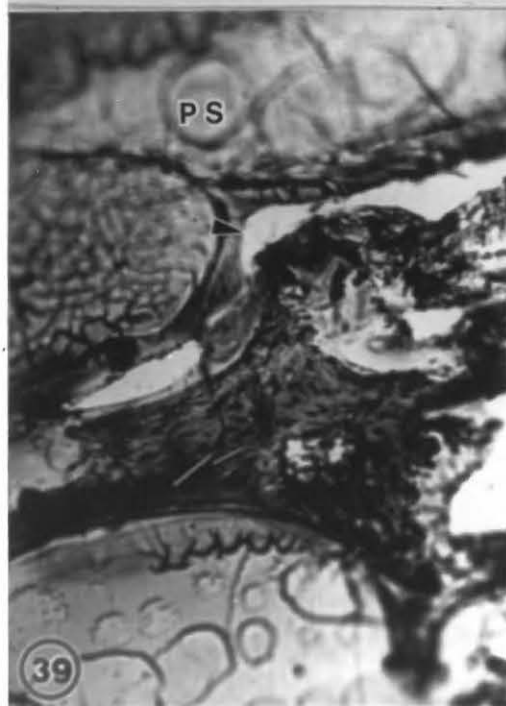
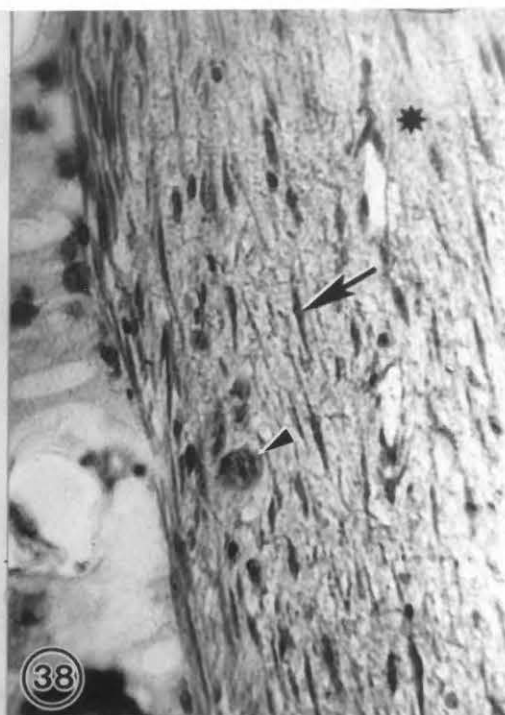
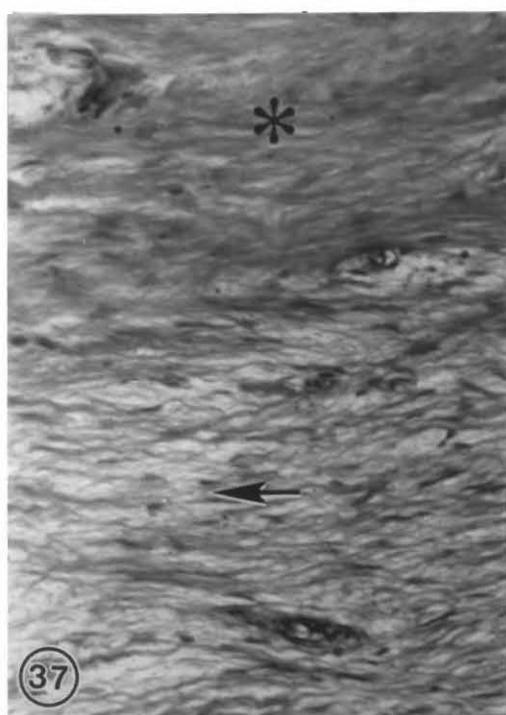


PLATE 11

FIGURE 41: Photomicrograph of a coronal section of the edentulous mandible 60 days following implantation of DBP + PPSF showing the connective tissue within the micropores (arrows) and around (arrowhead) the implant. Note the marble-like bone appearance within one of the macropores (asterisk).

FIGURE 42: Photomicrograph of a histologic section 60 days following implantation of DBP + PPSF showing the newly formed bone within the pores (arrow) and around the polysulfone (arrowhead) (H & E). (34 X)

FIGURE 43: Photomicrograph of a histologic section 60 days following implantation of DBP + PPSF showing the polysulfone (PS) completely covered by bone (arrow). Note bone (arrowhead) and fibrous tissue (asterisk) within the pores of PPSF (H & E). (55 X)

FIGURE 44: Photomicrograph of a histologic section 60 days following implantation of DBP + PPSF showing the polysulfone (PS) covered with bone (arrow) except a very small area (arrowhead). Note the presence of fibrous tissue (asterisk) and bone (arrow) in the pores of polysulfone (H & E). (55 X)

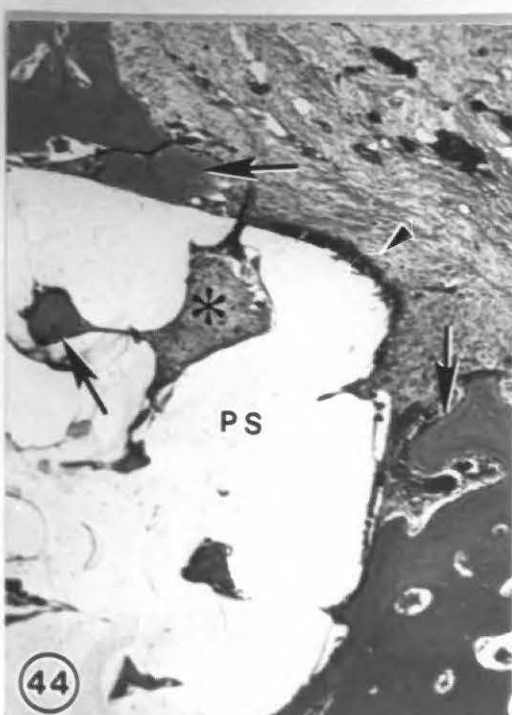
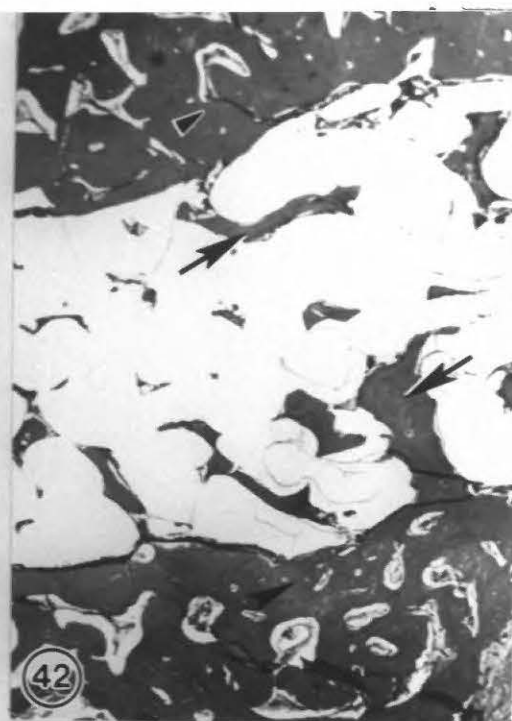
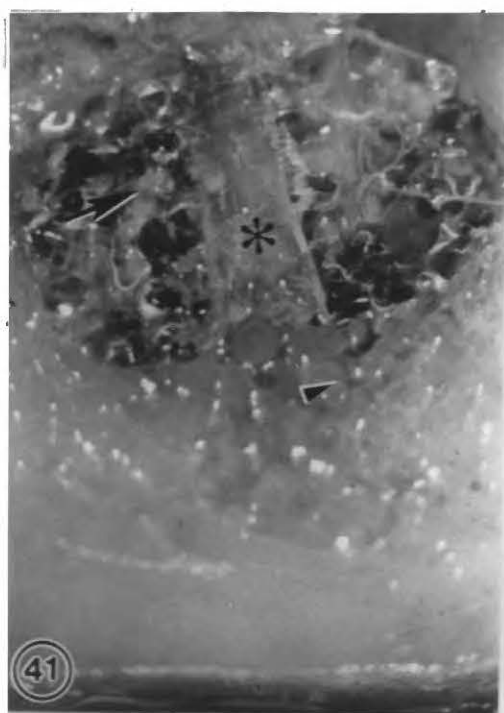


PLATE 12

FIGURE 45: Photomicrograph of a histologic section 60 days following implantation of DBP + PPSF showing the advancing edge of the newly formed bone (arrow) adjacent to the polysulfone (PS) (H & E). (34 X)

FIGURE 46: Photomicrograph of a histologic section 60 days following implantation of DBP + PPSF showing that the advancing edge of the newly formed bone contained osteocytes (arrowhead) and was covered with osteoblasts (arrow) (H & E). (220 X)

FIGURE 47: Photomicrograph of a histologic section 60 days following implantation of DBP + PPSF showing the bone-polysulfone interface (arrow). Note the vascular marrow (arrowhead) within the bone the apparent osseous integration of the polysulfone and bone (H & E). (55 X)

FIGURE 48: Photomicrograph of a histologic section 60 days following implantation of DBP + PPSF showing the newly formed bone and fibrous tissue (arrow) blend together within and around polysulfone (PS) (H & E). (41 X)

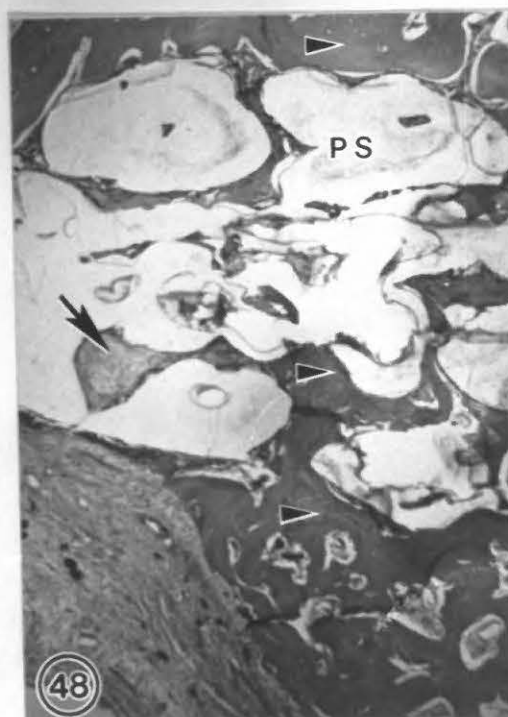
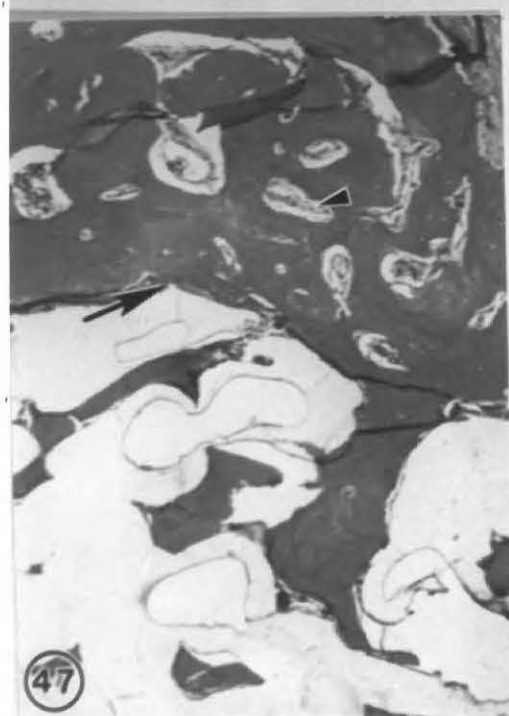
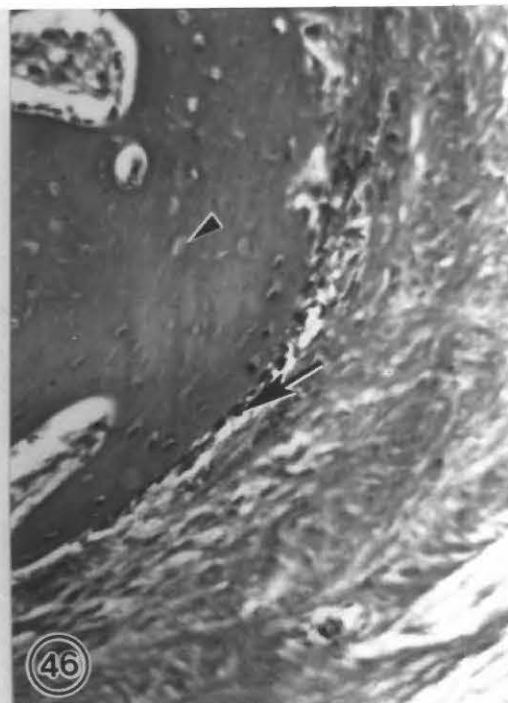
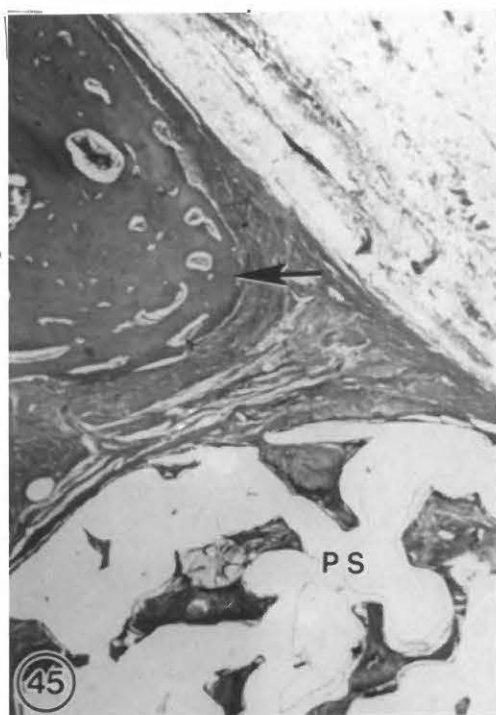


PLATE 13

FIGURE 49: Photomicrograph of a histologic section 60 days following implantation of DBP + PPSF showing that the newly formed bone adjacent to the implant contained osteocytes (arrow) and was covered with osteoblasts (arrowhead) (H & E). (55 X)

FIGURE 50: Photomicrograph of a histologic section 60 days following implantation of DBP + PPSF showing that a bone-polysulfone interface contained marrow (arrow) and was in close association with the polysulfone (PS) surface (H & E). (41 X)

FIGURE 51: Photomicrograph of a histologic section 60 days following implantation of DBP + PPSF showing direct contact (arrow) between the bone (arrowhead) and polysulfone (PS) with no intervening connective tissue (H & E). (55 X)

FIGURE 52: Photomicrograph of a histologic section 60 days following implantation of DBP + PPSF showing a thin fibrous layer (arrow) intervenes between the bone (arrowhead) and polysulfone (PS) (H & E). (55 X)

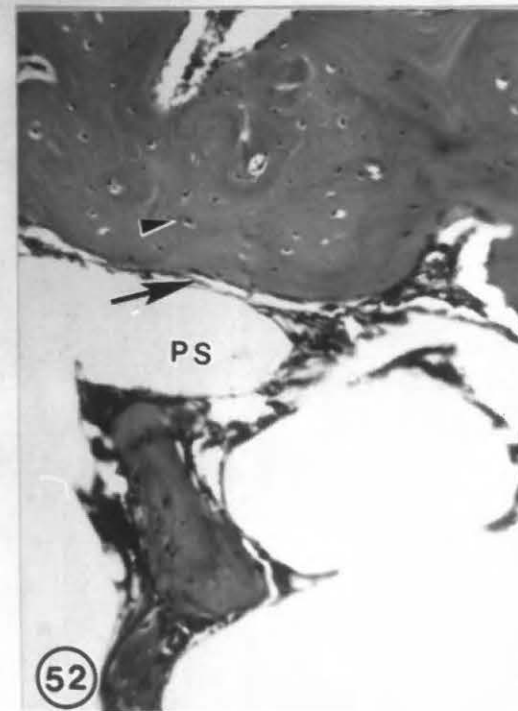
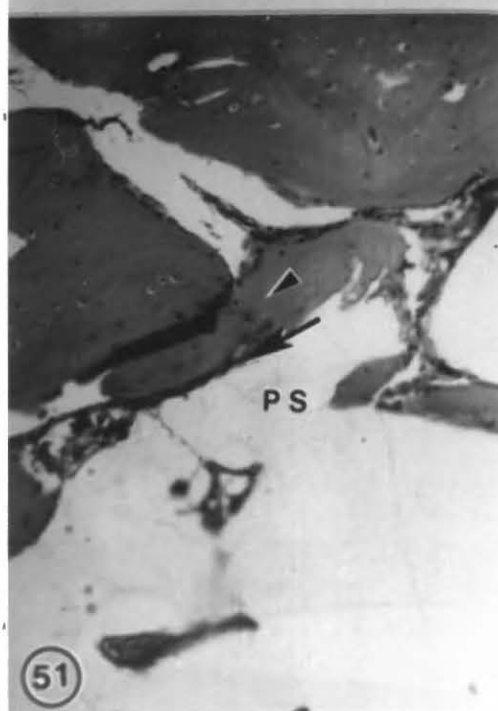
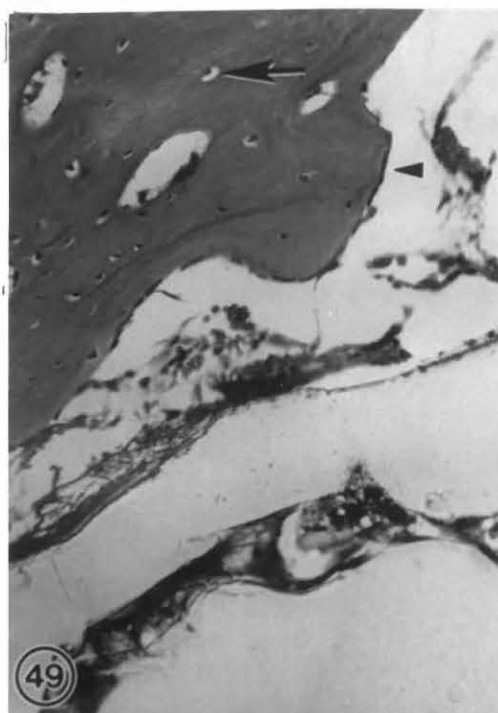


PLATE 14

FIGURE 53: Photomicrograph of a histologic section 60 days following implantation of DBP + PPSF showing a micropore that contain bone only. Note the osteocytes (arrow) in their lacunae (H & E). (344 X)

FIGURE 54: Photomicrograph of a histologic section 60 days following implantation of DBP + PPSF showing the osteoblasts (arrow) in juxtaposition to the bone surface within the micropores of polysulfone (PS) (H & E). (86 X)

FIGURE 55: Photomicrograph of a histologic section 60 days following implantation of DBP + PPSF showing blood vessels (arrow) within the pores of the polysulfone (H & E). (138 X)

FIGURE 56: Photomicrograph of a histologic section 60 days following implantation of DBP + PPSF showing a large blood vessel (arrow) just outside the fibrous layer which surrounded the polysulfone (H & E). (138 X)

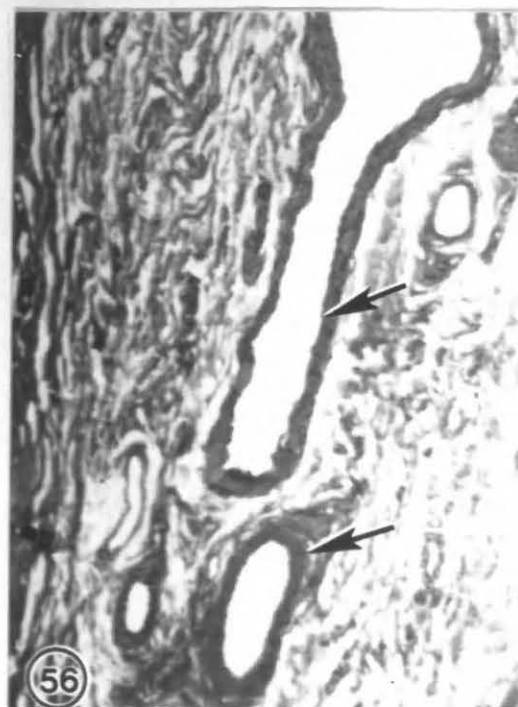
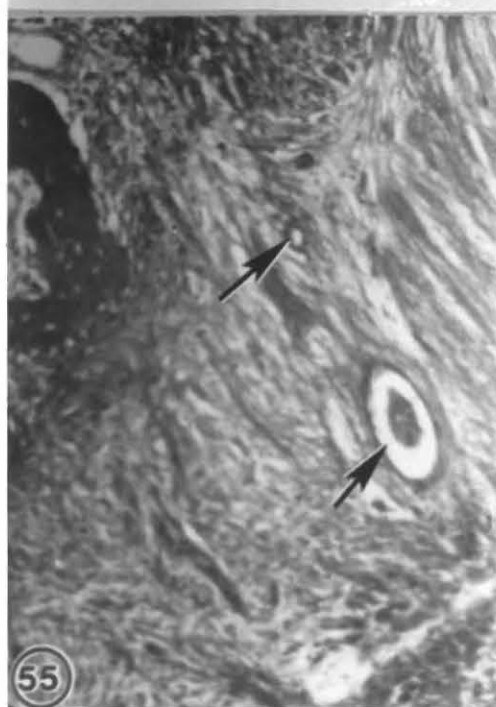
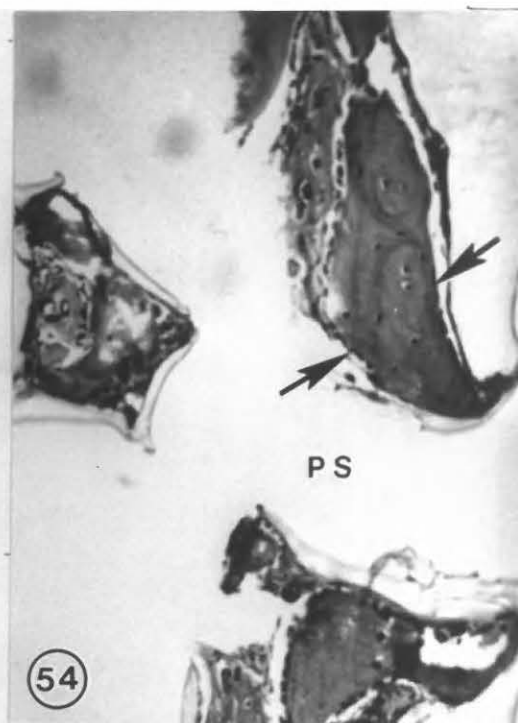
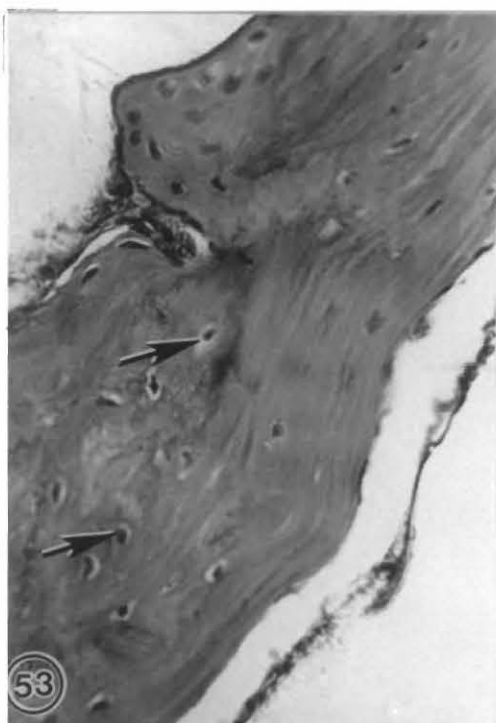


PLATE 15

FIGURE 57: Photomicrograph of a histologic section 60 days following implantation of DBP + PPSF showing blood vessels (arrow) on the mucosal tissue covering the polysulfone (H & E). (34 X)

FIGURE 58: Photomicrograph of a histologic section 60 days following implantation of DBP + PPSF showing the gingiva (arrow) overlying the implant area with no evidence of inflammatory reaction (H & E). (55 X)

FIGURE 59: Photomicrograph of a histologic undecalcified section 60 days following implantation of PPSF + DBP showing bone (blue), arrow) and osteoid (red, arrowhead) within the pores of the polysulfone (PS) (Modified Masson stain). (344 X)

FIGURE 60: Photomicrograph of a histologic section 60 days following implantation of PPSF - DBP showing bone (asterisk) and osteoid (arrow) at the polysulfone surface (PS) and within the micropores (arrowhead) (Modified Masson stain). (138 X)

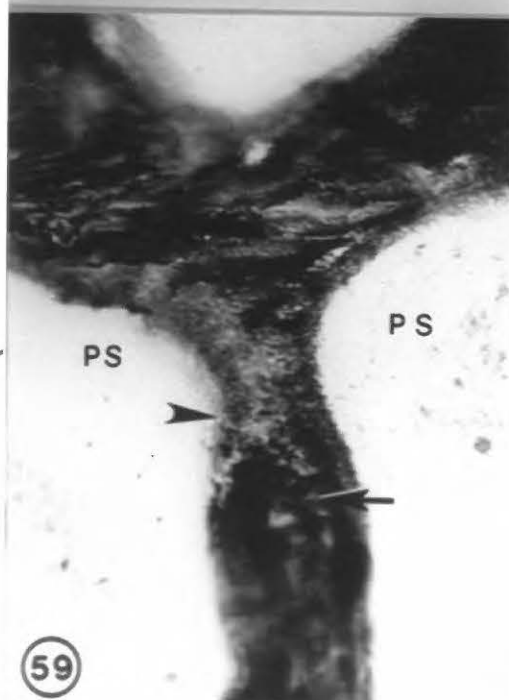
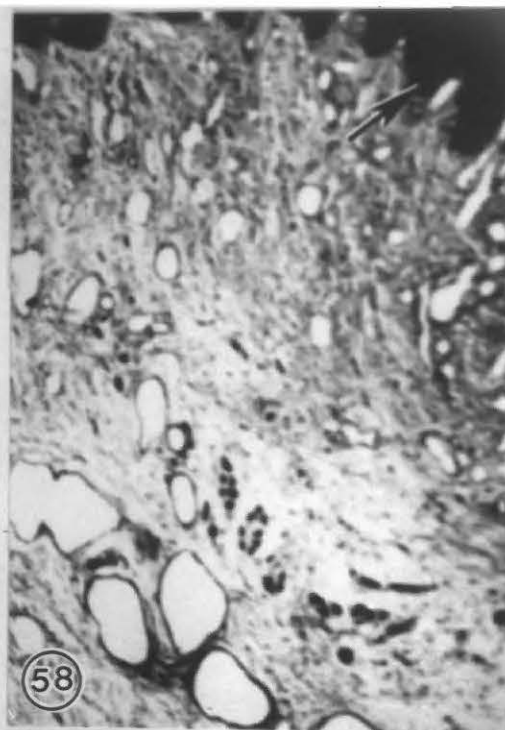
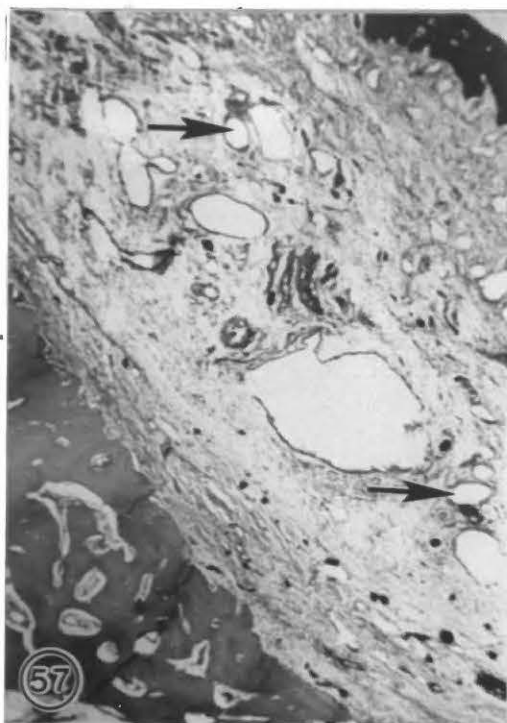


PLATE 16

FIGURE 61: Photomicrograph of a histologic section 60 days following implantation of DBP + PPSF showing bone-polysulfone interface (arrow) (M. Masson). (138 X)

FIGURE 62: Photomicrograph of a fluorescent histologic unstained section from an animal which received double tetracycline injection and sacrificed 60 days following implantation of DBP + PPSF, showing the newly formed bone (arrow) within the micropores of the polysulfone (PS). (41 X)

FIGURE 63: Photomicrograph of the previous section at higher magnification showing the the intense fluorescence of the newly formed bone (arrow) within the micropores of the polysulfone (PS). (55 X)

FIGURE 64: Photomicrograph of a fluorescent histologic unstained section from an animal which received the double tetracycline label 60 days following implantation of DBP + PPSF. The fluorescence was diffuse (arrow) within the micropores of polysulfone (PS). (86 X)

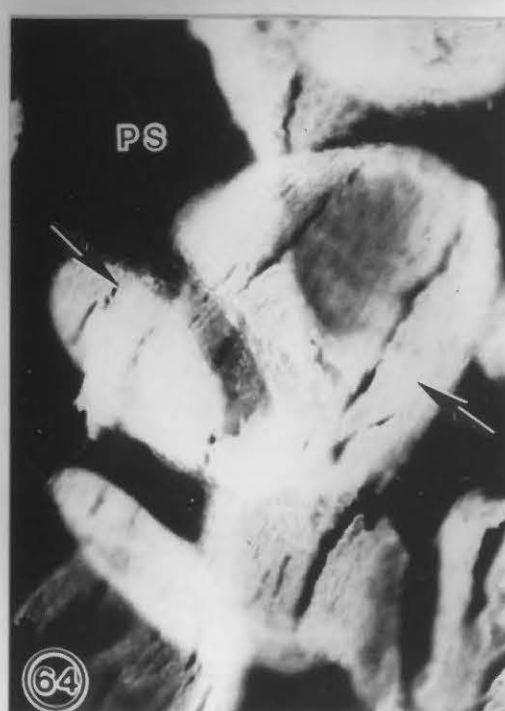
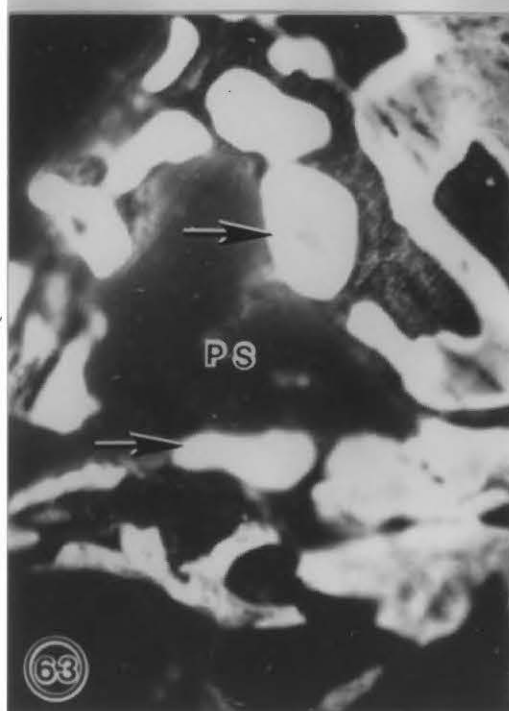


PLATE 17

FIGURE 65: Photograph showing the partially edentulous augmented (arrow) mandible 90 days following implantation of polysulfone.

FIGURE 66: Photograph showing the partially edentulous augmented mandible 90 days following implantation of polysulfone showing the implant on the outer top surface (arrow) of the edentulous ridge.

FIGURE 67: Higher magnification photomicrograph of the partially edentulous augmented mandible 90 days following implantation of polysulfone, showing normal covering mucosa (asterisk) overlying the implant.

FIGURE 68: Photomicrograph of a coronal section of the edentulous mandible 90 days following implantation of PPSF showing the connective tissue within the micropores (asterisk) and around the implant (arrowhead). Note the normal mucosa (arrow) overlying the implant.

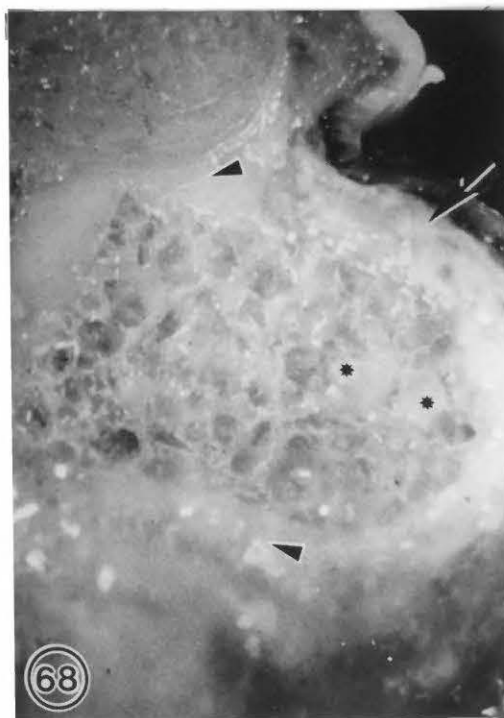


PLATE 18

FIGURE 69: Scanning electron micrograph of PPSF block showing the polysulfone particles (asterisk) and the micropores (arrowhead). (20 X)

FIGURE 70: Scanning electron micrograph of PPSF block showing the size and arrangement of the polysulfone particles (asterisk). (49 X).

FIGURE 71: Scanning electron micrograph of PPSF block showing the interconnecting micropores (arrowhead) and tunnels between the polysulfone particles (asterisk). (100 X)

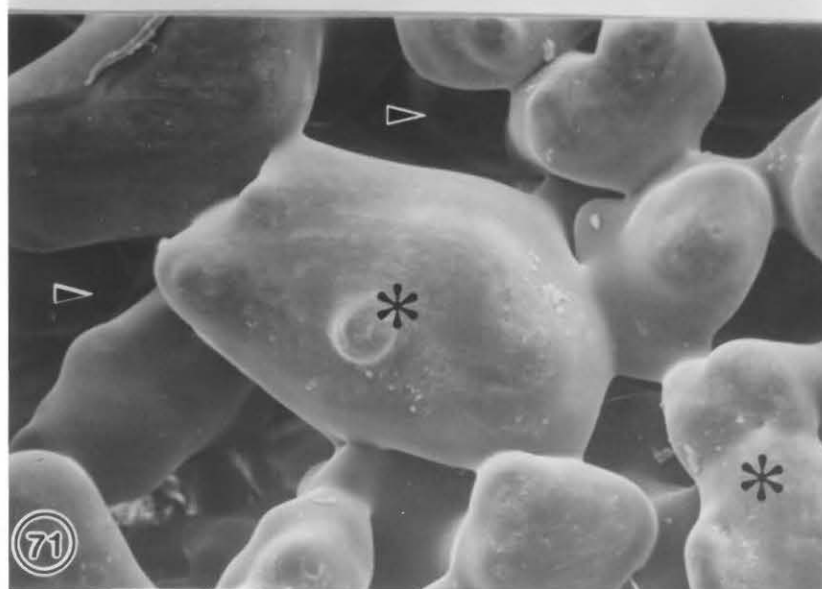
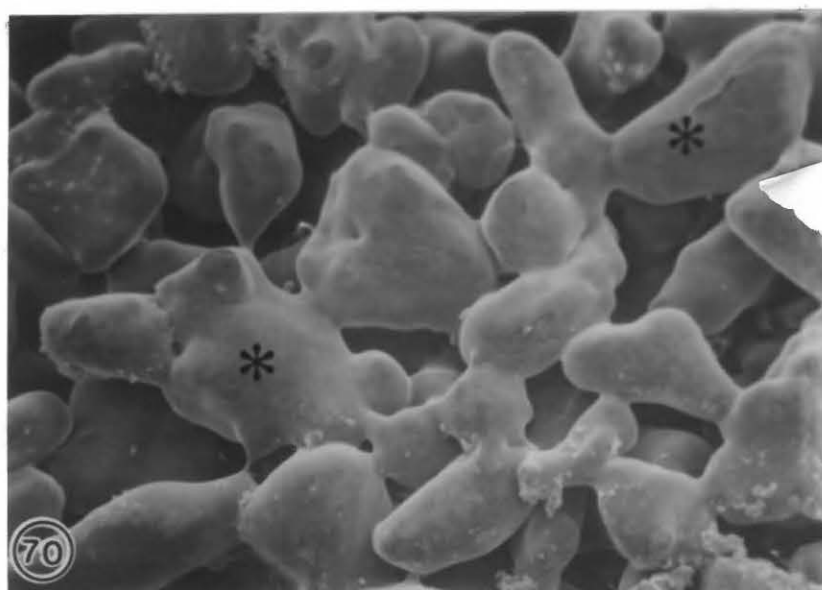
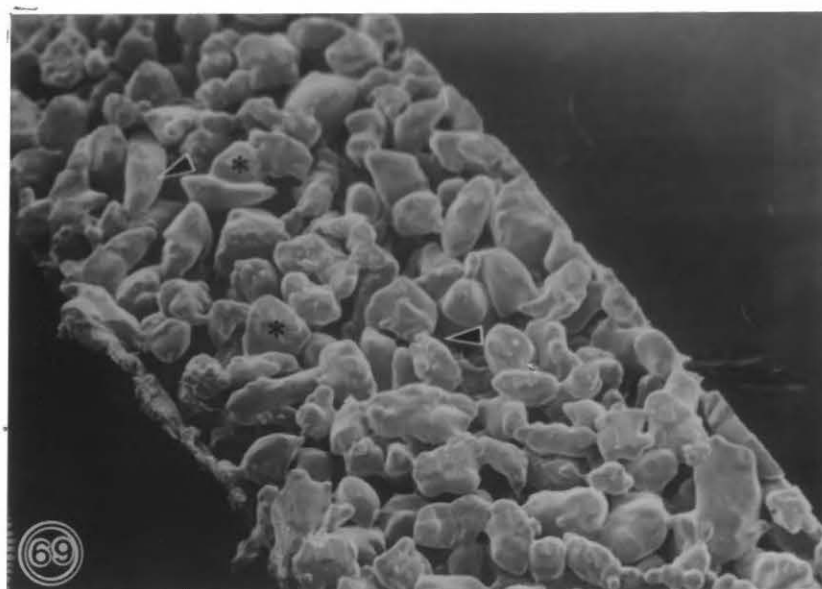


PLATE 19

FIGURE 72: Scanning electron micrograph of PPSF block showing the smooth contour and shape of polysulfone particles (asterisk). (200 X)

FIGURE 73: Scanning electron micrograph of PPSF 90 days following implantation showing the polysulfone (asterisk) completely surrounded and penetrated with connective tissue (arrowhead) and bone (arrow). (15 X)

FIGURE 74: Scanning electron micrograph of PPSF 90 days following implantation showing the fibrous tissue (asterisk) within the pores and around the polysulfone particles (arrowhead). (90 X)

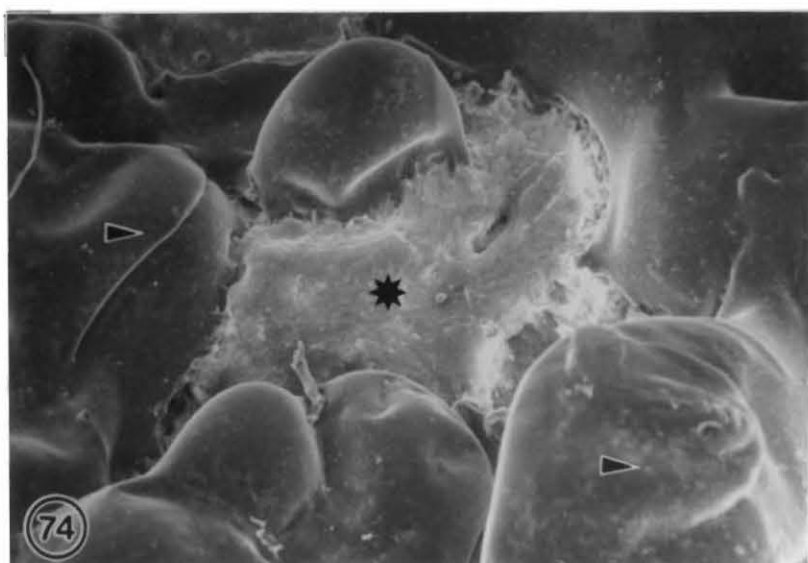
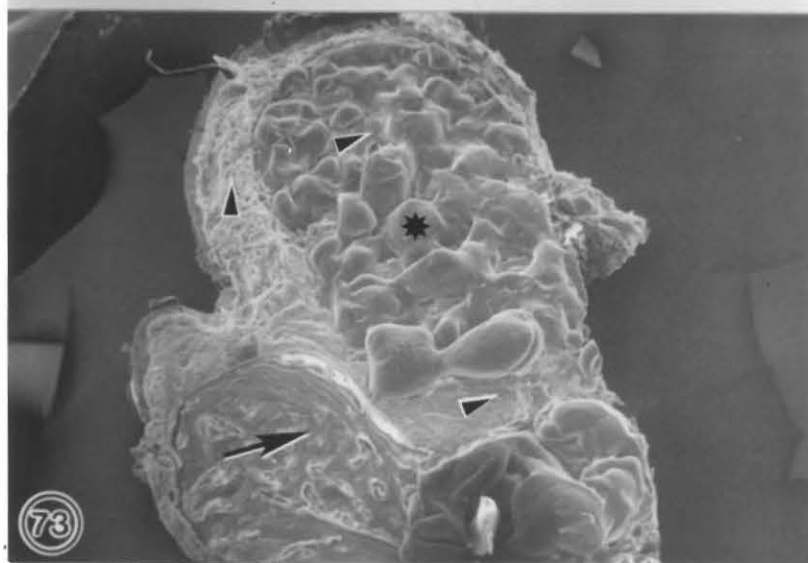
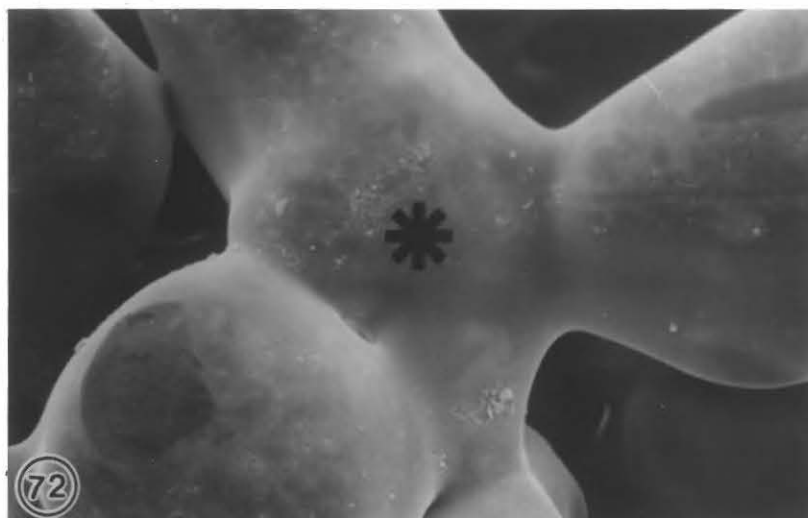


PLATE 20

FIGURE 75: Scanning electron micrograph of PPSF 90 days following implantation showing the interconnecting fibrous tissue (asterisk) in between the polysulfone particles (arrowhead). (100 X)

FIGURE 76: Scanning electron micrograph of PPSF 90 days following implantation showing the parallel arrangement of collagen fibers (arrows) within the pores of the polysulfone. (620 X)

FIGURE 77: Scanning electron micrograph of PPSF 90 days following implantation showing bundles of collagen fibers (arrow) within the pores of the polysulfone. (580 X)

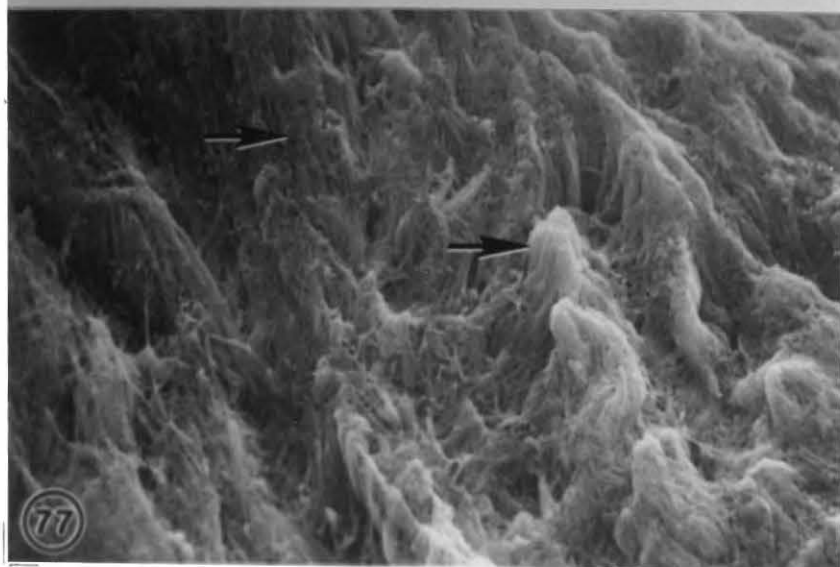
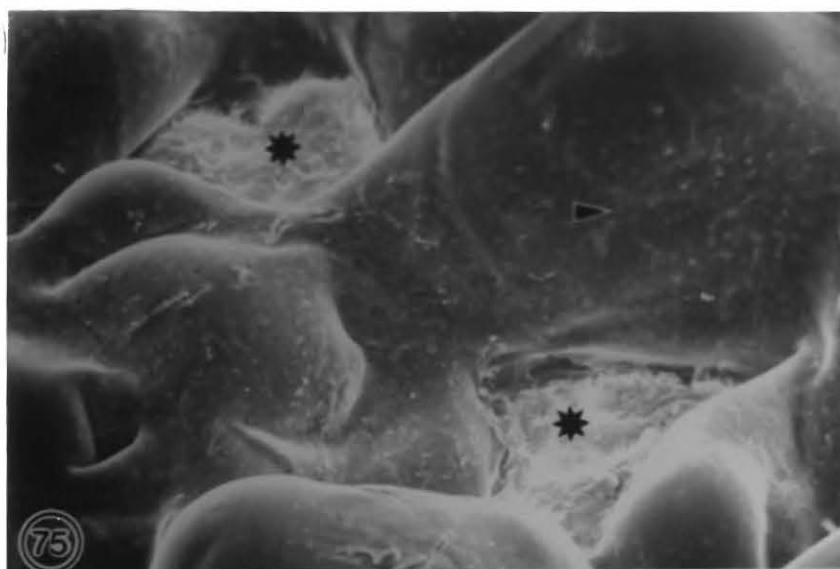


PLATE 21

FIGURE 78: Scanning electron micrograph of PPSF 90 days following implantation showing the network arrangement of collagen fibers (arrow). (5,800 X)

FIGURE 79: Scanning electron micrograph of PPSF 90 days following implantation showing the collagen fibers (arrowhead) and fibroblasts (arrow) within the pores of the polysulfone. (10,000 X)

FIGURE 80: Scanning electron micrograph of PPSF 90 days following implantation showing the close adaptation of the connective tissue (asterisk) to the polysulfone surface (arrowhead). (110 X)

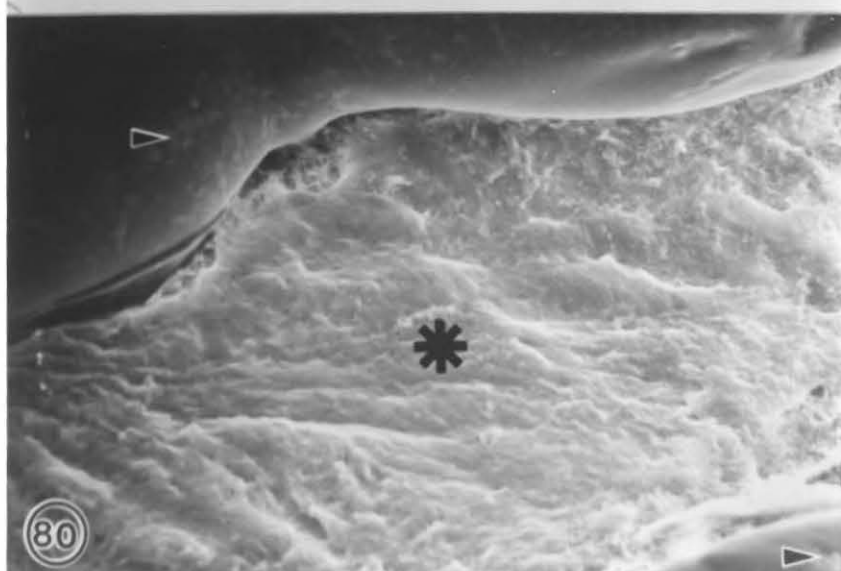
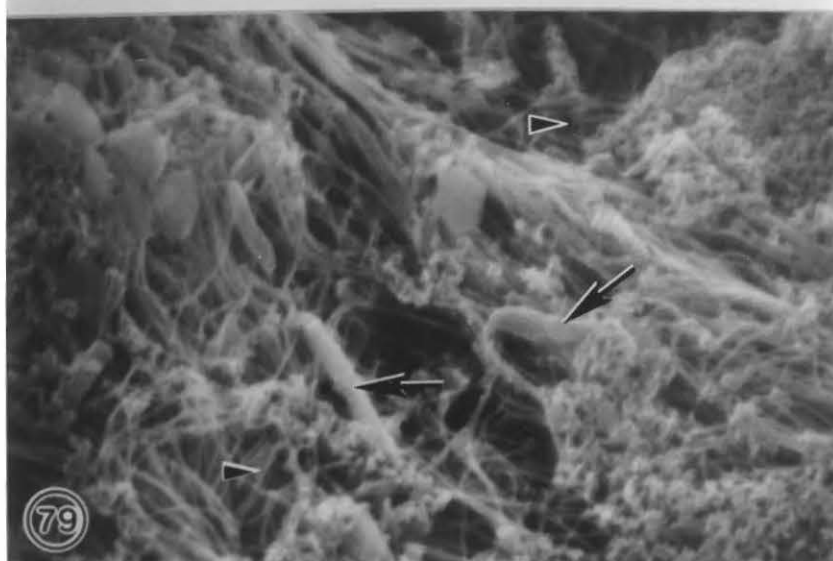
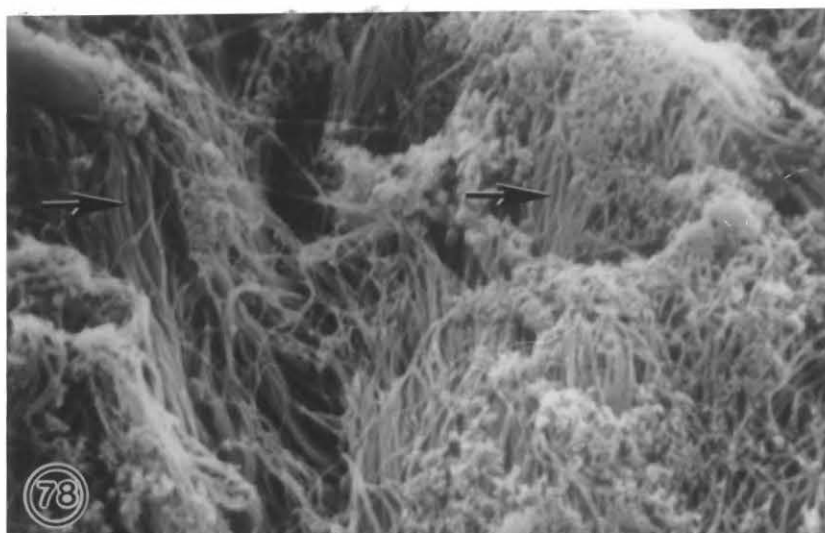


PLATE 22

FIGURE 81: Scanning electron micrograph of PPSF 90 days following implantation showing penetration of bone (asterisk) into the micropores of polysulfone (arrow). (70 X)

FIGURE 82: Scanning electron micrograph of PPSF 90 days following implantation at higher magnification showing bone within the micropores of the polysulfone (asterisk). Note the Haversian system (arrow) on the bone surface. (160 X)

FIGURE 83: Scanning electron micrograph of PPSF 90 days following implantation showing bone (arrow) surrounding polysulfone (asterisk). (61 X)

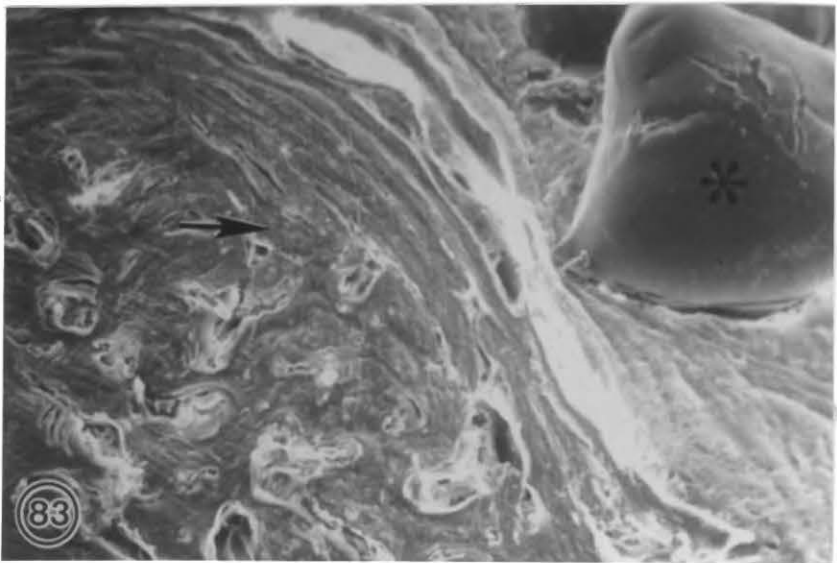
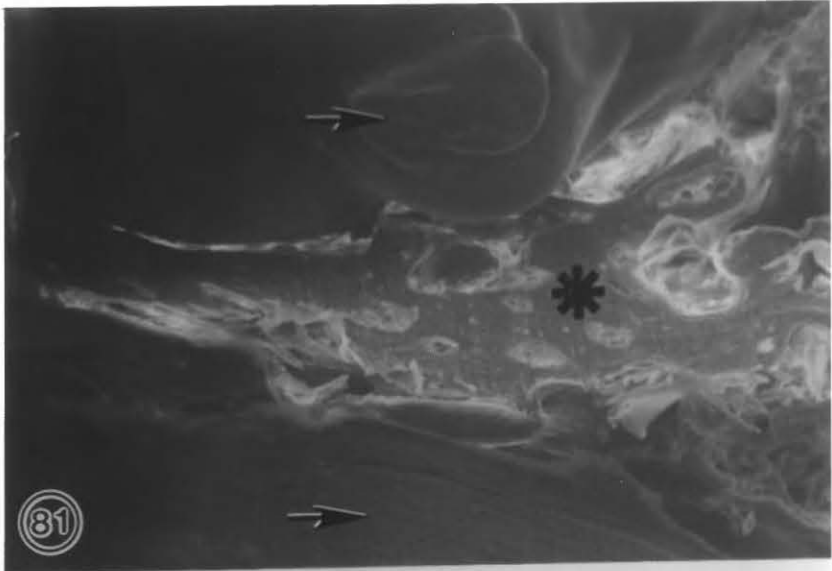


PLATE 23

FIGURE 84: Scanning electron micrograph of PPSF 90 days following implantation showing the epithelial (arrow) and submucosal (arrowhead) tissues covering the polysulfone (asterisk). (90 X)

FIGURE 85: Scanning electron micrograph of PPSF 90 days following implantation showing the mucosal covering (arrow) in close adaptation with the fibrous tissue (arrowhead) within the polysulfone (asterisk). (140 X)

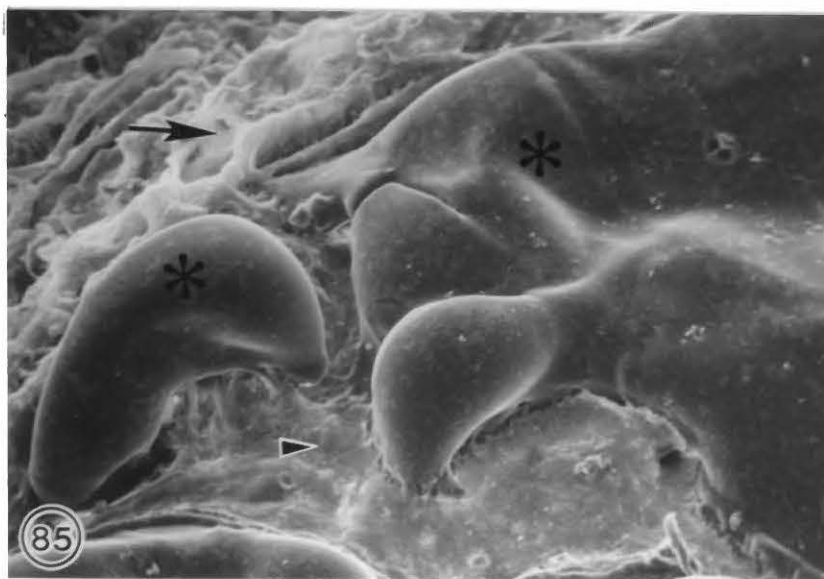
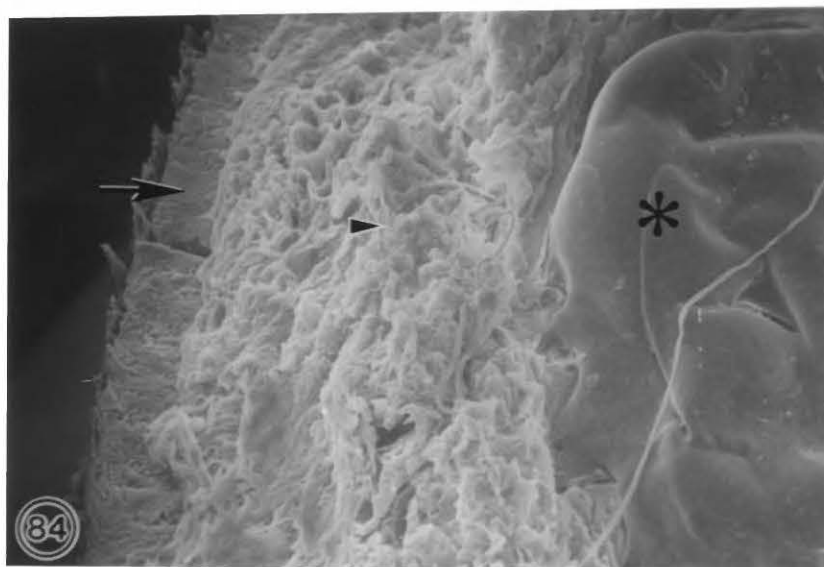


PLATE 24

FIGURE 86: Photomicrograph of a histologic section 90 days following implantation of PPSF showing the interconnecting fibrous tissue (arrow) within the micropores of the polysulfone (PS) (H & E). (44 X)

FIGURE 87: Photomicrograph of a histologic section 90 days following implantation of PPSF showing the collagen fibers (arrowhead) and fibroblasts (arrow) within the pores of polysulfone (PS) (H & E). (44 X)

FIGURE 88: Photomicrograph of a histologic section 90 days following implantation of PPSF showing the blood vessels (arrowhead) and arrangement of collagen fibers (arrow) within the pores of the polysulfone (PS) (H & E). (44 X)

FIGURE 89: Photomicrograph of a histologic section 90 days following implantation of PPSF showing the presence of bone (arrowhead) and fibrous tissue (arrow) within the same micropore of the polysulfone (PS) (H & E). (44 X)

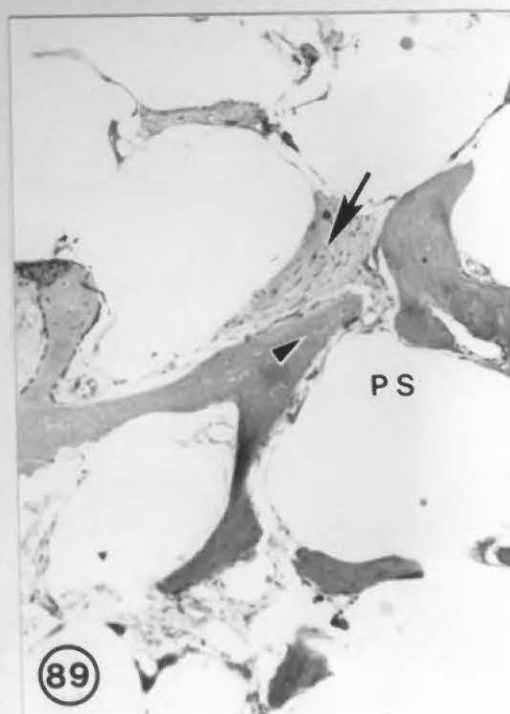
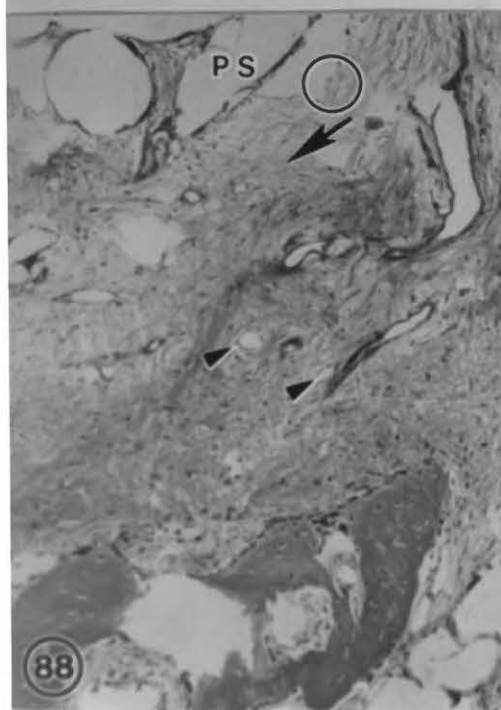
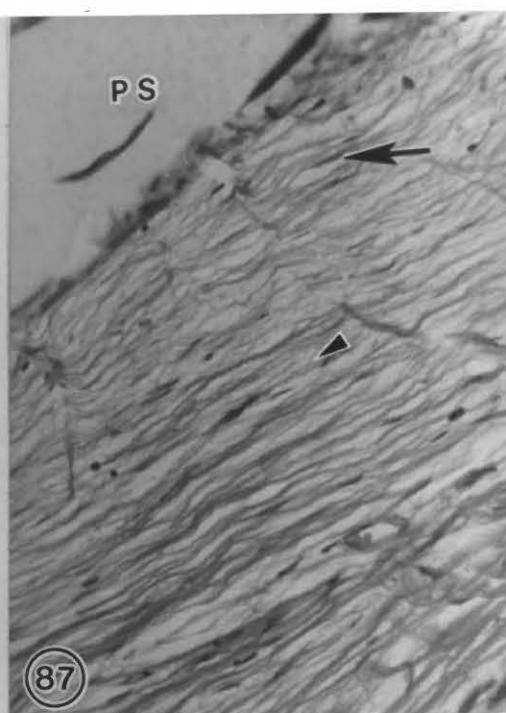
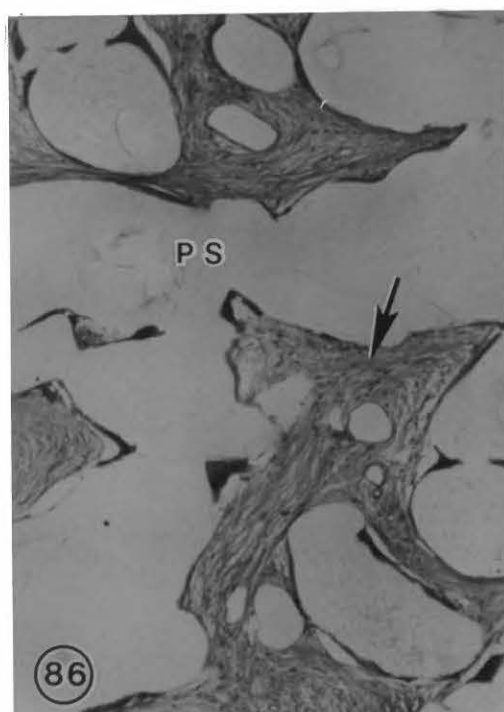


PLATE 25

- FIGURE 90: Photomicrograph of a histologic section 90 days following implantation of PPSF showing the newly formed bone (arrowhead) blended and continuous with the fibrous tissue (arrow) within the micropores of polysulfone (PS) (H & E). (44 X)
- FIGURE 91: Photomicrograph of a histologic section 90 days following implantation of PPSF showing the newly formed bone (arrow) within the micropores and around the polysulfone particles (PS) (H & E). (34 X)
- FIGURE 92: Photomicrograph of a histologic section 90 days following implantation of PPSF showing osteoblasts (arrow) covering the newly formed bone (arrowhead) within the micropores of the polysulfone (PS) (H & E). (352 X)
- FIGURE 93: Photomicrograph of a histologic section 90 days following implantation of PPSF showing osteocytes (arrowhead) and evidence of remodelling (arrow) of the newly formed bone within the micropores of polysulfone (H & E). (344 X)

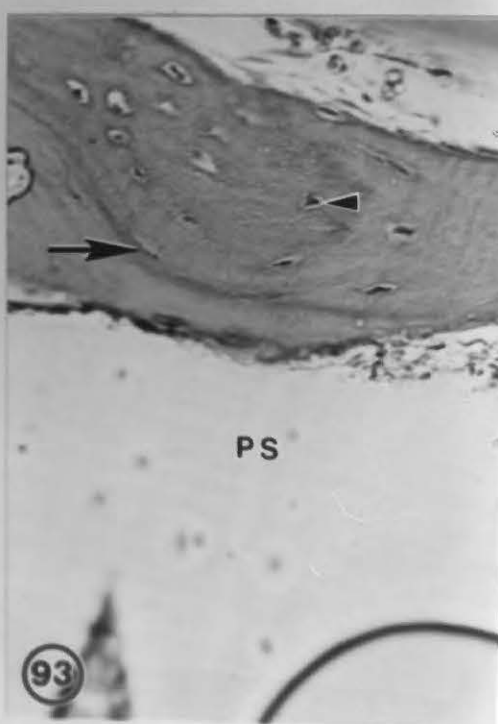
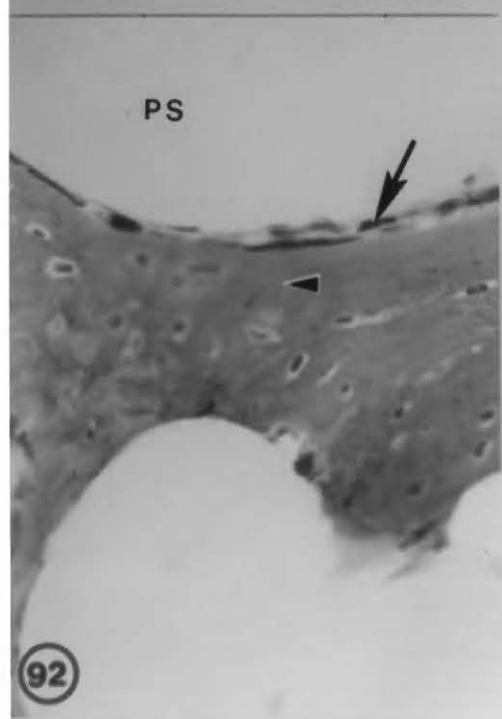
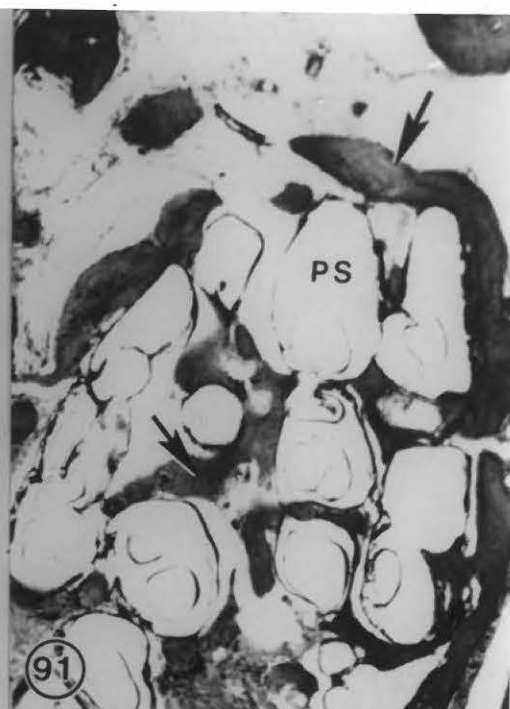
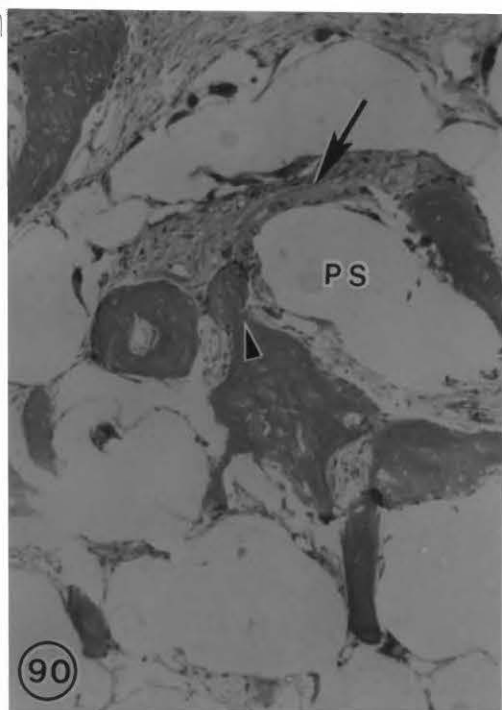


PLATE 26

FIGURE 94: Photomicrograph of an undecalcified histologic section 90 days following implantation of PPSF showing interconnecting bone (blue) arrowhead) and osteoid (red) arrow) within the pores of the polysulfone (PS) (Modified Masson stain). (55 X)

FIGURE 95: Photomicrograph of an undecalcified histologic section 90 days following implantation of PPSF showing the newly formed bone (arrow) and osteoid (arrowhead) within the micropores of the polysulfone (PS) (Modified Masson stain). (55 X)

FIGURE 96: Photomicrograph of an undecalcified histologic section 90 days following implantation of PPSF showing bone-polysulfone interface (asterisk). Note that bone contains marrow (M) and osteocytes (arrowhead) and was covered with osteoblasts (arrow) (Modified Masson stain). (86 X)

FIGURE 97: Photomicrograph of an histologic section 90 days following implantation of PPSF showing bone (asterisk) and osteoid (arrow) at the polysulfone surface (PS). Note the arrangement of osteoblasts (arrowhead) on the surface of the newly formed bone (Modified Masson stain). (138 X)

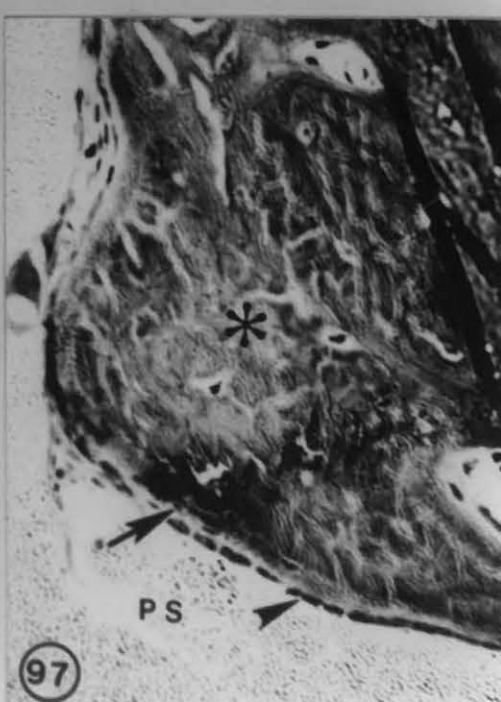
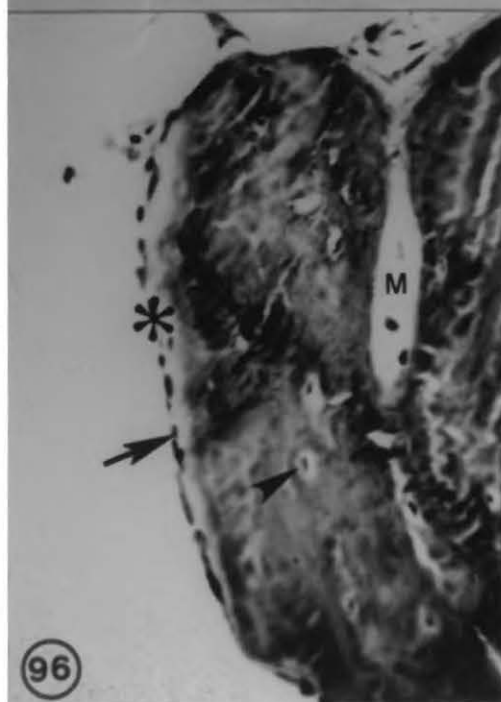
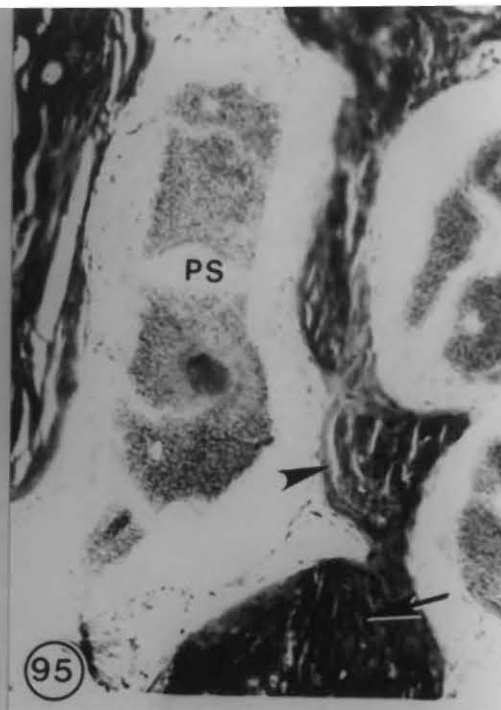
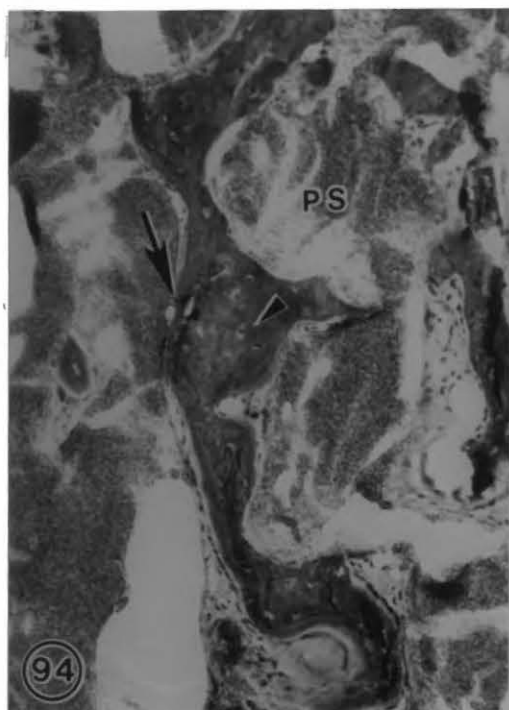
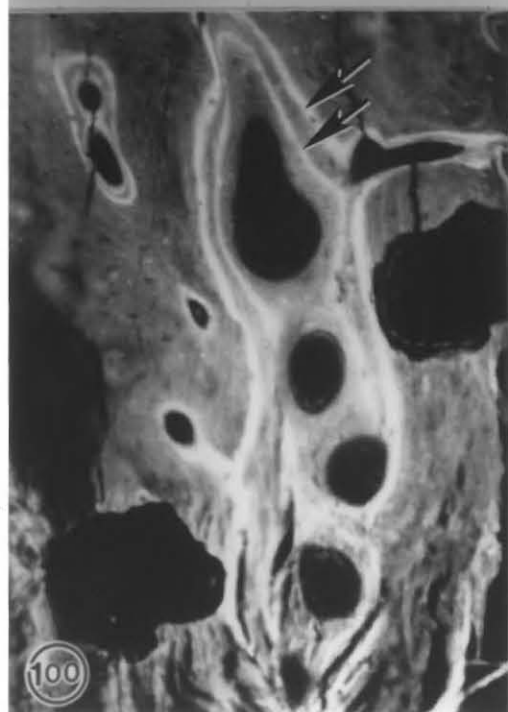
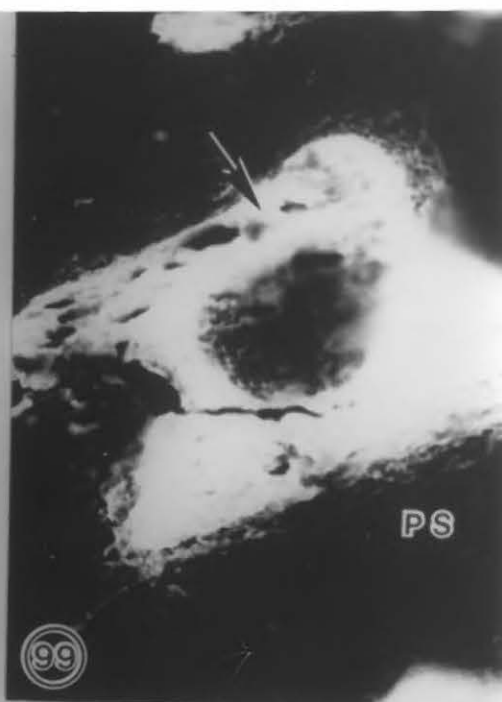
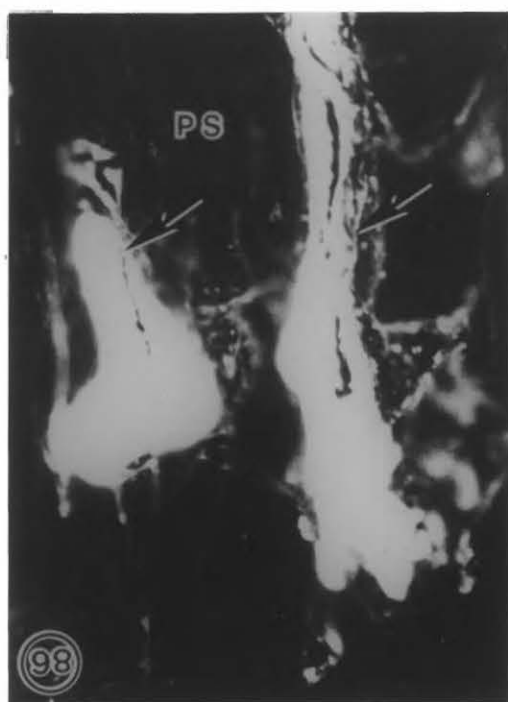


PLATE 27

- FIGURE 98: Photomicrograph of a fluorescent undecalcified histologic unstained section with the double tetracycline label 90 days following implantation of PPSF showing the newly formed bone (arrow) within the micropores of the polysulfone (PS). (34 X)
- FIGURE 99: Photomicrograph of a fluorescent undecalcified histologic unstained section with the double tetracycline label 90 days following implantation of PPSF showing diffuse (arrow), fluorescence with the micropores of polysulfone (PS). (34 X)
- FIGURE 100: Photomicrograph of a fluorescent histologic unstained section with the double tetracycline label 90 days following implantation of PPSF showing a distinct double layer (arrow) of fluorescence in the alveolar bone surrounding the polysulfone. (69 X)
- FIGURE 101: Photomicrograph of a fluorescent histologic unstained section with the double tetracycline label 90 days following implantation of PPSF showing the distinct double layer (arrow) fluorescence at higher magnification. (138 X)



REFERENCES

1. Albrektsson, T. Repair of bone grafts. A vital microscopic and histological investigation in the rabbit. Scand. J. Plast. Reconstr. Surg 14: 1-12, 1980.
2. Anderson, K.J. The behavior of autogenous and homogenous bone transplants in the anterior chamber of the eye: A histologic study of the effect of size of the implant. J. Bone Joint Surg. 43A: 980, 1961.
3. Ashman, A., Neuwirth, S.E. and Bruins, P. The HTRTM molded ridge for alveolar augmentation - an alternative to the subperiosteal implant autogenous bone graft or injectable bone grafting materials. J. Oral Implantology Vol. XII No. 4, 556-575, 1986.
4. Atkinson, P.J. and Woodhead, C. Changes in human mandibular structure with age. Archs Oral Biol. 13: 1453-1463, 1968.
5. Atkinson, P.J. and Woodhead, C. The development of osteoporosis. A hypothesis study based on a study of human bone structure. Clin. Ortho. and Rel. Res. 90: 217-228, 1973.
6. Atkinson, P.J., Woodhead, C., and Powell, K. The influence of remodelling on mandibular bone structure. J. Implantology 4: 263-293, 1974.
7. Atkinson, P.J., and Witt, S. Characteristics of bone. In: Biocompatibility of Dental Materials, CRC Press. Smith, D.C. and Williams, D.F., eds. Vol. I, Chapter 4, p. 95-131, 1978.
8. Atwood, D.A. A cephalometric study of the clinical rest position of the mandible, Part II, The variability in the rate of bone loss

- following removal of the occlusal contacts. J. Pros. Dent. 7: 544, 1957.
9. Atwood, D.A. Some clinical factors related to rate of resorption of residual ridges. J. Prosth. Dent. 12: 441-450, 1962.
 10. Atwood, D.A.: Postextraction changes in the adult mandible as illustrated by microradiographs of midsagittal sections and serial cephalometric roentgenograms. J. Pros. Dent. 13: 810-824, 1963.
 11. Atwood, D.A. Reduction of residual ridges: A major oral disease entity. J. Pros. Dent. Sept. 26(3): 266-279 1971.
 12. Atwood, D.A., Coy, W.A. Clinical cephalometric and densitometric study of reduction of residual ridges. J. Prosth. Dent. 26: 280-299, 1977.
 13. Axhausen, G., Ueber histologische vorgang bei der transplantation var gelenkendau. Arch Klin Chir, 99: 1-50, 1912.
 14. Bahn, S.L. Plaster: a bone substitute. Oral Surg. 21: 672, 1966.
 15. Baker, R.D., Hill, C. and Connole, P.W. Preprosthetic augmentation grafting-autogenous bone. J. Oral Surg. 35: 54-551, 1977.
 16. Baker, R.D., Terry, B.C., Davis, W.D., Connole, W.C. Long-term results of alveolar ridge augmentation. J. Oral Surg. 37: 486-489, 1979.
 17. Ballintyn, N.J. and Spector, M. Porous polysulfone as an attachment vehicle for orthopedic and dental implants. Biomat. Med. Dev. Art. Org. 7(1), 23-29, 1979.
 18. Barth, F. Ueber histologische befunde nach knachen implantation. Arch of Klin. Chir. 46: 409, 1893.

19. Bassett, C.A.L., and Herrmann, I. Influence of oxygen concentration and mechanical factors on differentiation of connective tissues in vitro. *Nature* 190: 460, 1961.
20. Bassett, C. Clinical implications of cell function. *Clin. Orthop.* 87: 49, 1972.
21. Baylink, J. Systemic factors in alveolar bone loss. *J. Pros. Dent.* 31: 486, 1972.
22. Behling, C.A. and Spector, M. Quantitative characteristic of cells at the interface of long-term implants of selected polymers. *J. of Biomed. Mat. Res.* 20: 653-666, 1986.
23. Beirne, O.R. and Greenspan, J.S. Histologic evaluation of tissue response to hydroxylapatite implanted on human mandibles. *J. Dent. Res.* 64(9):1152-1154, 1985.
24. Beirne, O.R., Curtis, T.A. and Greenspan, J.S. Mandibular augmentation with hydroxyapatite. *J. Pros. Dent.* 55(3): 362-367, 1986.
25. Blackstone, C.H. and Parker, M.L. Rebuilding the resorbed alveolar ridge. *J. Oral Surg.* 14: 45, 1956.
26. Blumenthal, N., Sabet, T. and Barrington, E. Healing responses to grafting of combined collagen decalcified bone in periodontal defects in dogs. *J. Periodontol* 57(2): 84, 1986.
27. Boucher, L.J.: Injected silastic in ridge extension procedures. *J. Pros. Den.* 14(3): 460-464, 1964.
28. Boucher, L.J. Injected silastic for tissue protection. *J. Pros. Den.* 15(1): 73-82, 1965.

29. Boucher's prosthetic treatment for edentulous patients. 9th ed. Hickey, J.C., Zarb, G.A. and Bolender, C.L. The C.V. Mosby Company, p. 7, 1985.
30. Boyde, A. and James, S.J. Bone modelling in the implantation bed. J. Biomed. Mat. Res. (19) 199-224, 1985.
31. Boyne, P.J. and Cooksey, D.E. Use of cartilage and bone implants in restoration of edentulous ridges. JADA 71: 1427-1435, 1965.
32. Boyne, P.J., Mikels, T.E. Restoration of alveolar ridges by intramandibular transposition osseous grafting. J. Oral Surg. 26: 569-576, 1968.
33. Brand, K.G., Johnson, K.H. and Buoen, L.C. Foreign body tumorigenesis, CRC Crit. Rev. Toxicol. 14: 353-394, 1976.
34. Brandies, E.F. and Dilert, E. Clinical uses of tricalcium phosphate and hydroxylapatite in maxillofacial surgery. J. Oral Surg. Implantology XII(1): 40-44, 1985.
35. Burchardt, H. The biology of bone graft repair. Clin. Orthop. 174: 28, 1983.
36. Bureau of economic research and statistics. A.D.A. Survey of Denture Wearers, 1976.
37. Buring, K. On the origin of cells in heterotropic bone formation. Clin. Orthop. 110: 293, 1975.
38. Burwell, R.G. Recent advances in orthopaedics. Baltimore, Williams and Wilkins Co., pp. 115-137, 1969.
39. Bush, L.F. The use of homogenous bone grafts: A preliminary report on the bone bank. J. Bone and Joint Surg. 29: 620, 1947.

40. Cameron, H.N., Pilliar, R.M. and Macnab, I. The effect of movement on the bonding of porous metal to bone. *J. Biomech. Mat. Res.* (7): 301, 1973.
41. Canalis, R.F., and Lechago, J. Tetracycline bone labeling. *Ann. Otol.* (91): 160-162, 1982.
42. Carlsson, G.E. and Persson, G. Morphologic changes of the mandible after extraction and wearing of dentures. *Odontol. Surg.* 18: 27, 1967.
43. Carlsson, G.E., Thilander, H. and Headegord, B. Histologic changes in the upper alveolar process after extractions with or without insertion of an immediate full denture. *Acta Odontol Scand.* 25(1): 21-43 1967.
44. Chalmers, J. Observations on the induction of bone in soft tissues. *J. Bone Joint Surg* 75(1): 36, 1975.
45. Chang, C.S., Matukas, V.J. and Lemons, J.E. Histologic study of hydroxylapatite as an implant material for mandibular augmentation. *J. Oral Maxillofac. Surg.* 41: 729-737.
46. Charnley, J. Reaction of bone to self curing acrylic cement. *J. Bone Joint Surg.* 52B, 340, 1970.
47. Clementschitch, F., *Über die wiederherstellung der prothesenfähigkeit des oberkiefers.* *Ost Zstomat* 50: 11, 1953.
48. Connoles, P.W. Mandibular cancellous bone grafts: Discussion of 25 cases. *J. Oral Surg.* 32: 745, 1974.
49. Craddock, F.W. *Prosthetic Dentistry*, ed. 2, St. Louis, 1951, The C.V. Mosby Co.

50. Cranin, A.N. Polyvinyl resin sponge implants in rebuilding atrophic ridges: A new surgical approach. In: Cranium Oral Implantology, Springfield III, Charles C. Thomas, pp. 314-319, 1970.
51. Curran, R.L. and Mager, J.A. Surface dependence of the perioneal response to agar gel. *Nature* 193: 494-495, 1962.
52. Davis, W.H. Transoral bone graft for atrophy of the mandible. *J. Oral Surg.* 28: 760, 1970.
53. Davis, W.H. Long-term ridge augmentation with rib graft. *J. Maxillofacial Surg.* 3: 103, 1975.
54. Desjardins, R.P. Hydroxylapatite for alveolar ridge augmentation: Indications and problems. *J. Pros. Dent.* 54(3): 374-383, 1985.
55. Egbert, M., Stoelinga, P.J., Blijdorp, P.A. and DeKoamen, H.A. The three-piece osteotomy and interpositional bone graft for augmentation of atrophic mandible. *J. Oral Maxillofac. Surg.* 44: 680-687, 1986.
56. Enlow, D.H. The principles of bone remodeling. Springfield III, 1963, Charles C. Thomas.
57. Enlow, D.H. The Human Face. New York, 1968, Hoeber Medical Division, Harper and Row Publishers.
58. Enlow, D.H.: Growth and the problem of the local control mechanism. *Am. J. Anat.* 136: 403-406, 1973.
59. Epstein, J.L. Use of polyvinyl alcohol sponge in alveoloplasty: A preliminary report, 18(6): 453-460, 1960.
60. F. Escales, J. Galante, W. Rostoker and P. Coogan. Biocompatibility of materials for total joint replacement. *J. Biomed. Mat. Res.* 10:175-195, 1976.

61. Farrell, C.D., Kent, N. and Guerra, L.R.: One-stage interpositional bone grafting and vestibuloplasty of the atrophic maxilla. *J. Oral Surg.* 34: 901-906, 1976.
62. Fazili, G.R., Overvest, V., Vernooy, A.M., Visser, W.J. and Waas, M.A. Follow-up investigation of reconstruction of the alveolar process in the atrophic mandible. *Int. J. Oral Surg.* 7: 400-404, 1978.
63. Ferraro, J.W. Experimental evaluation of ceramic calcium phosphate as a substitute for bone grafts. *Plastic Recon. Surg.* May, 63(5): 634-640, 1979.
64. Finn, R.A., Bell, W.H. and Brammer, J.A. Interpositional grafting with autogenous bone and coralline hydroxylapatite. *J. Maxillofac. Surg.* 8: 217-227, 1980.
65. Firschein, H.E. and Urist, M.R. Enzyme induction, accumulation of collagen and calcification in implants of bone matrix. *Clin. Ortho. and Rel. Res.* (84): 263-275, 1972.
66. Flohr, W.Z.: Implantation alloplastic material. *Zahnarztle Prox* 4: 1, 1953. Quoted by Thomas K.H. in: *Oral Surgery*, 5th ed. C.V. Mosby Company, p. 434.
67. Fonseca, R.J., Clark, P.J., Burkes, E.J. and Baker, R.D. Revascularization and healing of onlay particulate autogenous bone grafts in primates. *J. Oral Surg.* (38): 572-577, 1980.
68. Frost, H.M. Skeletal physiology and bone remodeling: An over view. In: *Fundamental and Clinical Bone Physiology*, Urist, M.R., ed. Philadelphia, J.P. Lippincott Co., 1980, p. 208-241.
69. Frost, H.M., Villanueva, B.A., Roth, H., Stanisavljeire, S. Tetracycline bone labelling. *J. New Drugs* (1): 206-216, 1961.

70. Gatewood, J.B. Reconstruction of the alveolar ridge with silicone-dacron implants: A pilot study. *J Oral Surg.* 26: 442-448, 1968.
71. Gerry, R.G. Alveolar ridge reconstruction with osseous autografts: *J Oral Surg.* 14: 74, 1956.
72. Glowacki, J., Altobelli, D. and Mulliken, B. Fate of mineralized and demineralized osseous implants in cranial defects. *Calcif. Tissue Int.* 33: 71-76, 1981.
73. Glowacki, J., Kahan, L.B., Murry, J.E., Folkman, J. and Mulliken, J.B. Application of the biological principle of induced osteogenesis for craniofacial defects. *The Lancet*, 959, 1981.
74. Goldberg, N.I., and Gershkoff, A. Full lower implant denture. *D. Digest* 56: 476, 1949.
75. Gray, D.H., et al. The control of bone induction in soft tissues. *Clin. Orthop.* 143: 245, 1979.
76. Greenfield, E.J. Implantation of artificial crown and bridge abutments. *D. Cosmos* 55: 364, 1913.
77. Guerra, L.R. Augmentation and overdenture prosthesis function and efficacy. *J. Oral Implantology, Special Issue, XII(3):* 1986.
78. Gumaer, K.I., Sherer, A.D., Slighter, R.G., Rothstein, S.S., Drobeck, H.P. Tissue response in dogs to dense HA implantation in the femur. *J. Oral Maxillofac. Surg.* 44: 618-627, 1986.
79. Gupta, D. and Tuli, S. Osteoinductivity of partially decalcified alloimplants in healing of large osteoperiosteal defects. *Acta Orthop Scand* 53: 857, 1982.

80. Hall, B.K. Types of skeletal tissues. In: Hall, B. (ed): Developmental and Cellular Skeletal Biology, New York, Academic Press, p. 1-20, 1978.
81. Ham, A. and Gordon S. The origin of bone that forms in association with cancellous chips transplanted into muscle. Br. J. Plastic Surg. 5: 154-160, 1952.
82. Ham, A. Histology, 7th ed. Philadelphia, J.B. Lippincott, p. 433-445, 1974.
83. Hammer, W.B. Augmentation of deficient mandible alveolar ridges with ceramics. IADR Abstract #257, p. 117, March, 1971.
84. Harakas, N.K. Demineralized bone matrix induced osteogenesis. Clin. Orthop. 188: 239, 1984.
85. Harle, F. Follow-up investigation of surgical correction of the atrophic ridge by visor osteotomy. J. Maxillofac. Surg. 7: 283-289, 1979.
86. Haroldsson, T., Karlsson, U. and Carlsson, G.E. Bite force and oral function in patients with complete dentures. J. Oral Rehabil. 6: 41, 1979.
87. Henefer, E.P., McFall, T.A. and Hauschild, D.C. Acrylate-amide sponge for repair of alveolar bone defects. J. Oral Surg. 26: 568, 1968.
88. Hey Groves, E. Methods of results of transplantation of bone in the repair of defects caused by injury or disease. Br. J. Surg. 5: 185, 1917.
89. Holland, D.J.: Alveoplasty with tantalum mesh. J. Pros. Dent. 3(3): 354-358, 1953.

90. Holmes, R., Mooney, V., Bucholz, R., and Tencer, A.: A coralline hydroxyapatite bone graft substitute. Clin. Orthop and Relat. Res. 188: 252-262, 1984.
91. Homsy, C.A. and Anderson, M.S. Functional stabilization of prostheses with a porous low modulus materials system. In: Biocompatibility of Implant Materials. Williams, D. Sector, ed. London, p. 85-92, 1976.
92. Hosny, M. and Sharawy, M. Osteoinduction in Rhesus monkey using demineralized bone powder allografts. J. Oral Maxillofac. Surg. 43: 837-844, 1985.
93. Hosny, M. and Sharawy, M. Osteoinduction in young and old rats using demineralized bone powder allografts. J. Oral Maxillofac. Surg. 43: 925-931, 1985.
94. Huggins, C. The formation of bone under the influence of epithelium of the urinary tract. Arch. Surg. 22: 377, 1931.
95. Hunter, J. Grafting of normal tissues. Birt. M.J. 2: 383, 1913.
96. Imai, Y., Kuo, Y.S., Watanohe, A. and Masuhara, E. Evaluation of polysulfone as a potential biomedical material. J. Biomedical Engin. 2(1-2): 103, 1978.
97. Inoue, T., Deporter, D.A. and Melcher, A.H. Induction of chondrogenesis in muscle, skin, bone marrow and periodontal ligament by demineralized dentin and bone matrix in vivo and in vitro. J. Dent. Res. 65(1): 12-22, 1980.
98. Jaul, D.H., McNamara, J.A., Carlson, D.S. and Upton, L.G. Acephalometric evaluation of edentulous Rhesus monkeys (*Macaca mulatta*): A long-term study. J. Pros. Dent. 44(4): 453-460, 1980.

99. Johnson, K.: A study of dimensional changes occurring in the maxilla after both extraction. Part II. Closed face immediate denture treatment. Aust. Dent. J. 9:6, 1964.
100. Johnson, K.: A study of dimensional changes occurring in the maxilla after tooth extraction. Part III. Open face immediate denture treatment. Aust. Dent. J. 9: 127, 1964.
101. Johnson, K.: A study of dimensional changes occurring in the maxilla after tooth extraction. Part IV. Interseptal alveolectomy and closed face immediate denture treatment. Aust. Dent. J. 9: 312, 1964.
102. Jones, J.C., Lilly, G.E., Hackett, P.B. and Osbon, D.B. Mandibular bone grafts with surface decalcified bone grafts. J. Oral Surg. 30: 269-276, April, 1972.
103. Kaban, L.B. and Glowacki, J. Induced osteogenesis in repair of experimental mandibular defects in rats. J. Dent. Res. 60: 1356, 1981.
104. Kaban, L.B. and Glowacki, J. Augmentation of rat mandibular ridge with demineralized bone implants. J. Dent. Res. 63(7): 998-1002, 1984.
105. Kajima, K. Interactions between polymeric materials and tissue-biodeterioration of polymeric materials. Bull, Tokyo Med. Dent. Univ. 22: 263-272, 1975.
106. Kaminski, E.J., Oglesby, R.J., Wood, N.K. and Sandrik, J. The behavior of biological materials at different sites of implantation. J. Biomed. Mat. Res. (2): 81-88, 1968.
107. Karp, R.D., Johnson, K.H., Buoen, L.C. Ghobrial, H.K.G. Brand, I. and Brand, K.G. Tumorigenesis by millipore filters in mice. Histology and

- Ultrastructure of Tissue Reactions as Related to Pore Size. J. Natl. Cancer Inst. 51: 1275-1285, 1973.
108. Kelly, J.F. and Friedlaender, G.E. Preprosthetic bone graft augmentation with allogenic bone. A preliminary report. J. Oral Surg. 35: 268-275, 1977.
109. Kent, J.N., Homsy, C.A., Gross, B.D. and Hinds, E.C. Pilot studies of a porous implant in dentistry and oral surgery. J. Oral Surg. 30: 608, 1972.
110. Kent, J.N., Homsy, C.A. and Hinds, E.C. Proplast in dental facial reconstruction. Oral Surg. 39(3): 347, 1975.
111. Kent, J.N., Zide, M.F., Jarcho, M., Quinn, J.H., Finger, I.M. and Rothstein, S.S. Correction of alveolar ridge deficiencies with non-resorbable hydroxylapatite. JADA 105: 993, 1982.
112. Kent, J.N., Quinn, J.H., Zide, M.E., Guerra, L.R. and Boyne, P.J. Alveolar ridge augmentation using non-resorbable hydroxylapatite with or without autogenous cancellous bone. J. Oral Maxillofac. Surg. 629-642, 1983.
113. Kent, J.N., Finger, I.M., Quinn, J.H. and Guerra, L.R. Hydroxylapatite alveolar ridge reconstruction: Clinical experiences, complications and technical modifications. J. Oral Maxillofac. Surg. 44: 37-49, 1986.
114. Kent, J.N. and Jarcho, M. Reconstruction of alveolar ridge with hydroxylapatite. In Fonseca and Davis: Reconstructive preprosthetic oral and maxillofacial surgery. W.B. Sanders Co., pp. 305-346, 1986.

115. Klawitter, J.J. and Hulbert, S.F. Application of porous ceramics for the attachment of load bearing internal orthopedic applications. J. Biomed. Mater. Res. Sym. #2 (Part 1), 161, 1971.
116. Kong, F. Reaction of cartilage to injury. Arch. Klin. Chir. 124: 1, 1923; Abstr. J.A.M.A. 81: 1646, 1923.
117. Koomen, H.A. Stoelinga, P.J. Tiderman, H. and Huybers, T.J. Interposed bone graft augmentation of the atrophic mandible. J. Maxillofac. Surg. 7: 129-135, 1979.
118. Kordan, H.A. Localized interfacial forces resulting from implanted plastics as possible physical factors involved in tumor formation. J. Theor. Biol. 17: 1-11, 1967.
119. Kraut, R.A., Composite graft for mandibular alveolar ridge augmentation: A preliminary report. J. Oral Maxillofac. Surg. 43: 856-859, 1985.
120. Kruger, G.O.: Ridge extension, review of indications and technics. J. Oral Surg. 16: 191-201, 1958.
121. Kruger, E. Rebuilding of alveolar ridge in the lower jaw by cartilage homografts. Trans. Second Int. Conf. Oral Surg. 197-202, 1967.
122. Kruger, G.O.: Textbook of oral and maxillofacial surgery. 6th ed. St. Louis, Toronto, 1984, p. 143-166.
123. Lammie, G.A. The reduction of edentulous ridges. J. Prost. Dent. 10: 605-612, 1960.
124. Lane, S.L. Plastic procedures as applied to oral surgery. J. Oral Surg. 16: 489, 1958.
125. Laskin, D.M.: A sclerosing procedure for hypermobile edentulous ridges. J. Pros. Dent. 23(3): 274, 1970.

126. Lew, D., Clark, P.J. and Jinenez, F. Autogenous rib graft. HA augmentation of the severely atrophic mandible: Preliminary report. J. Oral Maxillofac. Surg. 44: 606-608, 1986.
127. Lindholm, T., et al. Extraskkeletal and intraskkeletal new bone formation induced by demineralized bone matrix combined with bone marrow cells. Clinical Orthop. 171: 251, 1982.
128. Lye, T.L. A histologic evaluation of cartilage hemograft implant used in preprosthetic surgery. Oral Surg. 31(6): 745-753, 1971.
129. Maletta, J.A., Gasser, J.A., Fonseca, R.J. and Nelson, J.A. Comparison of the healing and revascularization of onlayed autologus and lyophilized allogenic rib grafts to the edentulous maxilla. J. Oral Maxillofac. Surg. 41: 487-499, 1983.
130. Marble, H.B. Grafts of cancellous bone and marrow for restoration of avulsion defects of the mandible: Report of two cases. J. Oral Surg. 28: 138, 1970.
131. Matlaga, B.F., Yasenchak, L.P. and Salthouse, T.N. Tissue response to implanted polymers: The significance of sample shape. J. Biomed. Mat. Res. 10: 391-397, 1976.
132. Mercier, P. and Lafontant, R. Residual alveolar ridge atrophy: classification and influence of facial morphology. J. Pros. Dent. 41(1): 90-100, 1979.
133. Mercier, P. and Inove, S. Bone density and serum minerals in cases of residual alveolar ridge atrophy. J. Prosthet. Dent. 46(3): 250-255, 1981.

134. Merwin, G.E., Rodgers, L.W., Wilson, J. and Martin, R.G.: Facial bone augmentation using bioglass in dogs. Arch Otolaryngol. Head and Neck Surg. 112: 280-284, 1986.
135. Miller, A.G.: A case of bone graft with decalcified chips. Lancet, 2: 618, 1890.
136. Moore, R.H., Smith, Q.M. and Field, J.L. Stimulation of new tissue growth as an adjunct to alveoplasty. J. Oral Surg. 6: 812, 1953.
137. Morris, A.L. The significance of complete denture prosthetics in the dental school curriculum today and in 1976. J. Pros. Dent. 19: 80, 1968.
138. Moses, C.H. Physical considerations in impression making. J. Pros. Dent. 3: 449, 1953.
139. Mulliken, J.B. and Glowacki, J. Induced osteogenesis for repair and construction in the craniofacial region. Plast. Recon. Surg. 65: 553, 1980.
140. Mulliken, J.B., Glowacki, J., Kaban, L.B., Folkman, J. and Murray, J. Use of demineralized allogenic bone implants for the correction of maxillofacial deformities. Ann. Surg. 194(3): 366-372, 1981.
141. Mulliken, J.B. Induced osteogenesis: The biologic principle and clinical applications. J. Surg. Res. 37: 487, 1984.
142. Narang, R., Well, H. and Laskin, D.M. Ridge augmentation with decalcified allogenic bone matrix grafts in dogs. J. Oral Surg. 30: 722-726, 1972.
143. Narang, R. and Wells, H. Demineralization of bone transplants in vivo. Oral Surg. 36: 291, 1973.

144. Neufeld, J.O. Changes in trabecular patterns of the mandible following loss of teeth. *J. Prosth. Dent.* 8: 685, 1958.
145. Neville, K. New linear polymers. McGraw-Hill Book Company, Aromatic polysulfones, Chapter 5, 103-127, 1967.
146. Nilles, J.L., Coletti, J.M. and Wilson, C. Biomechanical evaluation of bone porous material interfaces. *J. Biomed. Mat. Res.* (7): 231-251, 1973.
147. Nussbau: Zentrolbl F. Chir. Apr. 10, 1875, Cited by ORR, H.W.: The history of bone transplantation in general and orthopedic surg. *Am. J. Surg.*, 43: 547, 1939.
148. Nylen, M.U., Omuell, K.A., Cofgren, C.G. An electron microscope study of the tetracycline induced enamel defects in rat incisor enamel. *Scand J. Dent. Res.* 80: 384-409, 1972.
149. Oberg, T., Carlsson, G.E., and Fajers, C.M. The temporomandibular joint - A morphologic study on a human autopsy material. *Acta Odont Scand* 29: 350-384, 1971.
150. Ogden, J.A. Chondroosseous development and growth. In: Urist, M., ed. *Fundamental and Clinical Bone Physiology*. Philadelphia, J.B. Lippincott, p. 124-126, 1980.
151. Osbon, D. Lilly, G., Thompson, C. and Jost, T. Bone grafts with surface decalcified allogenic and particulate autologous bone. *J. Oral Surg.* 35: 276, 1977.
152. Page, M.E. Systemic and prosthodontic treatment to prevent bone resorption in edentulous patients. *J. Pros. Dent.* 33(5): 483-488, 1975.

153. Parkes, M.L., Kamer, F.M. and Merrin, M.L. Proplast chin augmentation. Plastic Recon. Surg. 1829-1835, 1975.
154. Peterson, L.J. and Slade, E.W. Mandibular ridge augmentation by a modified visor osteotomy: A preliminary report. J. Oral Surg. 35: 999-1004, 1977.
155. Phemister, D.B. The fate of transplanted bone and regenerative power of its various constituents. Surg. Gynecol. Obstet. 19: 303-323, 1914.
156. Piecuch, J.F. and Fedorka, N.J. Results of soft tissue surgery over implanted replamineform hydroxylapatite. J. Oral Maxillofac. Surg. 41: 801-806, 1983.
157. Piecuch, J. and Peterson, L. Interpore International 1985 Clinical Procedures Guidelines. Interpore 200TM porous hydroxylapatite block alveolar ridge construction.
158. Pietrokovski, J. and Massler, M. Alveolar ridge resorption following tooth extraction. J. Prosth. Dent. 17:21-27, 1967.
159. Privitzer, E., Uridera, O. and Tesk, J.A. Some factors affecting dental implant design. J. Biomedical Mat. Res. Symp. 6: 251, 1975.
160. Rath, A.H., Hand, A.R. and Reddi, A.H. Activity and distribution of lysosomal enzymes during collagenous matrix induced cartilage, bone and marrow development. Develop. Biol. 85: 89, 1981.
161. Ray, R.D. and Holloway, A. Bone implants: Preliminary report of an experimental study. J. Bone Joint Surg. 39(A): 1119, 1957.
162. Ray, R.D. and Sabet, T.Y. Bone grafts: Cellular survival versus induction. J. Bone Joint Surg. 45A: 337-344, 1963.

163. Raymond, J.F., Frost, D., Zeither, D. and Stoelinga, P.J.W. Osseous reconstruction of edentulous bone loss. In Fonseca and Davis: Reconstructive Preprosthetic Oral and Maxillofacial Surgery, W.B. Saunders Co., 1986, pp. 117-165.
164. Reddi, A.H. and Huggins, C.B. Biochemical sequence in the transformation of normal fibroblasts in adolescent rats. Proc. Nat. Sci. U.S.A. 69: 1601, 1972.
165. Reddi, A.H. and Huggins, C.B. Influence of geometry of transplanted tooth and bone on transformation of fibroblasts. Proc. Soc. Exp. Biol. Med. 143: 634, 1973.
166. Reddi, A.H. The matrix of rat calvarium as transformation of fibroblasts. Proc. Soc. Exp. Biol. Med. 150: 324, 1975.
167. Reddi, A.H. and Huggins, C.B. Formation of bone marrow in fibroblast transformation ossicle. Proc. Nat. Acad. Sci. U.S.A. 72: 2212, 1975.
168. Reddi, A.H. and Anderson, W.A. Collagenous bone matrix induced endochondral ossification and haemopoiesis. J. Cell Biol. 69: 557, 1976.
169. Reddi, A.H. and Huggins, C.B. Hormone dependent haemotopoiesis in fibroblast transformation ossicles. Nature 263: 514, 1976.
170. Reddi, A.H., Gay, R., Gay S. and Miller, E.J. Transition in collagen types during matrix induced cartilage and bone marrow formation. Proc. Natl. Acad. Sci. U.S.A. 74: 5589, 1977.
171. Reddi, A. Local and systemic mechanisms regulating bone formation and remodelling. Current Advances in Skeletogenesis p. 77, 1982.
172. Reddi, A.H. Extracellular bone matrix dependent local induction of cartilage and bone. J. Rheumatology (Supp. 11): 67, 1983.

173. Rehrmann, A. Creation of an alveolar ridge after bone transplantation. *J. Plast. Reconstr. Surg.* 24(2): 183, 1959.
174. Reitman, M.J., Brekke, J.H. and Bresuer, M. Augmentation of the deficient mandible by bone grafting to the inferior border. *J. Oral Surg.* 34: 916-918, Oct. 1976.
175. Revah, A., Pietrokovski, J. Extensive resorption of edentulous jaws following long-term dental care: Diagnosis and restorative treatments of two cases. *The Compendium of Continuing Education VI* (10): 707-723, 1985.
176. Rigdon, R.H. Plastic and inflammation: An in vivo experimental study. *J. Biomed. Mat. Res.* 8: 97-117, 1974.
177. Robert, A.B. The pathophysiology and anatomy of edentulous bone loss. In Fonseca and Davis: *Reconstructive Preprosthetic Oral and Maxillofacial Surgery*, W.B. Saunders Co., 1986, pp. 1-17.
178. Rubin, L.R., Bromberg, B.E. and Wolden, R.H. Long term human reaction to synthetic plastics. *Surg. Gynecol. Obstet.* 121: 603-608, 1971.
179. Salthouse, T.N. Effects of implant surface on cellular activity and evaluation of histocompatibility. In: *Advances in Biomaterials*, G.D. Winter, ed. Wiley, Chichester, U.K. In Press.
180. Salthouse, T.N. Some aspects of macrophage behavior at the implant interface. *J. Biomed. Mat. Res.* 18: 395-401, 1984.
181. Sampath, T. and Reddi, A.H. Role of extracellular matrix in local bone induction. *Current advances in skeletogenesis*, 66, 1982.
182. Sampath, T.K. and Reddi, A.H. Homology of bone inductive proteins from human, monkey, bovine and rat extracellular matrix. *Proc. Natl. Acad. Sci. USA* 80: 6591, 1983.

183. Sampath, T.K., Reddi, A.H. Distribution of bone inductive proteins in mineralized and demineralized extracellular matrix. *Biochem. Biophys. Res. Comm.* 119: 949, 1984.
184. Sampath, T.K., Nathanson, M.A. and Reddi, A.H. In vitro transformation of mesenchymal cells derived from embryonic muscle into cartilage in response to extracellular matrix components of bone. *Proc. Natl. Acad. Sci.* 81: 3419-3423, 1984.
185. Sanders, B. and Cox, R. Inferior border rib grafting for augmentation of the atrophic edentulous mandible. *J. Oral Surg.* 34: 897-900, 1976.
186. Sauer, B.W., Weinstein, A.M., Klawitter, J.J., Hulbert, S.F., Leonard, R.B. and Bagwell, J.G. The role of porous polymeric materials in prosthesis attachment. *J. Biomed. Mat. Res.* 5: 145, 1974.
187. Schack, C.C., Noyes, F.R. and Villaneura, A.R. Measurement of haversian bone remodelling by means of tetracycline labelling in ribs of Rhesus monkey. *Henry Ford Hosp. Med. J.* 20(3): 131-144, 1972.
188. Sears, V.H. Principles and techniques for complete denture construction. C.V. Mosby Co. 1949, p. 92-98.
189. Senn, N. On the healing of aseptic bone cavities by implantation of antiseptic decalcified bone. *Am. J. Med. Sci.* 98: 219, 1889.
190. Sharrard, W. and Collins, D. The fate of human decalcified bone grafts. *Proc. Ral. Soc. Med.* 54: 1101, 1961.
191. Sicher's Oral Anatomy. DuBrul, E.L. Chapter 7, The C.V. Mosby Company, 7th ed., p. 536-540, 1980.
192. Small, I. A., Brown, S. and Kobernick, S.D. Teflon and silastic for mandibular replacement: experimental studies and reports of cases. *J. Oral Surg.* 22: 378, 1964.

193. Spector, M., Droughn, R.A., Sauer, B.W. and Young, F.A. Effect of loading on the pores structure of low modulus porous implant materials. J. Dent. Res. 55B: B245, 1976.
194. Spector, M. Minchno, M.J. and Kwiatkowski, G.T. High modulus polymer for porous orthopedic implants: Biomechanical compatibility of porous implants. J. Biomed. Mat. Res. 12: 665, 1978.
195. Spector, M., Harmon, S.L., Irvin, M.P. and Ballintyn, N.J. Trans. of the 4th Annual Meeting of the Society for Biomaterials, San Antonio, Texas, April, 1978, p. 124.
196. Spector, M., Harmon, S.L. and Kruetner, A. Characteristics of tissue growth into proplast and porous polyethylene implants in bone. J. Biomed. Mat. Res. 13: 677-692, 1979.
197. Spector, M., Eldridge, J.T., Harman, S.L. and Kruetner, A. Porous polysulfone coated femoral prosthesis in dogs. Biomaterial, Vol. 3: 155-157, 1982.
198. Spector, M., Teichgraller, J.F. and Jackson, R.T. Tissue response to porous materials used for ossicular replacement prostheses. Biomaterial, 2: 29-40, 1983.
199. Spector, M., Davis, R.J., Lunceford, M.D. and Harmon, S.L. Porous polysulfone coatings for fixation of femoral stems by bony ingrowth. Clin. Orthoped. and Related Res. #176, 34-41, 1983.
200. Spector, M., Reese, N. and Hewan-Lawe, K. Response to particulate polysulfone and polyethylene in an animal model for tumorgency testing. Trans. of the 10th Annual Meeting of the Proc. for Biomat. 1984.

201. Stoelinga, P.J., Tideman, H., Berger, J.S. and Koamen, H.A. Interpositional bone graft augmentation of the atrophic mandible. A Preliminary Report. J. Oral Surg. 36: 30-32, 1978.
202. Swoope Jr., C.C. and Kydd, W.L. The effect of cusp form and occlusal surface area on denture base deformation. J. Pros. Dent. 16: 34, 1966.
203. Syftestad, G.T., Triffitt, J.T., Urist, M.R. and Caplan, A.I. An osteo-inductive bone matrix extract stimulates the in vitro conversion of mesenchyma into chondrocytes. Calcif. Tissue Int. 36: 625-627, 1984.
204. Tallgren, A. The effect of denture wearing on facial morphology. A 7-year longitudinal study. Acta Odontol. Scand. 25: 563, 1967.
205. Tallgren, A. Positional changes of complete dentures: A 7-year longitudinal study. Acta Odontol. Scand. 27: 539, 1969.
206. Tallgren, A. Alveolar bone loss in denture wearers as related to facial morphology. Acta Odontol. Scand. 28: 251, 1970.
207. Tallgren, A. The continuing reduction of the residual alveolar ridges in complete denture wearers: A mixed-longitudinal study covering 25 years. J. Pros. Dent. 27(2): 120, 1972.
208. Tam, C.S. and Anderson, W. Tetracycline labelling of bone in vivo. Calcif. Tiss. Inter. 39: 121-125, 1980.
209. Taylor, S.R. and Gibbons, D.F. Effect of surface texture on the soft tissue response to polymer implants. J. Biomed. Mat. Res. 17: 205-227, 1983.

210. Teichgraeber, J.F., Spector, M., Per-Lel, J.H. and Jackson, R.T. Tissue response to plasti-pore and proplast otologic implants in the middle ears of cats. *Amer. J. of Otolog.* 5(2): 127-136, 1983.
211. Terry, B.C., Albright, J.E. and Baker, R.D. Alveolar ridge augmentation in the edentulous maxilla with use of autogenous ribs. *J. Oral Surg.* 32: 429, 1974.
212. The United States Pharmacopeia XIX, Mack Publishing Co., Easton, PA, 1975, p. 644.
213. Thoma, K.H. and Holland, D.J. Atrophy of the mandible. *Oral Surg.* 4: 1977, 1951.
214. Thoma, K.H. *Oral Surgery*, Vol. I, Chapter 1, 5th ed. St. Louis, C.V. Mosby Co., 1969. p. 434-435.
215. Thomas, K.A. and Cook, S.D. An evaluation of variables influencing implant fixation by direct bone apposition. *J. Biomed. Mat. Res.* 19: 875-901, 1985.
216. Tilney, N.L. and Boor, P.J. Host response to implanted dacron grafts. *Arch Surg.* 110: 1469-1472, 1975.
217. Topazian, R.G., Hammer, W.B., Bauch, L.J. and Hulbert, S.F.: Use of alloplastics for ridge augmentation. *J. Oral Surg.* 29: 792-798, 1971.
218. Topazian, R.G. The use of ceramics in augmentation and replacement of portions of the mandible. *J. Biomed. Mat. Res.* No. 2, Part 2, 311-332, 1972.
219. Trehorne, R.W. and Brighton, C.T. The use and possible misuse of tetracycline as a vital stain. *Clin. Orthop. and Rel. Res.* 140: 240-246, 1979.

220. Tuli, S. and Singh, A. The osteoinduction property of decalcified bone matrix. *J. Bone Joint Surg.* 60(B): 116, 1978.
221. Tuli, S.M. In vitro calcification of human and rabbit bone matrix by physical and chemical methods. *Indian J. Med. Res.* 68: 164, 1978.
222. Tuli, S.M., and Gupta, K.B. Bridging of large chronic osteoperiosteal gaps by allogenic decalcified bone matrix implants in rabbits. *The J. of Trauma* 21(10): 894-897, 1981.
223. Urist, M.R. Bone formation by autoinduction. *Science* 150: 893-899, 1965.
224. Urist, M., et al. The bone induction principle. *Clin. Orthop.* 53: 243, 1967.
225. Urist, M. Surface decalcified allogenic bone (SDAB) implants. *Clin. Orthop.* 56: 37, 1968.
226. Urist, M.R. and Dowel, T.A. The inductive substratum for osteogenesis in pellets of particulate bone matrix. *Clin. Orthop.* 61: 61, 1968.
227. Urist, M.R. and Hay, P.H. Osteogenic competence. *Clin. Orthop.* 64: 194, 1969.
228. Urist, M.R. and Strates, B.S. Bone formation in implants of partially and wholly demineralized bone matrix. *Clin. Orthop.* 71: 271, 1970.
229. Urist, M.R., Twist, J.M. and Dubrec, B.S. Quantitation of new bone formation in intramuscular implants of bone matrix in rabbits. *Clin. Orthop.* 68: 279, 1970.
230. Urist, M.R. and Craven, P.L. Bone cell differentiation in avian species: including comments on multinucleation and morphogenesis. *Fed. Proc.* 29: 1680, 1970.

231. Urist, M.R. The substratum for bone morphogenesis. *Develop. Biol.* (Suppl.) 4: 125, 1971.
232. Urist, M.R. and Strates, B.S. Bone morphogenetic protein. *J. Dent. Res.* 50(4): 1392, 1971.
233. Urist, M.R. and Mikulski, A.J. A soluble bone morphogenetic protein extracted from bone matrix with a mixed aqueous and nonaqueous solvent. *Proc. Soc. Exp. Biol. Med.* 162: 48, 1979.
234. Urist, M.R., Leizte, A., Mizutani, H., Takagi, K., Triffitt, J.T., Amstutz, J., Delange, R., Termine, J. and Finerman, G.A.M. A bovine low molecular weight bone morphogenetic protein (BMP) fraction. *Clin. Orthop.* 162: 219-232, 1982.
235. Urist, M., et al. Bone cell differentiation and growth factors. *Science* 220: 680, 1983.
236. Urist, M.R., Huoy, K., Brownell, A.G., Hohl, W.M., et al. Purification of bovine bone morphogenetic protein by hydroxyapatite chromatography. *Proc. Natl. Acad. Sci.* 81: 371-379, 1984.
237. Van De Putte, K.A. and Urist, M.R. Osteogenesis in the intramuscular implants of decalcified bone matrix. *Clin. Orthop.* 43: 257, 1966.
238. Vandersteenhoven, J.J. and Spector, M. Osteoinduction within porous polysulfone implants at extraosseous sites using demineralized allogenic bone matrix. *J. Biomed. Mat. Res.* 17: 793-806, 1983.
239. Walter, J.B. and Gchiaromonte, L. The tissue responses of the rat to implanted ivalon, etheron, and polyfoam plastic sponges. *Br. J. Surg.* 52: 49-54, 1965.
240. Wang, J.H., Waite, D.E. and Steinhauser, E. Ridge augmentation: An evaluation and follow-up report. *J. Oral Surg.* 34: 600-602, 1976.

241. Wical, K.E. and Swoope, C.C. Studies of residual ridge resorption. Part II. The relationship of dietary calcium and phosphorous to residual ridge resorption. J. Pros. Dent. 32(1): 13-22, 1974.
242. Willezt, S.G. and Semlitsch, M. Reaction of the articular capsule to artificial joint prosthesis. In: Biocompatibility of Implant Materials, Williams, D., ed. Sector, Publishing Ltd., London, p. 40-48, 1976.
243. Williams, D.F. Prosthesis stabilization by tissue ingrowth into porous ceramics, Chapter 3, In: Williams, D.F., ed. Biocompatibility of Orthopedic Implants, Vol. II, 1982.
244. Winter, C.M., Woefel, J.B. and Igaraslin, T. Five year changes in the edentulous mandible as determined on oblique cephalometric radiographs. J. Dent. Res. 53: 1455, 1974.
245. Wittbjer, J. Osteogenic activity in composite grafts of demineralized compact bone and marrow. Clin. Orthop. 173: 229, 1983.
246. Zarb, G.A. Oral motor patterns and their relation to oral prosthesis. J. Pros. Dent. 47(5): 472-478, 1982.
247. Zeiss, I.M. Studies on transference of bone. Vascularization of autologus and homologus implants of cortical bone in rats. Br. J. Experimental. Pathol. 41: 345, 1960.

VII. APPENDIX

See attached sheet for Animal Use/Procedures Approval Form.



Medical College of Georgia
Augusta, Georgia 30912

Division of Research Administration

November 19, 1985

M E M O R A N D U M

TO: Dr. Mohamed M. Sharawy
Department of Oral Biology-Anatomy

FROM: Carolyn Lineberry, Secretary
Committee on Animal Use for Research and Education

SUBJECT: C.A.U.R.E. Review of Protocol

The Committee on Animal Use for Research and Education has reviewed your protocol entitled "Osteoinduction in Rhesus Monkeys Using Porous Polysulfane Material and Demineralized Bone Powder" (85-11-208; Amideast Fellowship) and has found that it adheres to the standards and guidelines for animal use in research and education. This memorandum will serve as your notice of approval. The approved Animal Use and Procedure Form will be retained in the Division of Research Administration along with the remainder of your application information.

cc: Dr. Malcolm Kling
Division of Research Administration